Information regarding the geologic, hydrogeologic and geochemical data of site conditions, and the waste stream characteristics at ExxonMobil facility are presented in earlier sections. That information is used in this section to provide a demonstration, via model simulation, that injected wastes will not migrate to a point outside the permitted Injection Zone within a period of 10,000 years. A discussion of the modeling approach and methodology is presented below.

7.1 Model Objectives and Approach

The modeling performed herein specifically addresses three considerations in order to demonstrate no-migration:

- 1. Injection Interval pressurization during the operational period;
- 2. Lateral waste transport and containment within the Injection Zone during the 10,000-year post-operational period; and,
- 3. Vertical waste transport and containment within the Injection Zone during the 10,000-year post-operational period.

To meet these objectives, three separate models were constructed using different approaches. Each model addresses specific considerations for a demonstration of no migration. The descriptions and approaches of the three models are shown in the table below.

General Model Description	General Modeling Approach	
Lateral Injection Interval Pressurization	Quasi-3-D Numerical Model (SWIFT)	
Lateral Plume Transport for Low and High Density Injectate	Quasi-3-D Numerical Model (SWIFT)	
Vertical Transport of Injectate	1-D Analytical Model	

The Sandia Waste Isolation Flow and Transport (SWIFT) code was employed in the lateral (numerical) models. The lateral models are three-dimensional in the sense that the Injection Interval is modeled based on approximate geologic structure, as defined in Section 4.0. There is, however, no vertical transport allowed, thereby maximizing the Injection Interval pressurization and lateral waste transport.

Analytical techniques were used in the vertical transport model. In accordance with 40 CFR §148.21(a)(3) and (5), the numerical and analytical models used to demonstrate no



migration have been verified and validated. The models are available to the public and are based on sound engineering and hydrogeologic principles.

7.1.1 The SWIFT for Windows Computer Code

The computer simulation code used for modeling the pressure buildup and lateral migration of injected waste at the ExxonMobil facility is SWIFT for Windows (HSI Geotrans, 2000). SWIFT for Windows is a version of the SWIFT code (Reeves and others, 1986; Finley and Reeves, 1982; Ward and others, 1987; Reeves and Ward, 1986; Intercomp, 1976). SWIFT was originally called SWIP (Survey Waste Injection Program) and was developed under contract to the U.S. Geological Survey (Intercomp, 1976). The code was developed to model waste injection in deep brine aquifers under conditions of variable fluid density, viscosity and temperature.

SWIFT is a three-dimensional finite difference code that can be used to simulate ground water flow, contaminant transport and heat transport in single or dual porosity media. Steady state or transient conditions can be simulated. In SWIFT, the equations governing ground water flow and solute transport are coupled through: 1) the pore fluid velocity; 2) the dependence of the fluid density on pressure, solute mass fraction and temperature; and 3) the dependence of fluid viscosity on solute mass fraction and temperature.

SWIFT has been extensively verified and validated. Ward and others (1984) documented the benchmarking of SWIFT against eleven analytical solutions and field problems. These problems explore a wide range of SWIFT's capabilities including variable density flow and disposal well injection. Illustrative problems using the SWIFT code have been published in two reports (Finley and Reeves, 1982; Reeves and others, 1987).

7.1.2 Analytical Model

The vertical transport of waste and dissolved waste constituents was calculated using analytical models. These models incorporated the effects due to both advection and molecular diffusion. The advective transport arises from the Injection Interval pressure buildup during the operational period, and the buoyant gradient resulting from the density contrast between the injectate and formation fluid. The molecular diffusion component of transport results from the concentration gradient between the Injection Interval and the overlying strata. Additionally, the diffusive transport through a mud-filled borehole is calculated to address the possibility of a mud-filled artificial penetration intersecting the Injection Interval and waste plume.



The analytical solutions are derived from published materials and employ sound hydrologic principles. Derivations and discussions of the mathematical models used in the vertical transport of waste are presented in Section 7.6.

7.2 General Modeling Methodology and Assumptions

In this modeling, a "conservative approach" methodology was applied. Model input parameters, initial conditions and boundary conditions were employed to ensure that the simulated Injection Interval pressurization and waste transport distance are overestimated. The general methods employed to ensure conservative modeling results are discussed below. Information regarding the specifics of each model are presented in the appropriate model discussions.

The ExxonMobil facility operates two Class I injection wells (WDW-397 and WDW-398) which inject into the Frio Formation. The ExxonMobil facility Injection Zone is contained within the Frio Formation. The Injection Zone and Injection Interval are present at the following depths in WDW-397 and WDW-398:

	WDW-397	<u>WDW-398</u>
Injection Zone	5,347 feet to 7,272 feet KB	5,370 feet to 7,295 feet KB
Injection Interval	5,922 feet to 7,272 feet KB	5,965 feet to 7,295 feet KB

Within the Injection Interval, select sands are utilized for the injection of waste. These sands are identified as the Frio D Sand, Frio E&F Sand and the Frio A/B Sand. Figure 7-1A is a portion of the Halliburton Array Induction Spectral Density Dual Spaced Neutron Log ran in WDW-397 on March 8, 2006. Figure 7-1B is a portion of the Halliburton Array Induction Log (3 Run Composite) ran in WDW-398 on July 18, 2009. The depths to the Injection Zone, Injection Interval and various Frio Sands are notated on both figures. Plates 4-2 and 4-3 are structural, stratigraphic cross sections through the ExxonMobil facility location which depict the sands of interest within the Injection Interval. The Frio Sands of interest to this demonstration are found at the following depths in the WDW-397 and WDW-398 injection wells:

Frio Sands	WDW-397	WDW-398
Frio D Sand	6,635 feet to 6,664 feet KB	6,670 feet to 6,715 feet KB
Frio E&F Sand	6,712 feet to 6,930 feet KB	6,756 feet to 6,940 feet KB
Frio A/B Sand	6,960 feet to 7,126 feet KB	6,991 feet to 7,155 feet KB



Although the Frio D Sand is present at the location of WDW-398, it is poorly developed. WDW-398 will not be completed to use the Frio D Sand. A fourth Frio sand is identified in the nearby Merisol plant injection wells (WDW-147 and WDW-319). The Frio C Sand is defined as the interval located at a log depth between 7,097 feet KB and 7,286 feet KB in Merisol Plant Well 1 (WDW-147). The Frio C Sand is below the total depth of the WDW-397 and WDW-398 injection wells. Figure 7-1 illustrates the relationship of the Frio sands in the WDW-398, WDW-397 and WDW-147 injection wells.

The depth to the center of the Injection Interval for the Frio D Sand in the reservoir modeling is placed at 6,650 feet KB in WDW-397 (based on top of Frio D Sand at 6,635 feet KB plus 50 percent of thickness at well (29 feet/2)). The depth to the center of the Injection Interval for the Frio E&F Sand in the lateral migration models and reservoir pressurization model is placed at 6,787 feet KB in WDW-397 (based on top of Frio E&F Sand at 6,712 feet KB plus 50 percent of modeled reservoir thickness (150 feet/2)). The depth to the center of the Injection Interval for the Frio A/B Sand in the lateral migration models and reservoir pressurization model is placed at 7,022 feet KB in WDW-397 (based on top of Frio A/B Sand at 6,960 feet KB plus 50 percent of modeled reservoir thickness (125 feet/2)).

The top of vertical model is placed within the Injection Interval at 6,178 feet GL (6,200 feet KB) in WDW-397 and 6,251 feet GL (6,276 feet KB) in WDW-398. ExxonMobil will stipulate that neither WDW-397 nor WDW-398 will be completed to inject into Injection Interval sands which are higher in the subsurface than 6,178 feet GL (6,200 feet KB) in WDW-397 or 6,251 feet GL (6,276 feet KB) in WDW-398. The top of the permitted Injection Interval is at 5,922 feet KB in WDW-397 and 5,965 feet KB in WDW-398.

Although the ExxonMobil well(s) may inject into varying sand horizons, the modeling scenario employed in this demonstration was designed to conservatively represent waste migration and reservoir pressurization for **collective** sand intervals. The lateral migration models (light density and heavy density waste) and pressurization model assumes a reservoir with a conservative reservoir thickness, and an appropriate reservoir permeability for the given scenario (i.e., higher permeability for the flow models and lower permeability for the pressurization model). The SWIFT models employed for this



demonstration are close approximations of the Frio D Sand, Frio E&F Sand and the Frio A/B Sand, with respect to structure, thickness and reservoir depth.

This demonstration considers disposal into the authorized Injection Interval at a cumulative injection rate (future) of 1,200 gallons per minute (gpm). In addition, this demonstration considers injection into either well (WDW-397 or WDW-398) at a maximum injection rate (future) of 1,200 gpm. WDW-397 was officially placed in service on December 11, 2008. Prior to placing the well in service, ExxonMobil performed an extensive stimulation and injected pre-injection buffer fluids into WDW-397 beginning on April 22, 2008. This pre-operation fluid injection is also incorporated in the demonstration. The injection rate (January 1, 2009 to December 31, 2020) was set at an average injection rate of 1,200 gpm.

Regional structural information was incorporated into the lateral transport models (variable structure) to address the possibility of "up-dip" or "down-dip" movement of injected wastes. This includes the presence of the South Houston Dome and Clinton Dome salt domes which are structural "highs" within the SWIFT model grid. transport models include the effects of advection, dispersion and molecular diffusion. The maximum injectate density was incorporated into the Injection Interval pressurization model to maximize pressure buildup. The minimum injectate density was incorporated into the low-density injectate lateral transport model and the vertical transport model to maximize up-dip and vertical movement during a 10,000-year operational period. The maximum injectate density was incorporated into the highdensity injectate lateral transport model to maximize down-dip movement during a Formation structural information was not 10,000-year post operational period. incorporated into the vertical transport model, thereby maximizing the upward driving forces of pressure buildup and buoyancy at the point of maximum concentration (wellbore).

7.2.1 Geologic and Hydrologic Model Assumptions

Several hydrologic and geologic assumptions were made in the modeling portion of this petition. General assumptions required for both the lateral SWIFT and vertical models are: 1) Darcy's law is valid, i.e. ground water flow is laminar; 2) the porous medium is fully saturated and confined; 3) hydrodynamic dispersion can be described as a Fickian process; 4) the initial model concentration is zero; 5) the injected and formation fluids are miscible and no reactions between waste constituents or between waste and formation or



formation fluids occur; and 6) the waste movement is modeled by considering the movement of a single conservative species, i.e., no sorption or decay of the waste occurs. Specific assumptions pertaining to each model is detailed in the appropriate following section.

7.2.2 Modeled Concentration Reduction

Table 7-1 is a summary of analytical results of chemical analyses of the waste proposed for injection at the ExxonMobil facility. Based on the hazardous constituents of concern to this petition demonstration, a 5-order of magnitude (100,000-fold) reduction in the initial concentration was used to define the limits of migration of hazardous constituents. This reduction is based on a maximum concentration measurement of constituents present in the waste stream with an additional order of magnitude increase in that concentration, so that the resulting reduction must be at least an order of magnitude greater than that which would actually be required, based on historically measured maximum concentrations. At this level of reduction, hazardous constituents in the ExxonMobil facility waste stream will have been conservatively reduced to levels which are below the accepted health based limits for those constituents. Table 7-2 presents a summary of the hazardous constituents (maximum historical concentration and maximum petitioned concentration) in the ExxonMobil facility's waste stream which are of concern to the this petition demonstration, the EPA health based limits or detection limits for the subject compounds, and the magnitude of reduction necessary to lower maximum anticipated concentrations below existing health based limits. Table 7-3 lists the maximum petitioned wellhead concentration for the hazardous constituents, the associated possible waste codes for each potentially hazardous constituent, the EPA health based limits or detection limits for the subject compounds, and the magnitude of reduction necessary to lower maximum petitioned concentrations below existing health based limits.

This petition demonstration is being made for the following waste codes: D002, D004, D005, D006, D007, D008, D009, D023, D024, D025, D030, and F039. The F039 waste code is made only for the constituents listed in Table 7-3.

7.2.3 Boundary Conditions

For lateral migration modeling, the Injection Interval is assumed to be open on all sides to maximize plume dimensions. This is accomplished by imposing transmissive Carter-Tracy boundaries on the lateral sides using the same transmissivities and porosity-



thickness values that are used throughout the model. For pressure buildup modeling, the faults located to the south of the facility location are modeled as sealing boundaries, thus maximizing pressure buildup in the area surrounding the WDW-397 and WDW-398 injection well.

The "top" and "bottom" of the Injection Interval in the lateral model are non-transmissive with the assignment of zero hydraulic conductivity in the z-direction, thus confining waste movement and Injection Interval pressurization within the modeled Injection Interval layer. This is a conservative condition since no waste transmission or pressure leakoff to the remaining injection reservoir can occur, thereby maximizing waste movement and pressure buildup within the Injection Interval.

The top of vertical model is placed within the Injection Interval at 6,178 feet GL (6,200 feet KB) in WDW-397 and 6,251 feet GL (6,276 feet KB) in WDW-398. ExxonMobil will stipulate that neither WDW-397 nor WDW-398 will be completed to inject into Injection Interval sands which are higher in the subsurface than 6,178 feet GL (6,200 feet KB) in WDW-397 or 6,251 feet GL (6,276 feet KB) in WDW-398. The top of the permitted Injection Interval is at 5,922 feet KB in WDW-397 and 5,965 feet KB in WDW-398. The transport model is 1-dimensional with no transverse component of movement (hydraulic conductivity or dispersivity), thereby maximizing vertical movement.

7.3 Model Input Parameters

The parameters used in the lateral and vertical models are presented in Table 7-4. The parameters employed in these models have been selected to result in maximum Injection Interval pressurization and waste transport distances. Some additional discussion is given below for parameters of particular importance.

7.3.1 Injection Interval Depth, Structure and Thickness

For the vertical migration model, all transport is directed upward from a depth of 6,200 feet KB (6,178 feet GL) within the Injection Interval of WDW-397 and from a depth of 6,276 feet KB (6,251 feet GL) within the Injection Interval of WDW-398. The permitted Injection Interval top is at 5,922 feet KB in WDW-397, and at 5,965 feet KB in WDW-398. The permitted top of the Injection Zone is at 5,347 feet KB in WDW-397. The screened interval for WDW-397 is from 6,644 feet to 7,139 feet KB. The permitted Injection Interval top in WDW-398 is at 5,925 feet KB, and the permitted top of the



Injection Zone is at 5,350 feet KB. The screened interval for WDW-398 is from 6,671 feet to 7,164 feet KB.

For the Frio D Sand reservoir modeling, a model reference point was selected in the middle of the Frio D Sand within the Injection Interval at the ExxonMobil facility location. The top of the Frio D Sand is present at a depth of about 6,603 feet below sea level (subsea); 6,613 feet relative to ground level (GL)); or about 6,635 feet relative to kelly bushing (KB) in WDW-397. The top of the Frio D Sand is present at a depth of about 6,633 feet subsea; 6,645 feet GL; or about 6,670 feet KB in WDW-398. A depth of 6,618 feet subsea (6,628 feet GL or 6,650 feet KB) was chosen as the reference depth for the depth specific SWIFT model parameters for the Frio D Sand.

The top of the Frio E&F Sand is present at a depth of about 6,680 feet subsea (6,690 feet GL; 6,712 feet KB) in WDW-397, and at about 6,719 feet subsea (6,731 feet GL; 6,756 feet KB) in WDW-398. A depth of 6,755 feet subsea (6,765 feet GL or 6,787 feet KB) was chosen as the reference depth for the depth specific SWIFT model parameters for the Frio E&F Sand.

The top of the Frio A/B Sand is present at a depth of about 6,928 feet subsea (6,938 feet GL; or about 6,960 feet KB in WDW-397, and at about 6,954 feet subsea (6,966 feet GL; or about 6,991 feet KB in WDW-398. A depth of 6,990 feet subsea (7,000 feet GL or 7,022 feet KB) was chosen as the reference depth for the depth specific SWIFT model parameters for the Frio A/B Sand.

Figures 7-1A is portion of the ExxonMobil WDW-397 electric log that illustrates the electric log signature across this portion of the Injection Zone and Injection Interval at the ExxonMobil facility location. Figure 7-1B is portion of the ExxonMobil WDW-398 electric log that illustrates the electric log signature across this portion of the Injection Zone and Injection Interval at the ExxonMobil facility location. Depths to the tops and bottoms of the Frio Sands have been noted on both figures.

Each light-density waste lateral migration model and each reservoir pressurization model considers the structure on top of the completion interval sands (Frio D; E&F and A/B Sands). Each high-density waste lateral migration model utilizes a constant dip on top of the completion interval sands. Collectively, the lateral migration models and reservoir pressurization models are referred to as SWIFT models. The structural information used



in the modeling is based on the regional and local geologic area of review at the ExxonMobil facility, as discussed in Section 4.0. Each SWIFT model also considers the thickness of the modeled sand interval.

Plate 4-9 is a net sand isopach map of the Frio D Sand. The Frio D Sand has a net thickness of about 29 feet at the WDW-397 injection well location, about 18 feet at the WDW-398 injection well location, and has an average net thickness value of 30 feet within the end-of-operations waste plume, and has an average net thickness of 36 feet within the projected path of the 10,000-year buoyant plume. Just north and east of the ExxonMobil facility location, the Frio D Sand is absent with a net sand thickness of 0 feet. Rather than incorporate a variable thickness into the SWIFT modeling scenario, the net sand of the area of interest was averaged. To account for the absence of the Frio D Sand, the grid cells within the approximate 10-foot thick contour interval line were made inactive via use of the R1-26 Card (FPV=0). A net sand thickness of 25 feet was selected as a representative thickness of the Frio D Sand interval within the remainder of the modeled area.

Plate 4-11 is a net sand isopach map of the Frio E&F Sand. The Frio E & F Sand has a net thickness of about 188 feet at the WDW-397 injection well location, about 184 feet at the WDW-398 injection well location, an average net thickness value of 189 feet within the end-of-operations waste plume, and an average net thickness of 133 feet within the projected path of the 10,000-year buoyant plume. Just north and east of the ExxonMobil facility location, the Frio E&F Sand net thickness is greater than 200 feet. The Frio E&F Sand thins to approximately 80 feet in thickness on top of the Clinton Dome located to the northwest of the facility. Rather than incorporate a variable thickness into the SWIFT modeling scenario, the net sand of the area of interest was averaged. A net sand thickness of 150 feet was selected as a representative thickness of the Frio E&F Sand interval within the local study area. In order to assess the potential additional plume migration in the Frio E&F Sand due to thinning of the sand near the Clinton Dome, a sensitivity run was prepared which employed a constant reservoir thickness of 132 feet (1 foot less than the average net thickness within the projected path of the 10,000-year buoyant plume). Sensitivity analyses are discussed in detail in Appendix H.

Plate 4-12 is a net sand isopach map of the Frio A/B Sand. The Frio A/B Sand is thinner in net sand content than the Frio E&F Sand. The Frio A/B Sand has a net sand thickness of about 152 feet at the WDW-397 well location, about 147 feet at the WDW-398



injection well location, an average net thickness value of 143 feet within the end-of-operations waste plume, and an average net thickness of about 91 feet within the projected path of the 10,000-year buoyant plume. The net sand of the Frio A/B Sand is greatest to the south and east of the ExxonMobil facility location (greater than 200 feet in thickness), and thins to between 50 and 75 feet in thickness on top of the Clinton Dome. Rather than incorporate a variable thickness into the modeling scenario for the Frio A/B, the net sand of the area of interest was averaged. A net sand thickness of 125 feet was selected as a representative thickness of the Frio A/B Sand interval within the local study area. In order to assess the potential additional plume migration in the Frio A/B Sand due to thinning of the sand near the Clinton Dome, a sensitivity run was prepared which employed a constant reservoir thickness of 91 feet, which is the average net thickness of Frio A/B Sand within the projected path of the 10,000-year buoyant plume. Sensitivity analyses are discussed in detail in Appendix H.

In summary, the SWIFT no-migration and non-endangerment model was assigned an Injection Interval thickness of 25 feet when modeling flow into the Frio D Sand interval. The SWIFT no-migration and non-endangerment model was assigned an Injection Interval thickness of 150 feet when modeling flow into the Frio E&F Sand interval. The SWIFT no-migration and non-endangerment model was assigned an Injection Interval thickness of 125 feet for any modeling scenario which considers flow into the Frio A/B Sand interval. This is conservative and served to maximize lateral plume dimensions and reservoir pressurization.

At the location of the ExxonMobil injection wells, flowmeter survey data (see Appendix C-9), demonstrate that these reservoir thickness values are appropriate for the modeled scenarios. It is understood that the Frio D Sand is both thin and non-continuous within the study area. Based on the flowmeter survey data included in Appendix C, this demonstration is made at a maximum flow rate of 360 gpm entering the Frio D Sand. A flow profile survey, acceptable to the Agency, shall be run annually to confirm flow distribution into the Frio D Sand, the Frio E&F Sand and the Frio A/B Sand and to confirm that the injection rate into the Frio D Sand does not exceed 360 gpm for any monthly average total injection rate into WDW-397 which exceeds (360 gpm) (1,440 minutes/day) (number of days in that month).

In the vertical model, all transport is directed upward from a depth of 6,178 feet GL (6,200 feet KB) in WDW-397 and 6,251 feet GL (6,276 feet KB) in WDW-398 into the



overlying confinement (or mud-filled artificial penetration). The transport model is 1-dimensional with no transverse component of movement, thereby maximizing vertical movement.

7.3.2 SWIFT Hydraulic Conductivity and Permeability

The hydraulic conductivity and permeability employed in the SWIFT models was selected based on a review of literature values for the Frio Formation, fall-off testing performed on WDW-397 and from a review of historical fall-off tests performed on other nearby Class I injection wells (Merisol WDW-147 and WDW-319).

WDW-397 Fall-Off Test Data

Fall-off test data were collected from WDW-397 after completion in June 2006. WDW-397 is completed across the Frio D Sand, Frio E&F Sand and the Frio A/B Sand. Therefore, fall-off test results represent an "average" for the sands, rather than a value representative of each group. For this reason, reservoir test data collected from the nearby Merisol injection wells are also relied on to provide reservoir permeability estimates for the reservoir sand below the ExxonMobil facility location.

Data from the June 2006 fall-off test are provided in Appendix C to demonstrate that the permeability values employed in this demonstration are reasonable. An analysis of the post-completion pressure fall-off test was performed to determine the pertinent Injection Interval characteristics, namely flow capacity. The net sand screened interval thickness (351 feet) was used in the analysis, as was the average core sample porosity of the cored interval within the Injection Interval in WDW-397. The injection test flow rate of 672 gallons per minute over the approximate 4-hour injection (pressure buildup) period was also used in the analysis. The analysis input parameters, results and relevant plots are also presented in Appendix C. The analysis yields a flow capacity (permeability-thickness product) of 407,511 milliDarcy-feet (mD-ft). Assuming 351 feet for the thickness, the derived permeability is 1,161 mD.

Fall-off test data were collected from WDW-397 in October 2008, as part of the annual reservoir test requirements. Data from the October 2008 fall-off test are provided in Appendix C. An analysis of the post-completion pressure fall-off test was performed to determine the pertinent Injection Interval characteristics, namely flow capacity. The net receiving interval thickness (h) of 309 feet was based on the information recorded on the October 22, 2008 flowmeter profile survey (Appendix C-9). The fluid viscosity for the



reservoir brine in the Frio E&F Sand was previously determined to be 0.487 cP at 169 °F. The injection test flow rate of 700 gallons per minute over the approximate 22-hour injection (pressure buildup) period was also used in the analysis. The analysis input parameters, results and relevant plots are also presented in Appendix C. The analysis yields a flow capacity (permeability-thickness product) of 216,659 milliDarcy-feet (mD-ft). Assuming 309 feet for the thickness, the derived permeability is 701 mD.

Fall-off test data were collected from WDW-397 in August 2009, as part of the annual reservoir test requirements. Data from the August 2009 fall-off test are also provided in Appendix C. An analysis of the post-completion pressure fall-off test was performed to determine the pertinent Injection Interval characteristics, namely flow capacity. The net receiving interval thickness (h) of 309 feet was based on the information recorded on the October 9, 2009 flowmeter profile survey (Appendix C-9). The fluid viscosity for the reservoir brine in the Frio E&F Sand was previously determined to be 0.487 cP at 169 °F. The injection test flow rate of 500 gallons per minute over the approximate 22-hour injection (pressure buildup) period was also used in the analysis. The analysis input parameters, results and relevant plots are also presented in Appendix C. The analysis yields a flow capacity (permeability-thickness product) of 160,754 milliDarcy-feet (mD-ft). Assuming 309 feet for the thickness, the derived permeability is **520 mD**.

WDW-397 Fall-Off Test Results Summary

Date	Test Type	Analysis Technique	k (mD)	h (fft)	u (/eP)	Transmissivity
Jun-06	Fall-off	Radial Flow	1,161	351	0.487	836,778
Oct-08	Fall-off	Radial Flow	701	309	0.487	444,884
Aug-09	Fall-off	Radial Flow	520	309	0.487	330,089

Fall-off test data were collected from WDW-398 in September 2009 at the conclusion of well construction. An analysis of the post-completion pressure fall-off test was performed to determine the pertinent Injection Interval characteristics, namely flow capacity. Based on the results of the October 1, 2009 WDW-398 spinner survey, the net receiving interval thickness (h) is 184 feet (note that the spinner survey injection rate was 210 gpm). A copy of the October 1, 2009 WDW-398 spinner survey is included in Appendix CC of Appendix J-3 (Volume XIII). At the spinner test flow rate of 210 gpm, all flow was entering the Frio E&F Sand. The fluid viscosity for the reservoir brine in the Frio E&F Sand was previously determined to be 0.487 cP at 169 °F. The injection test flow rate of 210 gallons per minute over the approximate 5-hour injection (pressure

buildup) period was also used in the analysis. Since the spinner survey and injection test were performed at 210 gpm, and the spinner survey results suggest that only the Frio E&F Sand accepts flow at this rate, the reservoir test analyses results are assumed to be representative of the Frio E&F Sand. Data and analysis results from the September 2009 WDW-398 fall-off test are provided in Appendix DD of Appendix J-3 (Volume XIII). A discussion of injection / fall-off test is also provided in Section 9.0 of Appendix J-1 (Volume XI). The analysis yields a flow capacity (permeability-thickness product) of 462,834 milliDarcy-feet (mD-ft) for the Frio E&F Sand. Assuming 184 feet for the thickness, the derived permeability for the Frio E&F Sand is 1,225 mD.

WDW-398 Fall-Off Test Results Summary

Date	Test Type	Analysis Technique	k (mD)	- h (ft)	μ(/cP)	Transmissivity kh/µ:(mD=ft/cP)
Sep-09	Fall-off	Radial Flow	1,225	184	0.487	462,834

WDW-147 and WDW-319 Fall-Off Test Data

WDW-397 is completed across the Frio D Sand, Frio E&F Sand and the Frio A/B Sand. Therefore, fall-off test results represent an "average" for the sands, rather than a value representative of each group. For this reason, reservoir test data collected from the nearby Merisol injection wells are also relied on to provide reservoir permeability estimates for the reservoir sand below the ExxonMobil facility location.

WDW-147 and WDW-319 injection wells are completed into the same Injection Interval, and it is assumed that the hydraulic conductivity and permeability for the ExxonMobil WDW-397 and WDW-398 injection wells are approximately equivalent to those determined for the Merisol WDW-147 and WDW-319 injection wells. A review of the historical fall-off test derived permeability values for the WDW-147 and WDW-319 injection wells provides a range of permeability values for use in the SWIFT models. To be conservative, a high or larger permeability is employed in the lateral plume model. This permeability serves to maximize lateral plume movement. A low or smaller permeability is employed in the non-endangerment (pressure buildup) model. The low end values are used in the SWIFT pressure models to ensure the maximum calculated pressure increases. The values used in the SWIFT models are summarized in Table 7-4.



Hydraulic conductivities used in the lateral and vertical models were calculated using permeabilities derived from well tests and literature review. Hydraulic conductivity can be determined for a specified fluid and permeability by:

$$K = \frac{k \rho g}{\mu}$$

where,

K = hydraulic conductivity, ft/day

 $k = intrinsic permeability, ft^2$ $\rho = fluid density, slugs/ft^3$

g = acceleration due to gravity, ft/sec²

 μ = fluid viscosity, lb-sec/ft²

A discussion of how the various hydraulic conductivities were determined is provided below.

Reservoir testing has been performed on the Merisol WDW-147 and WDW-319 injection wells for a number of years. Reservoir testing has been performed annually on WDW-147 wells since 1988 and on WDW-319 since initial construction in 2000. The results of the available historical fall-off test results derived from the fall-off tests performed on the two Merisol injection wells are summarized in Table 7-5. Copies of the fall-off test data for the Merisol wells are included in Appendix C.

Frio D Sand

The Frio D Sand is not present at the location of WDW-147 and WDW-319. The end member hydraulic conductivity and permeability derived for the Frio E&F Sand (discussed in the following paragraphs) are assumed to be representative of the Frio D Sand. In order to be conservative in the prediction of pressure buildup, a permeability of 650 mD is used in the SWIFT pressurization model for the Frio D Sand. This value is 56 percent of the WDW-397 June 2006 fall-off test derived permeability and 93 percent of the WDW-397 October 2008 fall-off test derived permeability. In order to be conservative in the prediction of waste plume migration, a permeability of 2,000 mD is used in the SWIFT lateral migration model for the Frio D Sand. This value is 172 percent of the WDW-397 June 2006 fall-off test derived permeability, and 285 percent of the WDW-397 October 2008 fall-off test. The Frio D Sand is poorly developed at the location of WDW-398 and will not be used by the WDW-398 injection well.



the Frio E&F Sand, a permeability of **2,000 mD** is used in the SWIFT lateral migration model for the ExxonMobil injection wells. This value is 1,099 percent of the average permeability calculated for the WDW-147 fall-off testing listed on Table 7-5, and 172 percent of the WDW-397 June 2006 fall-off test derived permeability, and 285 percent of the WDW-397 October 2008 fall-off test derived permeability.

Using model inputs of 150 feet for thickness, 0.487 cP for fluid viscosity in the Frio E&F Sand, and a permeability value of 650 mD, the derived transmissibility is 200,205 mD-ft/cP. This value of transmissibility is utilized in calculating the reservoir pressure buildup in the Frio E&F Sand to maximize pressure buildup during the operational timeframe of the well. Using model inputs of 150 feet for thickness, 0.487 cP for fluid viscosity in the Frio E&F Sand, and a permeability value of 2,000 mD, the derived transmissibility is 616,016 mD-ft/cP. This value of transmissibility is utilized in calculating the post-operational plume migration in the Frio E&F Sand to maximize transport during the 10,000-year modeling timeframe.

The formation hydraulic conductivity used in the SWIFT pressurization model of the Frio E&F Sand was 3.872 ft/day, based on a flow capacity of 97,500 mD-ft, formation fluid density of 66.02 lb/ft³, formation fluid viscosity of 0.487 cP and a receiving interval thickness of 150 feet.

The formation hydraulic conductivity used in the SWIFT lateral transport model for the Frio E&F Sand was 11.915 ft/day, based on a flow capacity of 300,000 mD-ft, formation fluid density of 66.02 lb/ft³, formation fluid viscosity of 0.487 cP and a receiving interval thickness of 150 feet.

Frio A/B Sand

Several injection/fall-off tests have been run on the Merisol WDW-319 injection well since completion in September 2000. This well is completed in the commingled Frio A/B Sand and the Frio C Sand Injection Interval. The initial test (following well completion) was run on September 26 and 27, 2000. Test derived transmissibility was 459,910 mD-ft/cP, for an average effective permeability of 1,035 mD (using an interval thickness of 240 feet and a viscosity of 0.540 cP). A listing of the derived transmissibility and calculated permeability for each of the tests is shown in Table 7-5. Interpretations for each well test are contained in Appendix C.



Using model inputs of 25 feet for thickness, 0.507 cP for fluid viscosity in the Frio D Sand, and a permeability value of 650 mD, the derived transmissibility is 32,051 mD-ft/cP. This value of transmissibility is utilized in calculating the reservoir pressure buildup in the Frio D Sand to maximize pressure buildup during the operational timeframe of the well. Using model inputs of 25 feet for thickness, 0.507 cP for fluid viscosity in the Frio D Sand, and a permeability value of 2,000 mD, the derived transmissibility is 98,619 mD-ft/cP. This value of transmissibility is utilized in calculating the post-operational plume migration in the Frio D Sand to maximize transport during the 10,000-year modeling timeframe.

The formation hydraulic conductivity used in the **SWIFT pressurization model** of the Frio D Sand was 3.725 ft/day, based on a flow capacity of 16,250 mD-ft, formation fluid density of 66.11 lb/ft³, formation fluid viscosity of 0.507 cP and a receiving interval thickness of 25 feet.

The formation hydraulic conductivity used in the SWIFT lateral transport model for the Frio D Sand was 11.460 ft/day, based on a flow capacity of 50,000 mD-ft, formation fluid density of 66.11 lb/ft³, formation fluid viscosity of 0.507 cP and a receiving interval thickness of 25 feet.

Frio E&F Sand

The average transmissibility for the Frio E&F Sand was approximated based on the reservoir testing of the Merisol WDW-147 injection well reported on Table 7-5. Average transmissibility of the Frio E&F Sand (based on fall-off testing of the WDW-147 injection well) is approximately 738,073 milliDarcy-feet/centiPoise (mD-ft/cP), for an average permeability of 1,828 mD (using a thickness of 218 feet and a viscosity of 0.540 cP). The fall-off test derived transmissibility for the WDW-147 injection well falls between a transmissibility of 524,815 mD-ft/cP (permeability of 1,300 mD) and 984,633 mD-ft/cP (permeability of 2,439 mD).

In order to be conservative in the prediction of pressure buildup in the Frio E&F Sand, a permeability of **650 mD** is employed in the SWIFT pressurization model. This value is 50 percent of the lowest permeability value derived for the WDW-147 fall-off testing listed on Table 7-5, 56 percent of the WDW-397 June 2006 fall-off test derived permeability and 93 percent of the WDW-397 October 2008 fall-off test derived permeability. In order to be conservative in the prediction of waste plume migration in



The September 2001, fall-off test transmissibility result of 131,023 mD-ft/cP, appears to be anomalously low in comparison to the other two tests. A critical review of that test, and the well's completion condition at the time of testing, shows that only a limited portion (125 feet) of the perforated interval was accepting flow. A series of remedial efforts were undertaken to restore injectivity to WDW-319 during the spring of 2001. Although acceptable wellhead pressures were re-established in the well by the end of May 2001, flow data taken at that time and during the September 2001 mechanical integrity testing program, showed a limited interval to be accepting flow. Therefore, data quality from the September 2001 test is questionable. A more aggressive well cleanout and stimulation program was conducted on WDW-319 during March 2002 and again in July 2004. This program re-established flow throughout the commingled Frio A/B Sand and Frio C Sand Injection Interval, as evidenced by flow logging. The greatly increased transmissibility of the well and the re-establishment of zero wellhead pressure during injection demonstrate the effectiveness of the well treatment.

The average transmissibility for the Frio A/B Sand was approximated based on the reservoir testing of the Merisol WDW-319 injection well reported on Table 7-5. Average transmissibility of the Frio A/B Sand based on fall-off testing of the WDW-319 injection well is approximately 323,444 milliDarcy-feet/centiPoise (mD-ft/cP), for an average permeability of 1,072 mD. Disregarding the questionable September 2001 fall-off test results, the fall-off test derived transmissibility for the WDW-319 injection well falls between a transmissibility of 258,137 mD-ft/cP (permeability of 864 mD) and 384,198 mD-ft/cP (permeability of 1,286 mD).

In order to be conservative in the prediction of pressure buildup in the Frio A/B Sand, a permeability of 650 mD is employed in the SWIFT pressurization model. This value is 76 percent of the lowest permeability value derived for the WDW-319 fall-off testing listed on Table 7-5, 56 percent of the WDW-397 June 2006 fall-off test derived permeability, and 93 percent of the WDW-397 October 2008 fall-off test derived permeability. In order to be conservative in the prediction of waste plume migration in the Frio A/B Sand, a permeability of 2,000 mD is used in the SWIFT lateral migration model. This value is 187 percent of the average permeability calculated for the WDW-319 fall-off testing listed on Table 7-5, 172 percent of the WDW-397 June 2006 fall-off test derived permeability, and 285 percent of the WDW-397 October 2008 fall-off test derived permeability

Using model inputs of 125 feet for thickness, 0.495 cP for fluid viscosity in the Frio A/B Sand, and a permeability value of 650 mD, the derived transmissibility is 164,141 mD-ft/cP. This value of transmissibility is utilized in calculating the reservoir pressure buildup in the Frio A/B Sand to maximize pressure buildup during the operational timeframe of the well. Using model inputs of 125 feet for thickness, 0.495 cP for fluid viscosity in the Frio A/B Sand, and a permeability value of 2,000 mD, the derived transmissibility is 505,051 mD-ft/cP. This value of transmissibility is utilized in calculating the post-operational plume migration in the Frio A/B Sand to maximize transport during the 10,000-year modeling timeframe.

The formation hydraulic conductivity used in the SWIFT pressurization model for the Frio A/B Sand was 3.840 ft/day, based on a flow capacity of 81,250 mD-ft, formation fluid density of 66.55 lb/ft³, formation fluid viscosity of 0.495 cP and a receiving interval thickness of 125 feet.

The formation hydraulic conductivity used in the SWIFT lateral transport model for the Frio A/B Sand was 11.816 ft/day, based on a flow capacity of 250,000 mD-ft, formation fluid density of 66.55 lb/ft³, formation fluid viscosity of 0.495 cP and a receiving interval thickness of 125 feet.

Vertical Model Hydraulic Conductivity

The vertical hydraulic conductivity (K_z) assigned to the overlying confinement interval for the vertical model is based on analyses of typical Gulf Coast shales at the depth of interest (5,000 feet to 6,000 feet). Several researchers, Borst (1983), Bryant and others (1975), Magara (1969) and Constant and others (1989), have attempted to establish a relationship between permeability and the other physical properties of shale (i.e., porosity, pore fluid pressure gradient, depth of burial and age).

Bryant and others (1975) measured the permeability of sediments from the Gulf of Mexico and formulated an empirical relationship between porosity and permeability with increasing depth of burial. Tables 7-6 and 7-7 offer depth, pressure, void ratio, porosity and density relationships for typical silty clays of the Gulf of Mexico and an equation which can be utilized to calculate permeability when given porosity. For example, a shale sediment compressed to an equivalent burial depth of 4,825 feet GL (depth to the top of the Confining Zone at the facility location) would have a porosity of about 31 percent. With this value, the equation for all data computes a permeability value of 3.19



 \times 10⁻¹⁰ cm/sec or 3.31 \times 10⁻⁴ mD [(3.19 \times 10⁻¹⁰ cm/sec)(1.04 \times 10⁶ mD per cm/sec)]. The conversion factor to convert hydraulic conductivity expressed in cm/sec to permeability expressed in milliDarcys is from Freeze and others (1979). The Bryant and others (1975) reference is included in Appendix D and provides figures which plot porosity versus permeability data in both hydraulic conductivity and permeability.

Bryant and others (1981) also considered the porosity-permeability relationship in a review of the geotechnical properties of oceanic sediments. Data from laboratory consolidation tests performed on sediments from the South Pass area of the Mississippi Delta, confirms that at a porosity of 26 percent, the permeability is approximately 1 x 10⁻⁵ mD. The Bryant and others (1981) reference is included in Appendix D

Clark (1989) studied typical Gulf Coast shales from the Oakville, Lagarto, Anahuac and Frio formations at Beaumont, Texas and determined that permeabilities were on the order of 1×10^{-5} to 1×10^{-6} mD. The Clark (1989) technical paper is included in Appendix D.

These studies offer insight into the very low permeability and porosity of Gulf Coast shales. This inherent characteristic makes Gulf Coast shales an excellent medium for use as confining strata in waste injection operations. In summary, based on literature the permeability of Gulf Coast shales, beneath the ExxonMobil facility, at depths of 4,000 to 5,000 feet, should be between 1×10^{-4} and 1×10^{-5} mD.

In addition to these values derived from various technical papers, shale cores were collected from the Confining Zone at the time of completion of WDW-397. These core data are included in Appendix C. Shale cores were collected between depths of 5,075 feet to 5,078 feet KB in the Anahuac Formation. Three core samples were subjected to liquid permeability measurement using synthetic Frio Formation brine as the pore fluid. The derived permeability ranged from 5.1×10^{-4} mD to 2.3×10^{-3} mD.

Based on the data included in the previous paragraphs, the value of 5.00 x 10⁻⁴ mD is assigned as the vertical shale intrinsic permeability in the containment interval. This value was converted to a hydraulic conductivity using the light density injectate at reservoir conditions in the Frio E&F Sand (viscosity of 0.438 and a density of 61.80 lb/ft³.



$$K_z = \frac{k\rho g}{\mu}$$

 $\rho g = \text{injectate fluid specific weight (density)} = 61.80 \text{ lb/ft}^3$

 μ = injectate fluid viscosity = 0.438 cP

 $k = \text{shale intrinsic permeability} = 5.00 \times 10^{-4} \text{ mD}$

Therefore:

$$K_z = \frac{(5 \times 10^{-4} \text{ mD})(61.80 \text{lb/ft}^3)(1.062 \times 10^{-11} \text{ ft}^2/\text{Darcy})(86,400 \text{ sec/day})}{(0.438 \text{ cP})(2.088 \times 10^{-5} \text{ lb - sec/ft}^2 - \text{cP})(1,000 \text{ mD/Darcy})}$$

$$K_z = 3.10 \times 10^{-6} \text{ ft/day}$$

The formation hydraulic conductivity used in the vertical migration model is 3.10×10^{-6} ft/day. The vertical hydraulic conductivity of the containment interval is assumed homogeneous (no variation in permeability along the vertical path). Additionally, since the vertical model is one-dimensional (vertically upward), the hydraulic conductivity is assumed to be isotropic.

7.3.3 SWIFT Model Reference Pressure and Fluid Gradients

Static BHP data were collected from WDW-397 at the time of completion. On May 30, 2006, static BHP data were collected after the well had been stimulated. The static BHP was 2,874 psig at 6,633 feet KB. The average wellbore fluid gradient at the time of measurement was 0.4416 psi/ft. At 6,785 feet subsea, the calculated static BHP was 2,956 psig, or 2,970 psia. On June 20, 2006, static BHP data were collected after the well had been completed to its current configuration. The static BHP was 2,906 psia at 6,700 feet KB. The average wellbore fluid gradient at the time of measurement was 0.4376 psi/ft. At 6,785 feet subsea, the calculated static BHP was 2,942 psig, or 2,957 psia.

The most recent reservoir testing for WDW-397 was performed in August 2009, and static BHP data were collected in WDW-397 on August 19, 2009. A static bottom-hole pressure measurement was made in WDW-397 at 6,787 feet KB at the conclusion of the pressure fall-off test. After about 19.44 hours, the bottom-hole pressure was stable at approximately 2,966 psia. The calculated fluid gradient in the well at the time of measurement was 0.442 psi/ft.



The static BHP at the reference depth for each of the Frio Sands of interest are summarized on the following table. BHPs were depth corrected using the fluid gradient measured at the time of collection of pressure data.

Frio Formation Injection Interval
Frio D. E&F and A/B Sands (WDW-397 Injection Well)

Date	Bottom Fluid Gradient (psi/ft)	Depth (ft KB)	BHP @ Depth (psia)	Static BHP (psia) @ D Sand Reference Depth (6,650 ft KB)	Static BHP (psia) @ E&F Sand Reference Depth (6,787 ft KB)	Static BHP (psia) @ A/B Sand Reference Depth (7,022 ft KB)
May-06	0.442	6,633	2,889	2,896	2,957	3,061
Jun-06	0.438	6,700	2,906	2,884	2,944	3,047
Oct-08	0.442	6,789	2,959	2,898	2,958	3,062
Aug-09	0.442	6,787	2,966	2,905	2,966	3,070

Static BHP data were collected from WDW-398 at the time of completion. On September 28, 2009, static BHP data were collected after the well had been stimulated. The static BHP was 2,925 psig at 6,750 feet KB. The average wellbore fluid gradient at the time of measurement was 0.4393 psi/ft. On September 30, 2009, static BHP data were collected at the conclusion of the reservoir test. The static BHP was 2,926 psig at 6,750 feet KB. The average wellbore fluid gradient at the time of measurement was 0.4393 psi/ft.

The static BHPs recorded in WDW-398 are summarized on the following table. BHPs were depth corrected using the fluid gradient measured at the time of collection of pressure data.

Frio Formation Injection Interval
Frio E&F and A/B Sands (WDW-398 Injection Well)

Date	Bottom Fluid Gradient (psi/ft)	Depth (ft KB)	BHP @ Depth (psia)	Static BHP (psia) @ E&F Sand Reference Depth (6,831 ft KB)	Static BHP (psia) @ A/B Sand Reference Depth (7,054 ft KB)
Sep-09	0.439	6,750	2,925	2,961	3,059
Sep-09	0.439	6,750	2,926	2,962	3,060

The static BHP data measured in WDW-398 are in close agreement with the initial static BHP data recorded in WDW-397.



The initial static BHPs collected in the nearby Merisol WDW-147 injection well were reviewed and compared to the WDW-397 static BHP data, as a means of verifying the WDW-397 BHPs.

As reported by Sandia Technologies, LLC in Revision No. 1 (December 2003) of the nomigration petition demonstration for WDW-147 and WDW-319, the June 1979 static BHP in WDW-147 was 2,866.3 psi (2,881 psia) at a reference depth of 6,564 feet KB (6,548 feet GL). Schlumberger reported a fluid level of 400 feet below ground level after the initial perforating gun run. The calculated fluid gradient is 0.465 psi/ft {[(2,881 psia – 14.7 psi)/(6,564 feet – 400 feet)] = 0.465 psi/ft average gradient}. Subsequent pressure measurements in WDW-147 suggest that the actual value of the original formation pressure may have been approximately 35 psi less than this initially measured static BHP.

The best estimate of formation pressure in the Frio E&F Sand is determined from the collective static pressures measured in WDW-147, since initial completion (static BHP measurements collected after June 1979). The historical static BHPs at the reference depth of 6,564 feet KB (6,548 feet GL) in WDW-147 collected after June 1979 range from 2,830 psia to 2,861 psia as shown on the following table:

Frio Formation Injection Interval Frio E&F Sand (WDW-147 Injection Well)

	Bottom Fluid	Deepest Gradient	BHP @ Gradient	Reference	Static
Date	Gradient	Stop	Stop	Depth	BHP
	(psi/ft)	(feet)	(psia)	(ft GL)	(psia)
Jul-86	0.518	6,700	2,904 ⁽¹⁾	6,548	2,848
Feb-88	0.498	6,720	2,915 ⁽¹⁾	6,548	2,852
Jan-89	0.468	6,700	2,912	6,548	2,848
Mar-90	0.490	6,700	2,906	6,548	2,839
Jan-91	0.587	6,700	2,910 ⁽¹⁾	6,548	2,845
Dec-91	0.507	6,700	2,914 ⁽¹⁾	6,548	2,860
Dec-92	0.517	6,680	2,899 ⁽¹⁾	6,548	2,854
Sep-93	0.446	6,692	2,909	6,548	2,852
Sep-94	0.438	6,700	2,907	6,548	2,847
Dec-96	0.449	6,700	2,910	6,548	2,849
Sep-97	0.452	6,700	2,924	6,548	2,863
May-01	0.430	6,620	2,872	6,548	2,848
Jul-02	0.434	6,620	2,874	6,548	2,850
Jul-03	0.435	6,620	2,873	6,548	2,849
Aug-04	0.431	6,620	2,877	6,548	2,853
Jul-05	0.429	6,623	2,882	6,548	2,857
Sep-06	0.433	6,620	2,884	6,548	2,860

(1) psi

The average static BHP of 2,851 psia is assumed to be representative of the original formation pressure at the reference depth 6,564 feet KB (6,548 feet GL or 6,523 feet subsea) for the Frio E&F Sand in WDW-147. The reference depth for the Frio E&F Sand is at a depth of 6,787 feet KB (6,765 feet GL or 6,755 feet subsea) below the ExxonMobil facility location. Correcting the pressure to 6,755 feet subsea using a fluid gradient of 0.438 psi/ft (June 20, 2006 bottom fluid gradient measured in WDW-397) yields an estimated static BHP of 2,952 psia. This value compares quite well with the static BHP values measured in WDW-397 (corrected to the Frio E&F Sand reference depth) in May and June 2006.

Merisol's WDW-319 is completed across the commingled Frio A/B and the Frio C Sand Injection Intervals. The initial and historical static BHPs measured in WDW-319 are therefore assumed to be representative of reservoir pressures for the Frio A/B Sands below the ExxonMobil facility.

]	Frio Formation Injection Interval Frio A/B Sand (WDW-319 Injection Well)								
Date	Bottom Fluid Gradient (psi/ft)	Deepest Gradient Stop (feet)	BHP @ Gradient Stop (psi)	Reference Depth (ft GL)	Static BHP (psia)				
Sep-00	0.430	6,950	3,036	6,816.5	2,987				
Sep-01	0.433	6,850	2,975	6,816.5	2,969				
Mar-02	0.438	6,854	2,983	6,816.5	2,975				
Mar-03	0.433	6,850	2,995	6,816.5	-2,989				
Jul-04	0.432	6,850	2,980	6,816.5	2,974				
Sep-05	0.431	6,850	2,992	6,816.5	2,986				
Sep-06	0.435	6,850	2,981	6,816.5	2,975				
Sep-07	0.431	6,820	2,969	6,816.5	-2,976				

The average static pressure of 2,980 psia is assumed to be representative of the original formation pressure at the reference depth 6,789 feet subsea (6,816.5 feet GL or 6,836 feet KB) for the commingled Frio A/B Sand and Frio C Sand. The reference depth for the Frio A/B Sand is at a depth of 6,990 feet subsea (7,000 feet GL or 7,022 feet KB) below the ExxonMobil facility location. Correcting the pressure to 6,990 feet subsea (7,000 feet GL) using a fluid gradient of 0.438 psi/ft yields an estimated static BHP of 3,068 psia. Again, this value compares quite well with the static BHP values measured in WDW-397 (corrected to the Frio A/B Sand reference depth) in May and June 2006.

Appendices C and D contain information and documentation concerning the native and current static BHPs of the Injection Interval recorded in the ExxonMobil WDW-397 and the Merisol WDW-147 and WDW-319 injection wells. Static BHP data collected in 2009 for WDW-398 are presented in Section 9.0 of Appendix J-1 (Volume XI) and Appenxices AA and BB of Appendix J-3 (Volume XIII). Based on these data, the SWIFT model reference pressures are as follows:

• SWIFT model reference pressure for the Frio D Sand is 2,884 psia at a depth of 6,618 feet subsea (6,628 feet GL or 6,650 feet KB)



- SWIFT model reference pressure for the Frio E&F Sand is 2,944 psia at a reference depth of 6,755 feet subsea (6,765 feet GL or 6,787 feet KB).
- SWIFT model reference pressure for the Frio A/B Sand is 3,047 psia at a depth of 6,990 feet subsea (7,000 feet GL or 7,022 feet KB)

7.3.4 Bottom-Hole Temperature

The bottom-hole temperature (BHT) of the Injection Interval was estimated based on the temperatures recorded on the original open-hole logs ran in WDW-397 at the time of completion, the temperature survey ran in WDW-397 on May 23, 2006 and temperature data collected in nearby Class I injection wells and artificial penetrations. A BHT of 160 °F at a depth of 6,638 feet KB was recorded on the February 9, 2006 Halliburton Array Induction Spectral Density Dual Spaced Neutron log. At the time of logging, 10.3 hours had elapsed since the well was last circulated. A BHT of 160 °F at a depth of 7,246 feet KB was also recorded on the February 27, 2006 Halliburton Array Induction Spectral Density Dual Spaced Neutron log. At the time of logging, 10 hours had elapsed since the well was last circulated. Copies of the log header for these logs are included in Appendix C. Given the short time duration between last circulation and the running of the subject logs, the BHT recorded on the logs had probably not returned to the native BHT. A temperature survey was ran in WDW-397 on May 23, 2006, approximately five (5) days after setting the gravel pack in the well. A copy of the relevant portions of the May 23, 2006 temperature log is included in Appendix C. The following data are taken from the May 23, 2006 temperature log from WDW-397.

		Average	Temperature	Temperature	Temperature
	Surface	Temperature	at Frio D	at Frio E&F	at Frio A/B
Facility Well	Temperature	Gradient	Sand*	Sand*	Sand*
	(°F)	(°F/100 feet)	(°F)	(°F)	(°F)
ExxonMobil WDW-397	77	1.47	164	169	168

^{*} Reference Depth = 6,618 feet subsea (6,628 feet GL or 6,650 feet KB) (Frio D Sand)

An examination of the May 23, 2006 Weatherford Temperature Log indicates a constant temperature gradient of 1.47 °F/100 feet from 630 feet KB to about 6,800 feet KB, and 1.74 °F/100 feet from 4,000 feet KB to 6,800 feet KB. Below 6,800 feet KB, the temperature remains constant at approximately 168.3 °F, before beginning to increase at a depth of 7,085 feet KB. The "flat" temperature gradient below 6,800 feet KB is attributed to the installation of the gravel pack across this approximate interval approximately five (5) days

^{*} Reference Depth = 6,755 feet subsea (6,765 feet GL or 6,787 feet KB) (Frio E&F Sand)

^{*} Reference Depth = 6,990 feet subsea (7,000 feet GL or 7,022 feet KB) (Frio A/B Sand)

prior to running the temperature log. The temperature data recorded for the reference depth in the Frio D Sand and Frio E&F Sand are consistent with the calculated temperature gradient. However, the temperature recorded at the reference depth for the Frio A/B Sand is inconsistent (appears to be low). Using the temperature gradient of 1.74 °F/100 feet (temperature gradient from 4,000 feet KB to 6,800 feet KB), the calculated BHT at the reference depth in the Frio A/B Sand is 173 °F (temperature of 120 °F at 4,000 feet KB plus [7,022 feet KB- 4,000 feet KB][1.74 °F/100 feet]).

A temperature survey was run in WDW-398 on September 28, 2009. No fluids had been pumped into WDW-398 over the six days preceding the performance of the temperature survey and the well had been shut-in for three days prior to running the temperature survey. A copy of September 28, 2009 temperature log is included in Appendix X of Appendix J-3 (Volume XIII). An examination of the Gulf Coast Well Analyses Differential Temperature Log indicates a constant temperature gradient of 1.43 °F/100 feet from 300 feet KB to about 6,700 feet KB. Between 6,760 feet and 6,800 feet KB, marked cooling is observed and is attributed to the significant volume of fluids pumps during gravel packing of the well. Below 6,800 feet KB, the temperature increases until a depth of about 7,000 feet KB is reached. Below about 7,000 feet KB, the temperature remains constant at approximately 166.6 °F to near total log depth of 7,100 feet. The "flat" temperature gradient below 7,000 feet KB is attributed to the installation of the gravel pack. Using the temperature gradient of 1.43 °F/100 feet (temperature gradient from 300 feet KB to 6,700 feet KB), the calculated BHT at the reference depth in the Frio D Sand; Frio E&F Sand and Frio A/B Sand at the horizon mid-point depths are:

		Average	Temperature	Temperature	Temperature
	Surface	Temperature	at Frio D	at Frio E&F	at Frio A/B
Facility Well	Temperature	Gradient	Sand*	Sand*	Sand*
	(°F)	(°F/100 feet)	(°F)	(°F)	(°F)
ExxonMobil WDW-398	82	1.43	164	167	170

- * Mid Point Depth = 6,648 feet subsea (6,660 feet GL or 6,685 feet KB) (Frio D Sand)
- * Mid Point Depth = 6,795 feet subsea (6,806 feet GL or 6,831 feet KB) (Frio E&F Sand)
- * Mid Point Depth = 7,016 feet subsea (7,028 feet GL or 7,053 feet KB) (Frio A/B Sand)

The temperature data recorded in WDW-398 on September 28, 2009 are nearly identical to the temperature data recorded in WDW-397 on May 23, 2006.

Offered for comparative purposes are other BHT data collected from nearby artificial penetration. The BHT obtained from the September 25, 2000 differential temperature survey run in Merisol WDW-319. The well had been static for approximately four (4) days



since inhibited brine was circulated prior to landing the injection tubing into the packer. A linear trend line fit to the data from the temperature log shows a mean surface temperature of 89°F and a temperature gradient of 0.82 °F/100 feet. Other additional temperature data are available from nearby Class I injection wells located at Lyondell Chemical Company in Channelview, Texas; Equistar in Channelview, Texas; and at Atofina in Crosby, Texas. All of these facilities are located northeast of the ExxonMobil facility location, but penetrate similar formations at similar depths. The subject temperature data is summarized below.

Facility Well	Regression Surface Temperature (°F)	Regression Temperature Gradient (°F/100 feet)	Temperature at Frio D Sand* (°F)	Temperature at Frio E&F Sand* (°F)	Temperature at Frio A/B Sand* (°F)
Merisol WDW-319	88.9	0.82	143	144	146
Lyondell WDW-148	81.1	1.09	153	155	157
Equistar WDW-36	57.5	1.31	144	146	149
Atofina WDW-230	61.5	1.43	156	158	162
Artificial Penetrations	73.6	1.15	150	151	154

- * Reference Depth = 6,618 feet subsea (6,628 feet GL or 6,650 feet KB) (Frio D Sand)
- * Reference Depth = 6,755 feet subsea (6,765 feet GL or 6,787 feet KB) (Frio E&F Sand)
- * Reference Depth = 6,990 feet subsea (7,000 feet GL or 7,022 feet KB) (Frio A/B Sand)

Temperature data was taken from the September 1990 temperature log run in the Lyondell Chemical Company WDW-148 injection well, the April 1994 temperature log run in the Atofina WDW-230 injection well, and the July 1988 temperature log run in the Equistar WDW-36 injection well. The temperature log from Atofina WDW-230 was taken on original installation of the well. Lyondell's WDW-148 injection well had been shut down approximately three (3) months prior to the 1990 temperature log, and Equistar's WDW-36 injection well was inactive for 18 months prior to the 1988 temperature log. Collectively, these temperature data fall generally below those data collected in WDW-397 and WDW-398, and thus confirm that WDW-397 and WDW-398 were shut-in for an adequate period of time such that the BHT in both wells attained near static and undisturbed BHT.

The BHT collected in WDW-397 provided the basis for estimating the BHT at a reference depth for each sand interval of interest. The SWIFT model reference temperature for the Frio D Sand is 164 °F at the reference depth of 6,618 feet subsea (6,628 feet GL or 6,650 feet KB). The SWIFT model reference temperature for the Frio E&F Sand is 169 °F at the reference depth of 6,755 feet subsea (6,765 feet GL or 6,787 feet KB). The SWIFT model reference temperature for the Frio A/B Sand is 173 °F at the reference depth of 6,990 feet subsea (7,000 feet GL or 7,022 feet KB).

READ R1-11 Initial Temperatures

The R1-11 card input parameter for the SWIFT model requires initial temperatures to be input relative to the SWIFT model reference plane. For the shallow depth, a depth of 4,968 feet subsea (4,978 feet GL or 5,000 feet KB) was selected and the temperature of 137 °F was recorded from the May 23, 2006 Weatherford Temperature Log ran in WDW-397. For the deeper depth, a depth of 8,200 feet subsea (8,210 feet GL or 8,232 feet KB) was selected and the temperature of 194 °F (temperature of 120 °F at 4,000 feet KB plus [8,232 feet KB-4,000 feet KB][1.74 °F/100 feet]) was calculated using the temperature gradient of 1.74 °F/100 feet (temperature gradient from 4,000 feet KB to 6,800 feet KB from the May 23, 2006 Weatherford Temperature Log ran in WDW-397).

READ R2-7-2 Injection Fluid Temperature

The R2-7-2 card requires that temperature of the injection fluid be input into the data set. The nature of the fluid for injection is such that the temperature of the fluid is at ambient conditions. The average temperature of 75 °F is used for the injection fluid and is input into the R2-7-2 Card. For the offset injection well locations, the native BHT at the center of grid block was estimated based on the temperature gradient derived for the data sets discussed in the previous paragraphs.

7.3.5 Porosity

During the drilling and completion of WDW-397, four (4) whole cores were collected between 5,596 and 6,857 feet KB from the permitted Injection Zone and permitted Injection Interval in WDW-397. In addition, a total of 39 quantifiable sidewall core samples from 5,350 to 7,124 feet KB, were collected from the permitted Injection Zone and permitted Injection Interval in WDW-397. During the drilling and completion of WDW-398, a total of 33 quantifiable sidewall core samples from 6,639 to 7,155 feet KB, were collected from the permitted Injection Zone and permitted Injection Interval in WDW-398. The core samples were sent to Core Laboratories in Houston, Texas for routine whole core and standard sidewall analysis. The WDW-397 Core Lab sidewall core and whole core analyses are included in Appendix C. The WDW-398 Core Lab sidewall core and whole core analyses are included in Appendix W of Appendix J-3 (Volume XIII).

Whole core analysis provided porosity values ranging from 25.68 to 33.91 percent across the Frio E&F Sand with the highest porosity being observed at 6,843.55 feet. No whole cores were collected from either the Frio D Sand or the Frio A/B Sand. The average



porosity for the sand portions of the whole core-sampled Frio E&F Sand is 30.82 percent. Since whole core test results are considered more reliable than sidewall core results (due to the percussive nature of sidewall core extraction resulting is some degree of sample crush), the average porosity value obtained from whole core testing is accepted as a representative value of the average porosity of the Frio E&F Sand.

Sidewall core were collected from both the Frio E&F Sand and the Frio A/B Sand. The sidewall core analysis from the Frio E&F Sand collected in WDW-397 provides porosity values ranging from 27.2 to 29.5 percent. The highest porosity exists within the interval at 6,785 feet. The average porosity for the sand portions of the sidewall core-sampled Frio E&F Sand in WDW-397 is 28.4 percent. The sidewall core analysis from the Frio A/B Sand in WDW-397 provides porosity values ranging from 28.3 to 29.6 percent. The highest porosity exists within the interval at 7,045 feet. The average porosity for the sand portions of the sidewall core-sampled Frio A/B Sand in WDW-397 is 29.0 percent.

The sidewall core analysis from the Frio E&F Sand collected in WDW-398 provides porosity values ranging from 23.6 to 32.9 percent. The highest porosity exists within the interval at 6,795 feet. The average porosity for the sand portions of the sidewall coresampled Frio E&F Sand in WDW-398 is 28.6 percent. The sidewall core analysis from the Frio A/B Sand in WDW-398 provides porosity values ranging from 25.5 to 33.3 percent. The highest porosity exists within the interval at 7,095 feet. The average porosity for the sand portions of the sidewall core-sampled Frio A/B Sand in WDW-398 is 31.6 percent.

The porosity of the Injection Interval sands in the WDW-397 and WDW-398 injection wells were confirmed by comparison to the porosity determined from analyses of whole and sidewall core samples taken from Merisol's WDW-147 and WDW-319 at the time of completion. Whole core porosity from cores collected from WDW-319 averages 32 percent in the Frio E&F Sand and 31 percent in the Frio A/B Sand. Average porosity of the whole cores taken in the Frio E&F Sand during construction of Merisol's WDW-147 injection well is 31 percent.

To be conservative in the modeling of both pressure buildup and plume transport, a porosity of **28 percent** is assigned to both the Frio E&F Sand and to the Frio A/B Sand Injection Intervals. This value is also selected as being representative of the Frio D Sand porosity.



The extent of vertical molecular diffusion of a contaminant species through the aquiclude layers overlying an injection sand is proportional to the aquiclude layer porosity, increasing roughly in direct proportion to the layer porosity. Therefore, in calculations utilized to predict a conservative upper-bound limit to vertical diffusion distance, a reasonable upper-bound limit to porosity, such as total shale porosity, should be used.

Sidewall core collected in WDW-397 at 5,900 feet, 6,026 feet and 6,527 feet from shale-rich intervals (based on SP log response in March 8, 2006 Halliburton High Res Array Ind Density Neutron Longspace Sonic Log) within the containment interval indicate an average porosity of 23.5 percent. The core data presented in Appendix C describe these sidewall core samples as being very fine-grained sand rather than shale. Regardless, these porosity values are accepted as being a very conservative estimate of porosity of the more mud-rich shale portions of the containment interval. Conventional core analyses of the shale overlying the Frio E&F Sand Injection Interval taken from 6,427 feet to 6,429 feet in Merisol's WDW-319 indicate porosity values ranging from 14.3 percent to 20.2 percent. Core data from WDW-147 are also presented in Appendix C.

For this petition demonstration, a total porosity value of **21 percent** is assigned to the shale layers overlying the Frio D Sand Injection Interval.

7.3.6 Tortuosity

The tortuosity factor is expressed as the square of the actual length of a flow path (which is sinuous in nature) divided by the straight-line distance between the ends of the flow path. Daniel & Shackleford (1988) report tortuosities (τ) varying from 0.01 in a clay matrix to 0.84 in a 100 percent sand matrix. Miller (1989) indicates that tortuosity is the reciprocal of the geometric correction factor which itself is equal to (shale porosity)² or (consolidated sandstone porosity)^{0.3} or (unconsolidated sandstone porosity)^{0.8} as upper bounds. The Injection Interval sand porosity is assumed to be 28 percent as determined from whole and sidewall core collected in WDW-397 and Merisol's WDW-147 and WDW-319 injection wells. The Confining Zone and Containment Interval shale porosity is assumed to be 21 percent based on whole and sidewall core data from WDW-397 and the nearby Merisol injection wells. The geometric correction factor was estimated to be **0.361** for the Injection Interval sands. In the vertical transport model, the geometric correction factor was estimated to be **0.044** for the containment interval shale.



7.3.7 Reservoir Dip Angle

The SWIFT models used to simulate lateral plume movement for the light density waste plume and reservoir pressure buildup employ a variable structure concept. Each grid block is set at a depth within the SWIFT model to closely match the mapped geologic structure on the Frio E&F Sand. The structure depth mapped on the Frio E&F Sand was then adjusted to the appropriate depth to simulate lateral migration within the Frio D Sand, Frio E&F Sand and Frio A/B Sand. Plate 7-4 depicts an overlay of the SWIFT Frio D Sand light density plume model grid structure onto the Frio D Sand structure map. Plate 7-5 depicts an overlay of the SWIFT Frio E&F Sand light density plume model grid structure onto the Frio E&F Sand structure map (as discussed in Section 4.0, a structure map was not prepared specifically for the Frio A/B Sand structure).

The SWIFT models used to simulate lateral plume movement in the Frio E&F Sand and the Frio A/B Sand for the high density waste plume employ a constant structure concept. The high density plume will also tend to drift up-dip within the Injection Interval due to the density contrast between the lighter density injected plume and the native reservoir fluid. However, ground water flow in the Injection Interval will move the injected waste plume in a down-dip direction. From northwest (up-dip) to southeast (down-dip), beginning northwest of the ExxonMobil injection well, the elevation decreases from about -5,800 feet subsea to about -7,300 feet subsea over a distance of about 75,050 feet (14.2 miles). This is an average dip angle of about 1.145 degrees. The dip is in a direction of approximately S45°E. A figure has been included in Appendix C (Figure C-9) which illustrates how the dip angle was derived. The average dip is employed in the lateral plume migration models (ExMob EF HiDens and ExMob AB HiDens).

7.3.8 Longitudinal and Transverse Dispersivity

In general, increasing plume migration distance equates to greater dispersion and, therefore, higher dispersivities. However, higher dispersivities allow the moving plume to spread out more (becoming more diffuse), which results in less transport. The longitudinal and transverse dispersivities used in the ExxonMobil facility models are given in Table 7-4. For the lateral model, the base case longitudinal dispersivity value of **100 feet** was chosen from a compilation of data from many field sites throughout the world provided by Gelhar (1986) and Anderson (1984). This scale dependency is generally thought to be caused by macroscopic aquifer heterogeneity (Davis and others,



1985 and Adams and Gelhar, 1992). However, studies suggest that near the source, dispersivities increase with distance from the source until an asymptotic value is reached at the Taylor or Fickian limit. This is the limit at which dispersion becomes essentially a Fickian process and can be adequately described by the advection dispersion equation (Gelhar and others, 1979). In the field, the Taylor limit is considered to be reached on the order of tens or hundreds of feet from the source and after a time period of tens to hundreds of days (Anderson, 1984).

Gelhar and others (1979) do not provide regressions for the dispersivity data. They have, however, spent a great deal of time in organizing and scrutinizing the data. The important fact is that Gelhar's work provides the best data set available. Among the top experts in the world, there is obviously no clear consensus on how the data should be analyzed. Copies of Gelhar (1986) and Gelhar and others (1992) are included in Appendix D.

Neuman (1990) removed what he considered to be unreliable data from the dispersivity values. His regression analysis provides for much higher dispersivities with increasing plume scale (Neuman, 1990; Neuman 1993; Xu and Eckstein, 1995, Figure 7-2). Xu and Eckstein (1995, Figure 7-2) provide their own interpretation on how Gelhar and his coworkers data set should be analyzed. Their weighted least squares regressions are by no means conclusive, however. Their analysis is based purely on the subjective assertion provided on page 907 that Gelhar and others (1992) consider their most reliable data to be accurate within a factor of 2 or 3. On this basis, Xu and Eckstein (1995) performed the various weighted regression analyses summarized in Figure 7-2. A copy of the Xu and Eckstein (1995) technical paper is included in Appendix D.

In conclusion, there is no clear consensus on how the dispersivity changes with plume scale. Therefore, it is appropriate to use an approach that falls in the middle of published results. This can be achieved by using the graph of equation 12b as depicted in Figure 1 of Xu and Eckstein (1995) (included as Figure 7-2). The fit of equation 12b falls significantly below Neuman's regression line. Therefore, justification exists for the use of much larger dispersivity values. The scale of the largest Injection Interval model plume for the ExxonMobil facility is on the order of 15,000 meters (49,000 feet). This means that the use of a more conservative 30.5 meters (100 feet) for the longitudinal dispersivity in the ExxonMobil facility models is justified, because from Figure 1 of Xu and Eckstein a larger value (80 meters or 265 feet) could be used. The base longitudinal



dispersivity value of 100 feet is appropriate given the range of values reported for the spatial and temporal scales of the lateral models.

Regarding the transverse horizontal dispersivity, the ExxonMobil facility models use a value of 10 feet which is one tenth of the longitudinal dispersivity. Gelhar and others (1992; p. 1970) state that although a ratio of longitudinal to transverse dispersivity of 3 to 1 is commonly used in models, there is no support for this assumption. Figure 6 of Gelhar and others (1992) is included as Figure 7-3. Gelhar and others state that the data support a longitudinal to transverse dispersivity ratio of one order of magnitude or greater. This is also reasonable and conservative given the accepted ratio of transverse to longitudinal dispersivity of 0.01 to 0.5 in MacKay and others (1985) and Anderson (1984). Therefore, the 10 to 1 ratio of longitudinal to transverse dispersivity ratio used in the ExxonMobil facility models is valid and conservative.

Dispersivity was not considered in the vertical model for two reasons. First, the vertical transport is modeled conservatively as one-dimensional; no transverse component of advection or diffusion was allowed (these would dilute the waste as it moves upward). The result is that the waste movement is maximized. Second, at the end of the operational period when the Injection Interval pressurization has subsided, it is assumed that there is no additional potential for fluid flow in any direction; diffusion is the only transport mechanism. The result is a zero fluid velocity and therefore, no dispersion, since dispersion is the product of the fluid velocity and dispersivity.

7.3.9 Molecular Diffusivity

The molecular diffusivity for arsenic was chosen for utilization in the lateral models because arsenic was determined to have the largest bulk (free water) molecular diffusivity.

Molecular Diffusivity - Inorganic Constituents

Arsenic has a free water molecular diffusivity of $1.043 \times 10^{-4} \text{ cm}^2/\text{sec}$ at the reservoir conditions present in the Frio D Sand, $1.095 \times 10^{-4} \text{ cm}^2/\text{sec}$ at the reservoir conditions present in the Frio E&F Sand, and $1.084 \times 10^{-4} \text{ cm}^2/\text{sec}$ at the reservoir conditions present in the Frio A/B Sand. The bulk diffusion coefficient for arsenic and all other inorganic waste constituents listed on Table 7-8 were determined using the Stokes-Einstein equation (Daniel and Shackleford, 1988):



$$D_{\rm m} = \frac{RT}{6\pi N \mu r}$$

where,

D_m = bulk molecular diffusion coefficient

R = ideal gas constant = 8.314 J-mol / K = 8.314 x 10⁷ cm²-g / (sec²-mol-K) N = Avagadro's number = 6.022 x 10²³ / mol

= absolute temperature = 164°F = 346°K (Frio D Sand)

= absolute temperature = 169°F = 349°K (Frio E&F Sand)

absolute temperature = 173°F = 351°K (Frio A/B Sand)

absolute viscosity = 0.507 cP (formation brine at 164°F) = 0.00507 g / (cm-sec) (Frio D Sand)

absolute viscosity = 0.487 cP (formation brine at 169°F) = 0.00487 g / (cm-sec) (Frio E&F Sand)

absolute viscosity = 0.495 cP (formation brine at 173 °F) = 0.00495 g / (cm-sec) (Frio A/B Sand)

ionic radius for arsenic valence $+5 = 4.6 \times 10^{-9}$ cm (CRC Handbook of Chemistry and Physics, 1991)

Substituting the values and solving:

$$\begin{array}{l} D_m \,=\, 1.09 \; x \; 10^{\text{-4}} \; cm^2/sec \;=\, 1.01 \; x \; 10^{\text{-2}} \; ft^2/day \; \text{(Frio D Sand)} \\ D_m \,=\, 1.14 \; x \; 10^{\text{-4}} \; cm^2/sec \;=\, 1.06 \; x \; 10^{\text{-2}} \; ft^2/day \; \text{(Frio E\&F Sand)} \\ D_m \,=\, 1.13 \; x \; 10^{\text{-4}} \; cm^2/sec \;=\, 1.05 \; x \; 10^{\text{-2}} \; ft^2/day \; \text{(Frio A/B Sand)} \end{array}$$

The free-water diffusivity for arsenic is 1.01 x 10⁻² ft²/day in the Frio D Sand. The freewater diffusivity for arsenic is 1.06 x 10⁻² ft²/day in the Frio E&F Sand. The free water diffusivity for arsenic is 1.05 x 10⁻² ft²/day in the Frio A/B Sand.

Molecular Diffusivity - Organic Constituents

The bulk (free liquid) diffusion coefficient for each of the organic hazardous constituents listed on Table 7-8 was determined using the Wilke-Chang equation (Johnson and others, 1989):

$$\frac{D_1}{D_2} = \left[\frac{MW_2\rho_1}{MW_1\rho_2}\right]^{0.6}$$

where D_1 and D_2 are the free solution (in water) molecular diffusivity of the compound of interest and the molecular diffusivity in water of a reference compound (benzene in this case), respectively. MW_1 and MW_2 are their molecular weights and ρ_1 and ρ_2 are the densities of the compounds at their boiling points. The densities and molecular weights were obtained from CRC Handbook of Chemistry and Physics (CRC, 1991). The use of densities at standard temperatures results in molecular diffusivities that are within 10 percent of experimental values (Johnson and others, 1989). As an example, the molecular diffusivity in water for 2,4-dinitrotoluene is:



$$D_{1} (2,4-\text{dinitrotoluene}) = 7 \times 10^{-10} \frac{m^{2}}{\text{sec}} \left[\frac{\left(78.1 \frac{g}{mole}\right) \left(1.3208 \frac{g}{cm^{3}}\right)}{\left(182.14 \frac{g}{mole}\right) \left(0.88 \frac{g}{cm^{3}}\right)} \right]^{0.6}$$

$$D_1$$
 (2,4-dinitrotoluene) = 5.37 x $10^{-10} \frac{\text{m}^2}{\text{sec}}$

The free water diffusivity for 2,4-dinitrotoluene is $5.37 \times 10^{-6} \text{ cm}^2/\text{sec}$. This is equivalent to $4.99 \times 10^{-4} \text{ ft}^2/\text{day}$.

Effective Molecular Diffusivity

Molecular diffusion is included in both the lateral and vertical models to account for transport facilitated by the concentration gradient of injected waste. Molecular diffusion is modeled by considering the movement of a conservative electrolyte species in a porous medium. In SWIFT, the relationship between the effective and free solution (in water) molecular diffusivity is:

$$D_{eff} = D_0 n \tau$$

where D_{eff} is the effective molecular diffusivity in a porous medium, D_0 is the molecular diffusivity in water, n is the porosity, and τ is the tortuosity.

Molecular Diffusion Through Injection Interval (Lateral Migration)

The SWIFT model requires that bulk molecular diffusion be input as effective molecular diffusion coefficient (D_{eff}). D_{eff} is derived by multiplying the bulk molecular diffusion coefficient (of the waste constituent having the highest bulk molecular diffusion coefficient (arsenic)) by the Injection Interval porosity and the tortuosity. The Frio D Sand, Frio E&F Sand and the Frio A/B Sand porosity is 28 percent. The tortuosity coefficient is 0.28.

Therefore:

 $\begin{array}{ll} D_{eff} = 1.01 \times 10^{-2} \; ft^2 / day \times 0.28 \times 0.28 = \textbf{7.93} \times \textbf{10}^{-4} \; \textbf{ft}^2 / \textbf{day} \; \text{(Frio D Sand)} \\ D_{eff} = 1.06 \times 10^{-2} \; ft^2 / day \times 0.28 \times 0.28 = \textbf{8.33} \times \textbf{10}^{-4} \; \textbf{ft}^2 / \textbf{day} \; \text{(Frio E\&F Sand)} \\ D_{eff} = 1.05 \times 10^{-2} \; ft^2 / day \times 0.28 \times 0.28 = \textbf{8.24} \times \textbf{10}^{-4} \; \textbf{ft}^2 / \textbf{day} \; \text{(Frio A/B Sand)} \end{array}$



Molecular Diffusion Through Containment Interval (Vertical Migration)

In the vertical transport model (analytical solution), the effective molecular diffusion coefficient (D_{eff}) for transport of waste constituents through the overlying containment interval (above Frio D Sand) was determined by multiplying the free water diffusion coefficient by Containment Interval porosity (0.21) and a tortuosity coefficient (0.21) assumed to be equal to the porosity of the Containment Interval layer shales. In the vertical transport model, the worst-case constituent movement is associated with arsenic.

Therefore:

$$D_{eff} = 1.01 \times 10^{-2} \text{ ft}^2/\text{day} \times 0.21 \times 0.21 = 4.46 \times 10^{-4} \text{ ft}^2/\text{day}$$
 (Frio D Sand)

Molecular diffusion through the containment interval for each of the waste constituents of concern was calculated and is presented on Table 7-8. As stated previously, the waste constituent having the farthest vertical movement through the containment interval is arsenic.

Molecular Diffusion Through a Mud Filled Borehole (Vertical Migration)

The effective molecular diffusion coefficient (D_{eff}) employed to calculate the movement of the waste constituents through a mud-filled borehole was determined by multiplying the free water diffusivity for arsenic (calculated for the Frio D, E&F and A/B Sands), by a tortuosity value of 0.5 and porosity of 0.9 for the drilling mud. This tortuosity value is chosen to reflect the tortuosity of the mud column, where the clay particles provide a substantial tortuosity effect.

Therefore:

$$\begin{array}{ll} D_{eff} = 1.01 \times 10^{\text{-2}} \ ft^2 / day \times 0.50 \times 0.90 = \textbf{4.55} \times \textbf{10}^{\text{-3}} \ \textbf{ft}^2 / \textbf{day} \ (\text{Frio D Sand}) \\ D_{eff} = 1.06 \times 10^{\text{-2}} \ ft^2 / day \times 0.50 \times 0.90 = \textbf{4.77} \times \textbf{10}^{\text{-3}} \ \textbf{ft}^2 / \textbf{day} \ (\text{Frio E\&F Sand}) \\ D_{eff} = 1.05 \times 10^{\text{-2}} \ ft^2 / day \times 0.50 \times 0.90 = \textbf{4.73} \times \textbf{10}^{\text{-3}} \ \textbf{ft}^2 / \textbf{day} \ (\text{Frio A/B Sand}) \end{array}$$

Molecular diffusion through a mud filled borehole for each of the waste constituents of concern were calculated and are presented on Table 7-8. The waste constituent having the farthest vertical movement in a mud filled borehole is arsenic.

7.3.10 Modeled Injection Rates

WDW-397 was officially placed in service on December 11, 2008. Prior to placing the well in service, ExxonMobil performed an extensive stimulation and injected pre-



injection buffer fluids into WDW-397 beginning on April 22, 2008. This pre-operation fluid injection is also incorporated in the demonstration. During 2008, ExxonMobil injected a total of 95,004,430 gallons of liquid (stimulation, treatment and wastewater fluids) into WDW-397. The volume of wastewater injected from December 11, 2008 to December 31, 2008 totals 17,048,690 gallons. For this modeling demonstration, it is assumed that WDW-397 was placed in service on July 1, 2008, and operated continuously at 700 gpm for the remainder of 2008. The total volume injected in the various model demonstrations for 2008 is 185,472,000 gallons, or about twice the volume actually injected into WDW-397. This results in a conservative reservoir pressure demonstration and artificially enlarges the end-of-operations waste plume dimensions. The future injection rate (January 1, 2009 to December 31, 2020) was set at an average injection rate of 1,200 gallons per minute (gpm). This demonstration considers disposal into the authorized Injection Interval at a cumulative injection rate (future) of 1,200 gpm. In addition, this demonstration considers injection into either well (WDW-397 or WDW-398) at a maximum injection rate (future) of 1,200 gpm.

Three nearby injection well operators also utilize the Frio E&F Sand and Frio A/B and commingled Frio C sands for injection purposes. These facilities include Merisol USA LLC (WDW-147 and WDW-319), Lyondell Chemical Company (WDW-148 and WDW-162) and Equistar Chemical Company (WDW-36).

Merisol: The Merisol WDW-147 injection well is completed into the Frio E&F Sand and the Merisol WDW-319 injection well is completed into the commingled Frio A/B Sand and Frio C Sand. WDW-147 was placed in service on August 9, 1979. WDW-319 was placed in service on December 27, 2000. Historical injection at Merisol is allocated accordingly. Future injection (beginning January 1, 2006) at Merisol is allocated at the maximum permit rate of 350 gpm to the Frio E&F Sand Injection Interval (WDW-147) and 350 gpm to the commingled Frio A/B Sand Injection Interval (WDW-319).

Lyondell: Historically, the Lyondell WDW-148 and WDW-162 injection wells were completed into the commingled Frio A/B Sand and Frio C Sand Injection Interval. WDW-148 was placed in service on August 9, 1979. WDW-162 was placed in service on July 28, 1980. WDW-162 was re-completed into the Frio E&F Sand in May 2003. WDW-148 was re-completed into the Frio E&F Sand in April 2004. Historical injection at Lyondell is allocated to the Frio A/B Sand Injection Interval. Injection into WDW-162 after May 2003 is allocated to the Frio E&F Sand. Injection into WDW-148 after April



2004 is allocated to the Frio E&F Sand. Future injection (beginning January 1, 2006) at Lyondell is allocated at the maximum permit rate of 700 gpm to the Frio E&F Sand Injection Interval (WDW-148 and WDW-162).

Equistar: WDW-36 was placed in service in March, 1969. The Equistar WDW-36 injection well was originally completed into the lower portion of the Frio A/B Sand (Frio B sand lobe) and the Frio C Sand. The well was recompleted into the Frio E&F Sand and the upper portion of the Frio A/B Sand (Frio A Sand lobe) in June 1977. Historical injection at Equistar is allocated to the Frio A/B Sand until its re-completion in 1977. At that point, injection is allocated to both the Frio E&F Sand Injection Interval (upper portion of the recompletion interval for Equistar) and the Frio A/B Sand (lower portion of the re-completion interval for Equistar). The full volume is modeled into each interval (i.e., modeled at 100 percent). Note that no cross flow is allowed between the intervals when the well is shut in. Future injection (beginning July 1, 2008) is allocated at the maximum permit rate of 350 gpm to both the Frio E&F Sand Injection Interval (upper portion of the re-completion interval for Equistar) and the commingled Frio A/B Sand and Frio C Sand Injection Interval (lower portion of the recompletion interval for This is conservative, since Equistar's injectate is currently disposed into Lyondell's two wells, and Equistar has no current plans in place to put WDW-36 back into service.

Cobra Operating Co.: The Cobra Operating, Co., Texas Northern Railroad #6 well, located approximately 34,030 feet northeast of the ExxonMobil WDW-397 injection well is permitted as a Class II saltwater injection well. The well is currently completed into the Frio C Sand (based on reported perforation depths and nearby wells with available logs). It is included in the commingled Frio A/B Sand Injection Interval modeling.

Other Injection Wells in Area: In the East Houston area, located along the south side of the Houston Ship Channel, there are several other industrial users of Class I injection wells. This includes the Shell Oil Company WDW-172 and WDW-173 injection wells (WDW-172 was plugged and abandoned in 1990; WDW-172 was plugged and abandoned in 1999) which are located about 4.5 miles east southeast of WDW-397, the Vopak WDW-157 injection well which is located about 5.8 miles east of WDW-397, the Texas Molecular WDW-169 and WDW-249 injection wells located about 6 miles east of WDW-397, and the Dow Hampshire WDW-222 and WDW-223 injection wells located about 6 miles east southeast of WDW-397. Well locations relative to the ExxonMobil

facility location for these Class I injection wells are shown on the structure maps (Plates 4-4, 4-6, 4-7, 4-8 and 4-10). The effects of injection into these off-set injection wells have not been included in the model demonstration. This is justified for several reasons. First, the subject injection wells are located at extended distances to the east of the ExxonMobil facility location. Second, the recent historical rates of injection (2008 and 2009) at each of the subject injection wells are quite low: less than 15 gpm for WDW-157; less than 65 gpm for WDW-169; less than 70 gpm for WDW-249; less than 15 gpm for WDW-222 and less than 35 gpm for WDW-223 (4th Quarter and/or Monthly Injection Reports [December] for 2008 and 2009 for these wells are provided in Appendix C-10). And lastly, two faults are mapped between the ExxonMobil location and the location of these specific injection wells. Moving from west to east from the ExxonMobil facility location, Fault A is downthrown to the east and has up to 100 feet of displacement and Fault B is downthrown to the east and has approximately 200 feet of displacement. Plates 4-3 and 4-16 demonstrate the offset of Faults A and B to the south of the ExxonMobil facility location and Plates 4-2 and 4-15 demonstrate the offset of Fault A to the east of the ExxonMobil injection well locations. Taken individually, neither of the faults have adequate displacement to create a barrier to flow between the subject injection wells and the ExxonMobil injection wells. However, collectively, these faults have substantial off-set and serve as a partial barrier, thus minimizing pressure and flow effects potentially induced by injection at these facilities on injection activities at the ExxonMobil facility.

Copies of the monthly injection rates, as reported to TCEQ for these facilities, are included in Appendix C. An annotated well log from each facility is also included in Appendix C. The SWIFT model requires that injection rate be input in ft³/day. Table 7-9 provides the annual injection rates and volumes in gallons, gallons per minute and cubic feet per day for the offset injection wells. These are the injection rates utilized in the SWIFT lateral no-migration model runs and reservoir pressurization model.

7.3.11 Modeled Brine and Injectate Fluid Densities

Reservoir brine and injected fluid density were calculated for input into the SWIFT model. The SWIFT model requires that the fluid densities be entered in pounds per cubic foot (lb/ft³). Density data was calculated at reservoir conditions of temperature and pressure.

Reservoir Brine Density

Due to substantial fluid loss of 9.0 lb/gal completion brine into the WDW-397 Injection Interval that occurred early in the completion of the well, it was not possible to obtain a



representative formation fluid sample from WDW-397. In addition, due to the large volume of 9.0 lb/gal completion brine utilized when gravel packing the WDW-398 screened interval, it was not possible to obtain a representative formation fluid sample from WDW-398. However, native formation fluid samples were obtained from a number of Class I injection wells completed into the Frio Formation Injection Interval in the Houston, Texas area. The analytical data is included in Appendix C. The analyses of these samples are summarized here:

	Merisol WDW-147 mg/L	Merisol WDW-319 mg/L	Lyondell WDW-148 mg/L	Equistar WDW-36 mg/L	Texas Molecular WDW-169 mg/L	Dow Hampshire WDW-222 mg/L
Sample Depth	6,700 - 6,780	6,850 - 7,260	6,881 - 7,167	6,590 - 6,650	7,103 - 7,415	7,194 - 7,508
Interval	Frio E&F	Frio A/B/C	Frio A/B/C	Frio F	Frio E/F/A/B	Frio E/F/A/B
Calcium	22,500*	1,610	2,740	6,400	2,400	2,200
Magnesium	475	214	340	1,400	480	457
Barium	66	49	44	190	60	63
Strontium	150	85	160	-	110	112
Sodium	-	45,700	39,200	55,664	43,000	39,400
Chloride	60,247	82,000	70,000	63,548	70,400	-
Sulfate	18	654	5	12	<100	•
Iron	-	1,170	-	5	35	61
Alkalinity (HCO ₃)	-	<5	115	99	10	80
рН	7.0	-	7.2	6.7	6.9	6.7
Specific Gravity	1.073 @ 21°C	· -	1.074	1.074	-	1.059 @ 150°F

*NOTE: The value for calcium reported for Merisol WDW-147 is highly suspect. The laboratory reports a value of 22,500 mg/L, but the value is an order of magnitude higher in concentration when compared to the values reported for other nearby injection wells. The actual value may be 2,250 mg/L rather than 22,250 mg/L.

Frio D Sand Reservoir Brine Density

The Merisol facility injection wells are the closest injection wells to the ExxonMobil facility location. The native formation fluids collected from the WDW-147 and WDW-319 injection wells at the time of construction are assumed to be representative of the formation fluid present at the ExxonMobil facility location. As reported above, the Injection Interval (Frio E&F Sand) formation fluid collected from WDW-147 has a specific gravity of 1.073 at 21°C. The equivalent density of the formation fluid is 1.0708 gm/cm³ or 66.85 lb/ft³. The fluid density is converted to 20 °C based on the density properties of water (ρ_{H2O}) (Table 2-28 of Perry's Chemical Engineers' Handbook (Perry, 1979) (Appendix C):



Density of Pure Water

Assuming
$$\frac{\rho_{\text{ff}(20\,^{\circ}\text{C})}}{\rho_{\text{ff}(21\,^{\circ}\text{C})}} = \frac{\rho_{\text{H2O}(20\,^{\circ}\text{C})}}{\rho_{\text{H2O}(21\,^{\circ}\text{C})}}$$
; then, $\rho_{\text{ff}(20\,^{\circ}\text{C})} = \rho_{\text{ff}(21\,^{\circ}\text{C})} \times \frac{\rho_{\text{H2O}(20\,^{\circ}\text{C})}}{\rho_{\text{H2O}(21\,^{\circ}\text{C})}}$

$$\rho_{\rm ff(20^{\circ}C)} = 66.85 \text{ lb/ft}^{3} \times \frac{0.998204 \text{ g/cm}^{3}}{0.997992 \text{ g/cm}^{3}} = 66.86 \text{ lb/ft}^{3}$$

The sodium chloride (NaCl) concentration for the fluid sample from the Frio E&F Sand was 115,911 mg/L or 11.59 percent NaCl and the total dissolved solids (TDS) is estimated to be 118,900 mg/L. It is assumed that the formation fluid present in the Frio D Sand is equivalent to that of the Frio E&F Sand. For purposes of this petition demonstration, the NaCl concentration is assumed be 118,900 mg/L or equal to the TDS content. The formation fluid weight percent for a 118,900 mg/L NaCl solution at standard atmospheric temperature and pressure (SATP) is in actuality 11.03 percent NaCl, calculated based on a correlation of mg/L to weight percent using data on Table 71 of the CRC Handbook of Chemistry and Physics, 58th Edition (CRC, 1979) (Appendix C). For purposes of this petition demonstration, SATP is defined as 20°C (68°F) and 1 atmosphere (14.7 lb/in²). The specific gravity for an 11.03 percent NaCl formation fluid at SATP was determined to be 1.0803. The density at this concentration of NaCl brine (11.03 percent), at SATP was determined to be 1.0784 g/cm³. This is equivalent to a density of 67.32 lb/ft³ [67.32 lb/ft³ = (1.0784 g/cm³)(3.527397 x 10⁻² oz/g)(1.0 lb/16 oz)(1 cm/0.0328084 feet)³].

To determine the density of the formation brine within the Frio D Sand, a density formation volume factor was calculated using the methodology given by Numbere and others (1977). This was used to correct the density of the reservoir brine calculated at standard ambient temperature and pressure (SATP) for reservoir conditions. For gas free water, the formation volume factor, BW, is

$$BW = A + BP + CP^2$$

Where:

A = $0.9947 + (5.8 \times 10^{-6})T + (1.02 \times 10^{-6})T^2$ B = $-4.228 \times 10^{-6} + (1.8376 \times 10^{-8})T - (6.77 \times 10^{-11})T^2$ C = $1.3 \times 10^{-10} - (1.3855 \times 10^{-12})T + (4.285 \times 10^{-15})T^2$ P = pressure at depth in psi T = temperature at depth in °F

The reference BHT at a depth of 6,618 feet subsea (6,628 feet GL or 6,650 feet KB) is 164°F. The static BHP is 2,884 psia (2,869 psi) at 6,618 feet subsea (6,628 feet GL or 6,650 feet KB) for the Frio D Sand in WDW-397.

A salinity correction, BWB, is then calculated for the Frio Formation (Frio D Sand brine using a NaCl value of 11.03 percent):

$$BWB = BW[\{(5.1x10^{-8})P + [(5.47x10^{-6} - 1.95x10^{-10})P](T - 60.0) + [-3.23x10^{-8} + (8.5x10^{-13})P](T - 60)^{2}\}\%NACL + 1]$$

$$BWB = 1.0183$$

The formation fluid densities at reservoir temperatures and pressures are then calculated:

Reservoir formation fluid density = Density at SATP/BWB = 67.32 lb/ft³/1.0183 = 66.11 lb/ft³

Assuming the fluid salinity is 11.03 percent NaCl (conservative assumption that maximizes the densities), the equation yields formation fluid densities of 66.11 lb/ft³ at the 6,618 feet subsea at 164 °F within the Frio D Sand of the Frio Formation Injection Interval.

Frio E&F Sand Reservoir Brine Density

The native formation fluids collected from the WDW-147 and WDW-319 injection wells at the time of construction are assumed to be representative of the formation fluid present at the ExxonMobil facility location. The Injection Interval (Frio E&F Sand) formation fluid collected from WDW-147 has a specific gravity of 1.073 at 21 °C. The equivalent density of the formation fluid is 1.078 gm/cm³ or 66.85 lb/ft³. The fluid density is converted to 20 °C based on the density properties of water (ρ_{H2O}) (Table 2-28 of Perry's Chemical Engineers' Handbook (Perry, 1979) (Appendix C):



Density of Pure Water

$$\rho_{\text{ff}(20 \text{ °C})} = 66.85 \text{ lb/ft}^3 \text{x} \frac{0.998204 \text{ g/cm}^3}{0.997992 \text{ g/cm}^3} = 66.86 \text{ lb/ft}^3$$

The sodium chloride (NaCl) concentration for the fluid sample from the Frio E&F Sand was 115,911 mg/L or 11.59 percent NaCl and the total dissolved solids (TDS) is estimated to be 118,900 mg/L. For purposes of this petition demonstration, the NaCl concentration is assumed be 118,900 mg/L or equal to the TDS content. The formation fluid weight percent for a 118,900 mg/L NaCl solution at standard atmospheric temperature and pressure (SATP) is in actuality 11.03 percent NaCl, calculated based on a correlation of mg/L to weight percent using data on Table 71 of the CRC Handbook of Chemistry and Physics, 58th Edition (CRC, 1979) (Appendix C). The specific gravity for an 11.03 percent NaCl formation fluid at SATP was determined to be 1.0803. The density at this concentration of NaCl brine (11.03 percent), at SATP was determined to be 1.0784 g/cm³. This is equivalent to a density of 67.32 lb/ft³ [67.32 lb/ft³ = (1.0784 g/cm³)(3.527397 x 10⁻² oz/g)(1.0 lb/16 oz)(1 cm/0.0328084 feet)³].

To determine the density of the formation brine within the Frio E&F Sand, a density formation volume factor was calculated using the methodology given by Numbere and others (1977). This was used to correct the density of the reservoir brine calculated at standard ambient temperature and pressure (SATP) for reservoir conditions. For gas free water, the formation volume factor, BW, is

$$BW = A + BP + CP^2$$

Where:

$$A = 0.9947 + (5.8x10^{-6})T + (1.02x10^{-6})T^2$$

$$B = -4.228x10^{-6} + (1.8376x10^{-8})T - (6.77x10^{-11})T^2$$

$$C = 1.3x10^{-10} - (1.3855x10^{-12})T + (4.285x10^{-15})T^2$$

$$P = \text{pressure at depth in psi}$$

$$T = \text{temperature at depth in } ^{\circ}F$$



The reference BHT at a depth of 6,755 feet subsea (6,765 feet GL or 6,787 feet KB) is 169 °F. The static BHP is 2,944 psia (2,929 psi) at 6,755 feet subsea (6,765 feet GL or 6,787 feet KB) for the Frio E&F Sand in WDW-397.

A salinity correction, BWB, is then calculated for the Frio Formation (Frio E&F Sand brine using a NaCl value of 11.03 percent):

$$BWB = BW[\{(5.1x10^{-8})P + [(5.47x10^{-6} - 1.95x10^{-10})P](T - 60.0) + [-3.23x10^{-8} + (8.5x10^{-13})P](T - 60)^{2}\}\%NACL + 1]$$

$$BWB = 1.0197$$

The formation fluid densities at reservoir temperatures and pressures are then calculated:

Reservoir formation fluid density = Density at SATP/BWB = $67.32 \text{ lb/ft}^3/1.0197 = 66.02 \text{ lb/ft}^3$

Assuming the fluid salinity is 11.03 percent NaCl (conservative assumption that maximizes the densities), the equation yields formation fluid densities of 66.02 lb/ft³ at the 6,755 feet subsea (6,765 feet GL or 6,787 feet KB) at 169 °F within the Frio E&F Sand of the Frio Formation Injection Interval.

Frio A/B Sand Reservoir Brine Density

The specific gravity and density of the Frio A/B Sand formation fluid was calculated based on the TDS determined from the September 2000 analysis of Frio brine collected from Merisol WDW-319. Neither a specific gravity measurement, nor a density measurement of the Frio A/B Sand formation fluid was performed as part of the analytical suite. The TDS of the reservoir brine was determined to be 135,000 mg/L. Since 95 percent of the TDS is NaCl, it is reasonable to assume that the reservoir brine density is approximately equivalent to a solution composed of 135,000 mg/L NaCl. The formation fluid weight percent for a 135,000 mg/L NaCl solution at SATP is in actuality 12.40 percent NaCl, calculated based on a correlation of mg/L to weight percent using data on Table 71 of the CRC Handbook of Chemistry and Physics, 58th Edition (CRC, 1979) (Appendix C). The specific gravity for a 12.40 percent NaCl formation fluid at SATP was determined to be 1.0906. The density at this concentration of NaCl brine (12.40 percent), at SATP was determined to be 1.0887 g/cm³. This is equivalent to a density of 67.97 lb/ft³ [67.97 lb/ft³ = (1.0887 g/cm³)(3.527397 x 10⁻² oz/g)(1.0 lb/16 oz)(1 cm/0.0328084 feet)³].

To estimate the density of the formation brine within the Frio A/B Sand, a density formation volume factor was calculated using the methodology given by Numbere and



others (1977). This was used to correct the density of the reservoir brine calculated at SATP for reservoir conditions. For gas free water, the formation volume factor, BW, is

$$BW = A + BP + CP^2$$

Where:

 $A = 0.9947 + (5.8x10^{-6})T + (1.02x10^{-6})T^{2}$ $B = -4.228x10^{-6} + (1.8376x10^{-8})T - (6.77x10^{-11})T^{2}$ $C = 1.3x10^{-10} - (1.3855x10^{-12})T + (4.285x10^{-15})T^{2}$ P = pressure at depth in psi $T = \text{temperature at depth in } ^{\circ}F$

The reference BHT at a depth of 6,990 feet subsea (7,000 feet GL or 7,022 feet KB) is 173°F. The static BHP is 3,047 psia (3,032 psi) at 6,990 feet subsea (7,000 feet GL or 7,022 feet KB) for the Frio A/B Sand in WDW-397.

A salinity correction, BWB, is then calculated for the Frio Formation (Frio A/B Sand brine using a NaCl value of 12.40 percent):

$$BWB = BW[\{(5.1x10^{-8})P + [(5.47x10^{-6} - 1.95x10^{-10})P](T - 60.0) + [-3.23x10^{-8} + (8.5x10^{-13})P](T - 60)^{2}\}\%NACL + 1]$$

$$BWB = 1.0212$$

The formation fluid densities at reservoir temperatures and pressures are then calculated:

Reservoir formation fluid density = Density at SATP/BWB = 67.97 lb/ft³/1.0212 = 66.55 lb/ft³

Assuming the fluid salinity is 12.40 percent NaCl (conservative assumption that maximizes the densities) the equation yields formation fluid densities of 66.55 lb/ft³ at the 6,990 feet subsea (7,000 feet GL or 7,022 feet KB) and 173 °F within the Frio A/B Sand of the Frio Formation Injection Interval.

Light Injectate Fluid Densities

The low-density injectate (up-dip) waste transport model uses an injectate fluid density of 62.43 lb/ft³ at SATP. This is equivalent to a density of 1.00 g/cm³ at SATP, and a specific gravity of 1.00 at SATP.

The density of the low-density injectate at reservoir temperature and pressure in the Frio D Sand was obtained by using the Numbere methodology used above to determine the Frio Formation brine density, assuming a salinity of 0.00 percent. The up-dip waste



transport (low density injectate) model uses an injectate fluid density of 61.54 lb/ft³ at reservoir conditions (164 °F and 2,869 psi) (see Appendix C).

The density of the low-density injectate at reservoir temperature and pressure in the Frio E&F Sand was obtained by using the Numbere methodology used above to determine the Frio Formation brine density, assuming a salinity of 0.00 percent. The up-dip waste transport (low density injectate) model uses an injectate fluid density of 61.45 lb/ft³ at reservoir conditions (169 °F and 2,929 psi) (see Appendix C).

The density of the low-density injectate at reservoir temperature and pressure in the Frio A/B Sand was also obtained by using the Numbere methodology used above, assuming a salinity of 0.00 percent. The up-dip waste transport (low density injectate) model uses an injectate fluid density of 61.38 lb/ft³ at reservoir conditions (173 °F and 3,032 psi) (see Appendix C).

Heavy Injectate Fluid Densities

The Injection Interval pressurization model and heavy-injectate (down-dip) waste transport model uses an injection fluid density of a 1.05 specific gravity Na₂SO₄ solution. At SATP, a 5.5 percent Na₂SO₄ solution has a specific gravity of 1.050 and a density of 1.048 g/cm³ (or 65.43 lb/ft³) (Table 82 of CRC Handbook (1979)). The CRC Handbook data is included in Appendix C.

In order to estimate the density at bottom-hole temperature, an assumption is made that the heavy-density injectate is composed of a 6.93 percent NaCl brine solution. A 5.5 percent sodium sulfate (Na₂SO₄) solution and a 6.93 percent NaCl brine solution have the same approximate density and specific gravity at surface conditions.

The density of the heavy-density injectate at reservoir temperature and pressure in the Frio D Sand was obtained by using the Numbere methodology used above, assuming a salinity of 6.93 percent NaCl brine solution. The high density injectate waste transport model uses an injectate fluid density of 64.34 lb/ft³ at reservoir conditions (164 °F and 2,869 psi) (see Appendix C for the formation volume factor calculations).

The density of the heavy-density injectate at reservoir temperature and pressure in the Frio E&F Sand was obtained by using the Numbere methodology used above, assuming a salinity of 6.63 percent NaCl brine solution. The high density injectate waste transport



model uses an injectate fluid density of **64.25** lb/ft³ at reservoir conditions (169 °F and 2,929 psi) (see Appendix C for the formation volume factor calculations).

The density of the high-density injectate at reservoir temperature and pressure in the Frio A/B Sand was also obtained by using the Numbere methodology used above, assuming a salinity of 6.63 percent NaCl brine solution. The waste high density injectate transport model uses an injectate fluid density of 64.18 lb/ft³ at reservoir conditions (173 °F and 3,032 psi) (see Appendix C for the formation volume factor calculations).

7.3.12 Modeled Brine and Injectate Fluid Viscosities

The formation brine viscosities used in the SWIFT lateral transport and pressurization models are assigned to be that of an 11.03 percent sodium chloride solution in the Frio E&F Sand and that of a 12.40 percent sodium chloride solution in the Frio A/B Sand. The low density injectate is expected to be approximately equivalent to that of fresh water. The high density waste stream is best described as a calcium sulfate (CaSO₄) – sodium sulfate (Na₂SO₄) solution. Each of the subject fluid viscosities and is temperature-dependent, as shown in following paragraphs.

Formation Brine Viscosities

The formation brine viscosities used in the SWIFT lateral transport and pressurization models are assigned to be that of an 11.03 percent sodium chloride solution in the Frio D Sand and Frio E&F Sand and that of a 12.40 percent sodium chloride solution in the Frio A/B Sand. These viscosities are temperature-dependent. This selection maximizes waste movement in the models. The viscosities shown below were determined using a concentration of 11.03 percent sodium chloride, as available in the Fig. D.35 NaCl nomograph provided in Earlougher (Appendix C). The Injection Interval brine viscosity in the Frio D Sand at 164 °F was determined to be **0.507 cP**. The Injection Interval brine viscosity in the Frio E&F Sand at 169 °F was determined to be **0.487 cP**

11.03% NaCl Brine Viscosity

Temperature (°F)	Formation Brine Viscosity (cP)
60	1.35
80	1.06
100	0.84
120	0.71
140	0.60
160	0.51
180	0.46
200	0.41



The viscosities shown below were determined using a concentration of 12.40 percent sodium chloride, as available in the Fig. D.35 NaCl nomograph provided in Earlougher (Appendix C). The Injection Interval brine viscosity at 173 °F was determined to be **0.495 cP**.

12.40% NaCl Brine Viscosity

Temperature (°F)	Formation Brine Viscosity (cP)
60	1.40
80	1.10
100	0.89
120	0.73
140	0.62
160	0.53
180	0.48
200	0.43

Light Injectate Viscosities

The low density injectate is expected to be approximately equivalent to that of fresh water. Therefore, the low density injectate fluid viscosities used in the lateral migration plume model were estimated, based on the equivalent salinity of a fluid having a density of 62.43 lb/ft³ at SATP, and are temperature-dependent. This selection maximizes waste movement in the model. The viscosities shown below were determined using a concentration of 0.00 percent sodium chloride, as available in the Fig. D.35 NaCl nomograph provided in Earlougher (1977, Appendix C). The low density injectate viscosity at 164 °F (Frio D Sand) was determined to be **0.378 cP**. The low density injectate viscosity at 169 °F (Frio E&F Sand) was determined to be **0.364 cP**. The low density injectate viscosity at 173 °F (Frio A/B Sand) was determined to be **0.353 cP**.

Light Injectate (Fresh Water) Viscosity

Temperature (°F)	Freshwater Viscosity (cP)
60	1.12
80	0.86
100	0.68
120	0.57
140	0.46
160	0.38
180	0.34
200	0.30

Heavy Injectate Viscosities

The high density waste stream is best described as a calcium sulfate (CaSO₄) – sodium sulfate (Na₂SO₄) solution. The high density injectate fluid viscosities used in the



Injection Intervals' pressure and heavy-injectate lateral models are assigned to be that of the maximum density injectate of a 5.5 percent Na₂SO₄ solution (1.048 g/cm³ at SATP), and are temperature-dependent. This selection maximizes pressure buildup and post-operational plume movement in the models. The viscosity values calculated below were extrapolated by using a 6.93 percent NaCl brine solution (1.048 g/cm³ at SATP) to approximate viscosity values at various temperatures and concentrations for a 5.5 percent Na₂SO₄ solution. The viscosity values for a 6.93 percent NaCl brine solution (1.048 g/cm³ at SATP) are depicted in the Fig. D.35 NaCl nomograph provided in Earlougher (1977, Appendix C). The high density injectate viscosity at 164 °F (Frio D Sand) was determined to be **0.452 cP**. The high density injectate viscosity at 169 °F (Frio E&F Sand) was determined to be **0.439 cP**. The high density injectate viscosity at 173 °F (Frio A/B Sand) was determined to be **0.428 cP**.

Heavy Injectate (6.93% NaCl Brine) Viscosity

Temperature (°F)	Heavy Injectate Viscosity (cP)
60	1.24
80	0.97
100	0.78
120	0.64
140	0.54
160	0.47
180	0.42
200	0.37

7.3.13 Regional Ground Water Flow

Natural regional hydraulic gradients of deep saline aquifers in the coastal Gulf of Mexico were ascertained during the geology study to be gulfward. The saline waters of the Frio Formation were calculated to move laterally between 0.0 to 1.6 ft/year. Studies reviewed and referenced for compilation of the information on area geology conclude that water movement in many regional deep saline aquifers in the Gulf Coast is extremely slow due to the lack of discharge pathways because of burial and enclosure of sand bodies by fine-grained muds. Original formation pressure gradient data for the Frio Formation in the East Houston area substantiates the lack of a large hydraulic gradient for the basal Frio sands. The southwest (down-dip) direction established for the Frio Formation in Clark (1988), is consistent with the theory of deep basin flows and the physical mechanisms (topographic relief near outcrops and deep basin compaction) identified as contributing to natural formation drift (Bethke and others 1988; Kreitler, 1986). Two reference papers



are provided which support the down-dip gradient value and the gulfward direction of the gradient (Kreitler and Akhter, 1989 and Clark, 1989) and are included in Appendix E.

For the "light-density" plume migration models, the ground water flow velocity was set at **0.0 ft/year**. This was done to ensure that the maximum up-dip injectate plume movement would be realized, since regional ground water (down-dip) flow would act to counter the up-dip force of buoyancy.

For the "high-density" plume movement demonstration, the ground water flow velocity was set at **1.2 ft/year**. This was done to ensure that the maximum down-dip injectate plume movement would be realized. The background velocity of 1.2 ft/yr is conservative given the presence of faults to the southeast of the facility and the presence of the Clinton Dome and South Houston Dome, all of which potentially "slow" the regional ground water flow rate. In addition, lateral facies changes which result in sand pinchouts are also known to occur in the direction of the recharge area, resulting in a background hydraulic gradient which is greatly exaggerated in this demonstration. The background velocity was implemented in the "high-density" plume models by: (1) running the lateral migration model with a 0 ft/yr ground water gradient to account for plume drift due to buoyancy; and (2) shifting the center of mass for the 10,000-year waste plume in the downdip direction by 12,000 feet (10,000 years x 1.2 ft/yr).

7.3.14 Rock and Fluid Compressibilities

The compressibility values were chosen conservatively to maximize the pressure increases in the models. The compressibility value affects the magnitude of the storativity, which has a relationship with the amount of model pressure increase. The smaller the storativity, the greater the pressure increase. Smaller compressibilities also maximize the plume extents. This is accomplished via the coupling equations for porosity and density in SWIFT (Reeves and others, 1986, p. 6). The porosity and fluid density are minimized with decreasing rock and water compressibility. The total compressibility is equal to the compressibility of the formation rock plus the compressibility of the formation fluid. Compressibility values are small (on the order of 10^{-6} psi⁻¹) and the values lie within a relatively small range. Total system compressibility (fluid and rock compressibility) was chosen for water and rock in order to maximize the pressure increases and the plume sizes in the models.



Fluid Compressibility

The brine compressibility for the Injection Interval was calculated using a method provided in Hewlett Packard (1982, p. 94):

Compressibility of water =
$$Cw = \frac{A + BT + CT^2}{1x10^6}$$

A = 3.8546 - (0.000134)(P)

 $B = -0.01052 + (4.77 \times 10^{-7})(P)$

 $C = 3.9267 \times 10^{-5} - (8.8 \times 10^{-10})(P)$

T = temperature in °F

P = pressure in psi

Compressibility brine =

$$Cb = Cw\{[-0.052 + 2.7 \times 10^{-4}(T) - 1.14 \times 10^{-6}(T^2) + 1.121 \times 10^{-9}(T^3)]\% NACL^{0.7} + 1\}$$

For the Frio D Sand, the compressibility of reservoir brine is calculated as follows:

A = 3.4570154

B = -0.009151487

C = 3.67423E-05

%NaCl = 11.03

 $T = 164 \, {}^{\circ}F$

P = 2,869 psi

$Cb = 2.43 \times 10^{-6} / psi^{-1}$

For the Frio E&F Sand, the compressibility of reservoir brine is calculated as follows:

A = 3.455414

B = -0.009099017

C = 3.66455E-05

%NaCl = 11.03

 $T = 169 \, ^{\circ}F$

P = 2,979 psi

$Cb = 2.43 \times 10^{-6} / psi^{-1}$

For the Frio A/B Sand, the compressibility of reservoir brine is calculated as follows:

A = 3.448312

B = -0.009073736

C = 3.65988E-05

%NaCl = 12.40

 $T = 173 \, {}^{\circ}F$

P = 3,032 psi

 $Cb = 2.39 \times 10^{-6} / psi^{-1}$

Rock Compressibility

For the formation compressibilities, a value of 3.2 x 10⁻⁶ psi⁻¹ was approximated for the Injection Interval sands, based on a porosity of 28 percent for the Frio D Sand, the Frio E&F Sand and the Frio A/B Sand. This value was obtained from Hall's correlation for unconsolidated sandstones in Earlougher (1977, p. 229, Fig. D.12) (see Appendix C).

Total System Compressibility

The total system compressibility for the Frio D Sand is the sum of the fluid compressibility $(2.43 \times 10^{-6}/\text{psi}^{-1})$ and rock compressibility $(3.2 \times 10^{-6} \text{ psi}^{-1})$, which is 5.63 x 10^{-6} psi⁻¹. The total system compressibility for the E&F Sand is the sum of the fluid compressibility $(2.43 \times 10^{-6}/\text{psi}^{-1})$ and rock compressibility $(3.2 \times 10^{-6} \text{ psi}^{-1})$, which is 5.63 x 10^{-6} psi⁻¹. The total system compressibility for the A/B Sand is the sum of the fluid compressibility $(2.39 \times 10^{-6}/\text{psi}^{-1})$ and rock compressibility $(3.2 \times 10^{-6} \text{ psi}^{-1})$, which is 5.59 x 10^{-6} psi⁻¹.

7.3.15 Well Index Values

The well index is calculated using the following equation (Reeves and others, 1986; equation 4-3):

$$WI = 2\pi K_s \sum_{k} \frac{\Delta z_k}{\ell n \binom{r_1}{r_w}}$$

where:

 K_s = hydraulic conductivity of the wellbore skin $\Sigma \Delta z$ = sum of the thickness for the model layers

 $|\mathbf{r}| = r_1 = [(\Delta \mathbf{x} \Delta \mathbf{y})/\pi]^{0.5}$

 $\Delta x \Delta y = \text{product of } x \text{ and } y \text{ grid dimensions at the well location}$

 r_w = the well radius

 $\ell n(r_1/r_w) = r_w \{1 + (r_1/r_w)[\ell n (r_1/r_w) - 1]\}/(r_1-r_w)$

For all the models, wellbore skin was ignored and the sand hydraulic conductivity was used.



Frio D Sand

For the Frio D Sand low-density and high-density plume models, the well index was calculated for WDW-397 and WDW-398 using the following values:

 K_s = hydraulic conductivity of wellbore skin = 11.460 ft/day $\Sigma \Delta z$ = sum of the thickness for the model layers = 25 feet $r| = [(\Delta x \Delta y)/\pi]^{0.5} = 14.1$ feet $\Delta x \Delta y$ = product of x and y grid dimensions at the well location = 625 ft² r_w = the well radius = 0.667 feet $\ell n(r_1/r_w) = 2.203$

For the low-density and high-density plume models in the Frio D Sand, the well index for WDW-397 and WDW-398 is as follows:

$$WI = 817.2 \text{ ft}^2/\text{day}$$

For the Frio D Sand pressure increase model, the well index for WDW-397 and WDW-398 was calculated using the following values:

 K_s = hydraulic conductivity of wellbore skin = 3.725 ft/day $\Sigma\Delta z$ = sum of the thickness for the model layers = 25 feet $r|=[(\Delta x \Delta y)/\pi]^{0.5}=14.1$ feet $\Delta x \Delta y$ = product of x and y grid dimensions at the well location = 625 ft² r_w = the well radius = 0.667 feet $\ell n(r_1/r_w) = 2.203$

For the Frio D Sand pressure increase model, the well index for WDW-397 and WDW-398 is as follows:

$$WI = 265.6 \text{ ft}^2/\text{day}$$

Frio E&F Sand

For the Frio E&F Sand low-density and high-density plume models, the well index was calculated for WDW-397 and WDW-398 using the following values:

 K_s = hydraulic conductivity of wellbore skin = 11.915 ft/day $\Sigma\Delta z$ = sum of the thickness for the model layers = 150 feet $r|=[(\Delta x\Delta y)/\pi]^{0.5}=14.1$ feet $\Delta x\Delta y$ = product of x and y grid dimensions at the well location = 625 ft² r_w = the well radius = 0.667 feet $\ell n(r_1/r_w) = 2.203$



For the low-density and high-density plume models in the Frio E&F Sand, the well index for WDW-397 and WDW-398 is as follows:

$$WI = 5,097.6 \text{ ft}^2/\text{day}$$

For the Frio E&F Sand pressure increase model (high-density injectate), the well index for WDW-397 and WDW-398 was calculated using the following values:

 K_s = hydraulic conductivity of wellbore skin = 3.872 ft/day $\Sigma\Delta z$ = sum of the thickness for the model layers = 150 feet $r|=[(\Delta x\Delta y)/\pi]^{0.5}=14.1$ feet $\Delta x\Delta y$ = product of x and y grid dimensions at the well location = 625 ft² r_w = the well radius = 0.667 feet $\ell n(r_1/r_w) = 2.203$

For the Frio E&F Sand pressure increase model, the well index for WDW-397 and WDW-398 is as follows:

$$WI = 1,656.5 \text{ ft}^2/\text{day}$$

Frio A/B Sand

For the Frio A/B Sand low-density and high-density plume models, the well index was calculated for WDW-397 and WDW-398 using the following values:

 K_s = hydraulic conductivity of wellbore skin = 11.816 ft/day $\Sigma \Delta z$ = sum of the thickness for the model layers = 125 feet r_s = $[(\Delta x \Delta y)/\pi]^{0.5}$ = 14.1 feet $\Delta x \Delta y$ = product of x and y grid dimensions at the well location = 625 ft² r_w = the well radius = 0.667 feet $\ell n(r_1/r_w)$ = 2.203

For the low-density and high-density plume models in the Frio A/B Sand, the well index for WDW-397 and WDW-398 is as follows:

$$WI = 4,212.7 \text{ ft}^2/\text{day}$$

For the Frio A/B Sand pressure increase model, the well index for WDW-397 and WDW-398 was calculated using the following values:

 K_s = hydraulic conductivity of wellbore skin = 3.840 ft/day $\Sigma\Delta z$ = sum of the thickness for the model layers = 125 feet rbar = $[(\Delta x \Delta y)/\pi]^{0.5}$ = 14.1 feet $\Delta x\Delta y$ = product of x and y grid dimensions at the well location = 625 ft² r_w = the well radius = 0.667 feet $\ell n(r_1/r_w)$ = 2.203



For the Frio A/B Sand pressure increase model, the well index for WDW-397 and WDW-398 is as follows:

$WI = 1,369.0 \text{ ft}^2/\text{day}$

In order to be conservative, well index values were employed in the modeling demonstration which were smaller (72 percent of the calculated value) than the calculated values. With all other parameters being equal, a higher well index value lessens the derived wellbore pressure and brings it closer to the grid block pressure value, while a lower index value has the opposite effect. The following well index values were utilized in the various SWIFT model runs:

	Frio D Sand	
Well	Well Index Value	Well Index Value
	(hydraulic conductivity = 11.460 ft/day)	(hydraulic conductivity = 3.725 ft/day)
WDW-397	589.9	191.8
WDW-398	589.9	191.8

Frio E&F Sand			
Well	Well Index Value	Well Index Value	
	(hydraulic conductivity = 11.915 ft/day)	(hydraulic conductivity = 3.872 ft/day)	
WDW-397	3,680.1	1,195.9	
WDW-398	3,680.1	1,195.9	

Frio A/B Sand			
Well	Well Index Value (hydraulic conductivity = 11.816 ft/day)	Well Index Value (hydraulic conductivity = 3.840 ft/day)	
WDW-397	3,041.2	988.4	
WDW-398	3,041.2	988.4	

7.3.16 Boundary Conditions

The review of the geologic study area suggests that the Injection Interval is laterally continuous across the local study area. However, a series of southwest-to-northeast trending parallel faults located to the southeast of the ExxonMobil facility location, collectively serve to partially bound the reservoir. The lateral transmissivity of these faults (Faults A, A' and B) is discussed in detail in Section 4.2.6.

In the lateral transport models for the Frio E&F Sand light density waste plume, Frio E&F Sand heavy density waste plume, Frio A/B Sand light density waste plume and Frio A/B Sand heavy density waste plume, all of the lateral boundaries are "open" to



maximize waste plume movement. This is accomplished by imposing transmissive Carter-Tracy boundaries on the sides using the same transmissivities and porosity-thickness values that are used throughout the model. Flow is allowed to move equally across the lateral boundaries by assigning a SWIFT input variable VAB (card R1-30) of 1.0.

In the lateral transport model for the Frio D Sand light density waste plume and Frio D Sand high density waste plume, the southeast (bottom edge) lateral boundary is closed and the remaining three (3) sides are "open." The distance to the closed boundary from the WDW-397 injection well in the Frio D Sand SWIFT models is 7,625 feet, which is the approximate distance to the location of Fault B. As discussed in Section 4.2.6., displacement along Fault B is sufficient to displace the Frio D Sand against low permeability shale to the southeast of the injection well location. Although Fault A passes at a closer proximity to the ExxonMobil injection well location, displacement along Fault A is minimal (on the order of 20 feet), and sand-to-sand contact is maintained across the fault trace. For the boundary which parallels the fault traces (approximate location of Fault B), the boundary is closed by assigning a SWIFT input variable VAB (card R1-30) of 0.0.

As discussed in the previous paragraph, a series of parallel faults located to the southeast of the ExxonMobil facility location collectively serve to partially bound (Frio E&F and Frio A/B Sands) or completely bound (Frio D Sand) the reservoir to the southeast. In the reservoir pressure buildup models for the Frio D Sand, Frio E&F Sand and Frio A/B Sand, the lateral boundaries are "open" on three (3) sides and closed along the model boundary which parallels the approximate location of Fault B (see Section 4.2.6). This is accomplished by imposing transmissive Carter-Tracy boundaries on three (3) of the sides using the same transmissivities and porosity-thickness values that are used throughout the model. Flow is allowed to move equally across these lateral boundaries by assigning a SWIFT input variable VAB (card R1-30) of 1.0. For the boundary which parallels the fault traces, the boundary is closed by assigning a SWIFT input variable VAB (card R1-30) of 0.0. This prevents fluid movement across this boundary.

Permeability-Thickness and Porosity-Thickness

The aquifer transmissivity, Kh, and porosity thickness, ϕ h, were calculated for the lateral migration models and reservoir pressure models as given below.



For the Frio D Sand, the Carter-Tracy boundary inputs were calculated using the following values:

```
Kh = (11.460 \text{ ft/day})(25 \text{ ft}) = 286.5 \text{ feet}^2/\text{day} (for the lateral plume model)
Kh = (3.725 \text{ ft/day})(25 \text{ ft}) = 93.1 \text{ feet}^2/\text{day} (for the pressure buildup model)
\phi h = (0.28)(25 \text{ feet}) = 7 \text{ feet}
```

For the Frio E&F Sand, the Carter-Tracy boundary inputs were calculated using the following values:

```
Kh = (11.915 \text{ ft/day})(150 \text{ ft}) = 1,787.3 \text{ feet}^2/\text{day} (for the lateral plume model)
Kh = (3.872 \text{ ft/day})(150 \text{ ft}) = 580.8 \text{ feet}^2/\text{day} (for the pressure buildup model)
\phi h = (0.28)(150 \text{ feet}) = 42 \text{ feet}
```

For the Frio A/B Sand, the Carter-Tracy boundary inputs were calculated using the following values:

Kh =
$$(11.816 \text{ ft/day})(125 \text{ ft}) = 1,477.0 \text{ feet}^2/\text{day}$$
 (for the lateral plume model)
Kh = $(3.840 \text{ ft/day})(125 \text{ ft}) = 480.0 \text{ feet}^2/\text{day}$ (for the pressure buildup model)
 $\phi h = (0.28)(125 \text{ feet}) = 35 \text{ feet}$

Equivalent Aquifer Radius

For purposes of this discussion, it is important to distinguish between the term "reservoir" and the term "aquifer." The reservoir is that portion of the system for which the simulation is desired. The aquifer is the area outside the reservoir that provides boundary conditions for the reservoir. The radius of the reservoir (r_e) for a Cartesian geometry is typically chosen as the radius of a circle of equal surface area. The radius of the aquifer (r_q) may be chosen to be either finite or infinite (HIS GeoTrans, 2000). For this model demonstration, a finite equivalent aquifer radius or RAQ (card R1-31) was assigned. The RAQ value was derived by determining the radius of a circle of surface area equal to the width of the SWIFT model multiplied by three (3) and length of the SWIFT model multiplied by three (3). Within this approximate area, "aquifer" properties are expected to mimic the modeled "reservoir" properties. The Frio E&F Sand and Frio A/B Sand lateral migration models are 68,000 feet wide and 70,000 feet in length. Thus,



$$RAQ = \pi r^2 = (68,000 \text{ feet x 3})(70,000 \text{ feet x 3})$$

 $RAQ = 116,775 \text{ feet}$

The Frio D Sand lateral migration model is 70,250 feet wide and 60,000 feet in length. Thus,

$$RAQ = \pi r^2 = (70,250 \text{ feet x 3})(60,000 \text{ feet x 3})$$

 $RAQ = 109,887 \text{ feet}$

The Frio D Sand, Frio E&F Sand and Frio A/B Sand reservoir pressurization models are 68,000 feet wide and 48,000 feet in length. Thus,

$$RAQ = \pi r^2 = (68,000 \text{ feet x 3})(48,000 \text{ feet x 3})$$

 $RAQ = 96,699 \text{ feet}$

Angle of Influence

The angle of influence, THETAQ (card R1-31), was assigned to be 360 degrees in the lateral migration model for the Frio E&F Sand and the Frio A/B Sand, based on the location of the injection wells with respect to the model boundaries (aquifer-influence boundaries).

The angle of influence, THETAQ (card R1-31), was assigned to be 270 degrees in the reservoir pressurization models for the Frio D Sand, the Frio E&F Sand and the Frio A/B Sand, based on the location of the injection wells with respect to the model boundaries (aquifer-influence boundaries).

7.3.17 Coefficient of Thermal Expansion

For the Frio D Sand, the initial reservoir temperature at the reference depth of 6,618 feet subsea (6,628 feet GL or 6,650 feet KB) was estimated to be 164 °F. For the Frio E&F Sand, the initial reservoir temperature at the reference depth of 6,755 feet subsea (6,765 feet GL or 6,787 feet KB) was estimated to be 169 °F. For the Frio A/B Sand, the initial reservoir temperature at the reference depth of 6,990 feet subsea (7,000 feet GL or 7,022 feet KB) was estimated to be 173 °F. Based on these temperature values, the coefficient of thermal expansion of the fluid based on Reeves and others (1986, p. 14, Figure 3-1) (see Appendix J) is approximately 0.0003 °F⁻¹. The value of 0.0003 °F⁻¹ is appropriate because it lies within the range given for experimental data as bracketed by the constant



values of 0.0002 °F⁻¹ and 0.0005 °F⁻¹ given in Figure 3-1 of Reeves and others (1986). Although a coefficient of thermal expansion value of 0.0003 °F⁻¹ is appropriate for the ExxonMobil facility SWIFT model runs, a value of **0.00** °F⁻¹ is utilized to be conservative.

7.3.18 Fluid and Rock Heat Capacities

The fluid heat capacity input is only used if the equations for heat flow are being solved. In the simulations, only the brine and pressure equations are solved. The value of 1.0 Btu/lb-°F was input for completeness and has no impact on the SWIFT calculated pressure or brine concentration.

The rock heat capacity input is only used if the equations for heat flow are being solved. In the simulations, only the brine and pressure equations are solved. The value of 1.0 Btu/ft³-oF was input for completeness and has no impact on the SWIFT calculated pressure or brine concentration.

7.3.19 Thermal Conductivity of the Fluid Saturated Porous Medium

The thermal conductivity of the fluid saturated porous medium in the x, y and z directions was assigned to be 116 Btu/ft-d-°F. This input is only used if the equations for heat flow are being solved. In the ExxonMobil facility simulations, only the brine and pressure equations are solved. The value of 116 Btu/ft-d-°F was input for completeness and has no impact on the SWIFT calculated pressure or brine concentration.

7.3.20 Solid Particle Density of the Formation

The solid particle density of the formation is chosen to be 165 lb/ft³. This input is only used if the equations for heat flow or radionuclide movement are being solved. In the ExxonMobil facility simulations, only the brine and pressure equations are solved. The value of 165 lb/ft³ was input for completeness and has no impact on the SWIFT calculated pressure or brine concentration.

7.3.21 Gridding Scheme and Gridded Area

Plate 7-1 depicts the grid employed for lateral migration modeling for the Frio D Sand and the Frio E&F Sand and Frio A/B Sand. There are 125 grid blocks in the X direction and 110 grid blocks in the Y direction for the low density lateral migration model for the Frio D Sand. The model distance is 70,250 feet along the X axis and 60,000 feet along



the Y axis. The gridding scheme for both the Frio D Sand low density lateral migration modeling and the high density lateral migration modeling is as follows:

X SPACING

3000.0 20*750.0 8*500.0 2*246.0 100.5 75.0 50.0 25.0 50.0 75.0 95.0 13*185.0 95.0 75.0 50.0 25.0 2*50.0 100.0 187.5 21*500.0 45*750.0

Y SPACING

12*500 5*250.0 150.0 100.0 62.5 50.0 25.0 50.0 80.0 3*145.0 80.0 50.0 25.0 50.0 72.5 2*110.0 300.0 21*500.0 54*750.0

WDW-397 is in the 55th block in the X direction and the 22nd block in the Y direction. The distance to WDW-397 from the 0, 0 coordinate is 25,600 feet in the X direction and 7,625 feet in the Y direction. WDW-398 is in the 35th block in the X direction and the 30th block in the Y direction. The distance to WDW-398 from the 0, 0 coordinate is 22,730 feet in the X direction and 8,345 feet in the Y direction.

There are 115 grid blocks in the X direction and 122 grid blocks in the Y direction for the low density lateral migration models for the Frio E&F Sand and the Frio A/B Sand. The model distance is 68,000 feet along the X axis and 70,000 feet along the Y axis. The gridding scheme for the Frio E&F Sand and the Frio A/B Sand low density lateral migration modeling is as follows:

X SPACING

35*750.0 8*500.0 197.5 150.0 100.0 50.0 25.0 50.0 100.0 145.0 7*275.0 145.0 100.0 50.0 25.0 50.0 100.0 137.5 150.0 10*500.0 39*750.0

Y SPACING

25*750.0 13*500 217.5 150.0 100.0 50.0 25.0 50.0 100.0 160.0 5*175.0 160.0 100.0 50.0 25.0 50.0 100.0 137.5 20*500.0 43*750.0

WDW-397 is in the 62nd block in the X direction and the 55th block in the Y direction. The distance to WDW-397 from the 0, 0 coordinate is 33,300 feet in the X direction and 27,300 feet in the Y direction. WDW-398 is in the 48th block in the X direction and the 43rd block in the Y direction. The distance to WDW-398 from the 0, 0 coordinate is 30,760 feet in the X direction and 25,780 feet in the Y direction.

Plate 7-2 depicts the grid employed for high density lateral migration modeling for the Frio E&F Sand and Frio A/B Sand. There are 113 grid blocks in the X direction and 129



grid blocks in the Y direction. The model distance is 68,000 feet along the X axis and 70,000 feet along the Y axis. The gridding scheme for Frio E&F Sand and Frio A/B Sand high density lateral migration modeling is as follows:

X SPACING

56*750.0 7*500.0 190.0 2*150.0 2*100.0 50.0 25.0 50.0 100.0 220.0 100.0 50.0 25.0 50.0 100.0 140.0 2*200.0 14*500.0 18*750.0

Y SPACING

18*750.0 13*500 3*245.0 2*125.0 3*100.0 50.0 25.0 50.0 2*100.0 7*150.0 2*235.0 7*150.0 2*100.0 50.0 25.0 50.0 100.0 150.0 3*355.0 680.0 58*750.0

WDW-397 is in the 76th block in the X direction and the 64th block in the Y direction. The distance to WDW-397 from the 0, 0 coordinate is 46,797.5 feet in the X direction and 24,447.5 feet in the Y direction. WDW-398 is in the 70th block in the X direction and the 41st block in the Y direction. The distance WDW-398 from the 0, 0 coordinate is 46,252.5 feet in the X direction and 21,352.5 feet in the Y direction.

Plate 7-3 depicts the grid employed for **pressure modeling** for the Frio D Sand, Frio E&F Sand and Frio A/B Sand. There are 125 grid blocks in the X direction and 94 grid blocks in the Y direction. The model distance is 68,000 feet along the X axis and 48,000 feet along the Y axis. The gridding scheme for the Frio D Sand, Frio E&F Sand and Frio A/B Sand pressure modeling is as follows:

X SPACING

21*750.0 8*500.0 2*246.0 100.5 75.0 50.0 25.0 50.0 75.0 95.0 13*185.0 95.0 75.0 50.0 25.0 2*50.0 100.0 187.5 21*500.0 45*750.0

Y SPACING

12*500.0 5*250 150.0 100.0 62.5 50.0 25.0 50.0 80.0 3*145.0 80.0 50.0 25.0 50.0 72.5 2*110.0 300.0 21*500 38*750.0

WDW-397 is in the 55th block in the X direction and the 22nd block in the Y direction. The distance to WDW-397 from the 0, 0 coordinate is 23,350 feet in the X direction and 7,625 feet in the Y direction. WDW-398 is in the 35th block in the X direction and the 30th block in the Y direction. The distance to WDW-398 from the 0, 0 coordinate is 20,480 feet in the X direction and 8,345 feet in the Y direction.



7.3.22 SWIFT Model Reference Point and Grid Block Centers

Frio D Sand: For the Frio D Sand reservoir modeling, a model reference point was selected in the middle of the Frio D Sand within the Injection Interval at the ExxonMobil facility location. The top of the Frio D Sand is present at a depth of about 6,603 feet below sea level (subsea); 6,613 feet relative to ground level (GL)); or about 6,635 feet KB. A depth of 6,618 feet subsea (6,628 feet GL or 6,650 feet KB) was chosen as the reference depth for the depth specific SWIFT model parameters for the Frio D Sand.

For the Frio D Sand SWIFT model runs, the depth to the center of the grid block at which WDW-397 is located was set at 6,618 feet subsea. For a model reservoir thickness of 25 feet, the top of the grid block at the well location is at 6,605 feet subsea.

Frio E&F Sand: For the Frio E&F Sand reservoir modeling, a model reference point was selected near the middle of the Frio E&F Sand within the Injection Interval at the ExxonMobil facility location. The top of the Frio E&F Sand is present at a depth of about 6,680 feet subsea (6,690 feet GL; 6,712 feet KB). A depth of 6,755 feet subsea (6,765 feet GL or 6,787 feet KB) was chosen as the reference depth for the depth specific SWIFT model parameters for the Frio E&F Sand.

For the Frio E&F Sand SWIFT model runs, the depth to the center of the grid block at which WDW-397 is located was set at 6,755 feet subsea. For a model reservoir thickness of 150 feet, the top of the grid block at the well location is at 6,680 feet subsea.

Frio A/B Sand: For the Frio A/B Sand reservoir modeling, a model reference point was also selected near the middle of the Frio A/B Sand. The top of the Frio A/B Sand is present at a depth of about 6,928 feet subsea (6,938 feet GL; or about 6,960 feet KB). A depth of 6,990 feet subsea (7,000 feet GL or 7,022 feet KB) was chosen as the reference depth for the depth specific SWIFT model parameters for the Frio A/B Sand.

For the Frio A/B Sand SWIFT model runs, the depth to the center of the grid block at which WDW-397 is located was set at 6,990 feet subsea. For a model reservoir thickness of 125 feet, the top of the grid block at the well location is at 6,928 feet subsea.



7.3.23 Time Step Allocation and Model Solution Method

The direct solver option was used for the SWIFT models. Time steps were specified to be small initially, and then were allowed to increase over time. In some cases, time stepping was allowed to vary automatically within specified limits.

During the stabilization period, the smallest automatic time step allowed was 0.01 days, with a maximum of 30 days for each SWIFT model. During injection for the pressure buildup and lateral migration plume models, the smallest time steps allowed was 1.0 day, which was allowed to automatically increase to maximums of 30 days. After injection ceased, the automatic time step was as small as 1.0 day initially, and then allowed to increase over time to a maximum of 10,000 days. For the pressure model, after injection ceases, the smallest time step was maintained at 1.0 day, and the maximum time step was maintained at 30 days.

7.3.24 Stabilization Period

The length of the stabilization period for each the ExxonMobil facility model was chosen to be 10,000 days. Automatic time stepping was allowed to take incrementally larger time steps from 0.01 days to 30 days until the 10,000-day stabilization period ended.

7.3.25 Darcy Velocity

During the SWIFT model stabilization period, small residual background velocity gradients occur. These remnant velocity values are inherently present due to the variable structure nature (variable dip in X and/or Y direction) of the models, and decrease in magnitude through time. The resultant X and Y Darcy velocity values and directional vectors from the pre-injection stabilization periods for the light injectate model after 10,000 days are included as Figures 7-4 (Frio D Sand Migration Model) and 7-5 (Frio E&F Sand Migration Model) and 7-6 (Frio A/B Sand Migration Model). The contour/vector maps illustrate the small residual background velocity gradient present in the SWIFT models prior to initiating injection.

The 10,000-year light plume movement distances for the Injection Interval models were not adjusted to account for the resultant background velocities at the end of the 10,000-day stabilization period. The Darcy velocity from the Injection Interval velocity maps (Figure 7-4, Figure 7-5 and Figure 7-6) is small, and on the order of approximately 3.0 x 10^{-5} ft/day (average), within the area of light density plume movement. The Darcy velocity (in ft/day) was converted to an average linear velocity by dividing by the



Injection Interval's porosity value (28 percent). The linear movement over the 10,000-year period was calculated to be approximately 391 feet. This distant is negligible (less than 1.0 percent of up-dip plume movement distance) given the extent of the 10,000-year plume dimensions.

The Darcy velocity from the Injection Interval velocity maps (Figure 7-7 and Figure 7-8) for the 10,000-year heavy plume movement demonstrate the negligible background velocities at the end of the 10,000-day stabilization period. The Darcy velocity (in ft/day) was converted to an average linear velocity by dividing by the Injection Interval's porosity value (28 percent). The average Darcy velocity in the updip direction (x-direction) in the Frio E&F Sand (SWIFT Model ExMob_EF HiDens) is small, and on the order of 2.36 x 10⁻⁵ ft/day. The linear movement over the 10,000-year period was calculated to be approximately 308 feet. This distant is negligible (less than 1.0 percent of heavy density plume movement distance) given the extent of the 10,000-year plume dimensions. The average Darcy velocity in the updip direction (x-direction) in the Frio A/B Sand (SWIFT Model ExMob_AB HiDens) is 2.33 x 10⁻⁵ ft/day. The linear movement over the 10,000-year period was calculated to be approximately 304 feet. Again, this distance is negligible (less than 1.0 percent of heavy density plume movement distance) given the extent of the 10,000-year plume dimensions.

7.3.26 Flowing and Static Bottom-Hole Pressure Data

Flowing and static BHP data for the Frio Formation Injection Interval were gathered from historical fall-off test analyses of the nearby Merisol Class I injection wells. The historical static BHP data suggests that there has been very little pressure buildup in the Frio Formation Injection Interval due to the operation of the subject Class I injection wells. The initial static BHP values for the ExxonMobil WDW-397 injection well are discussed in Section 7.3.3.

Flowing BHPs measured during fall-off testing of the nearby WDW-147 and WDW-319 injection wells are shown on a table included in Appendix C (Table 2-14 from the Merisol 2000 HWDIR Exemption Petition Reissuance Request prepared by Sandia Technologies, LLC, 2000). These data illustrate the viability of the Injection Interval sands with respect to disposal. These data suggest that there has been very little reservoir pressure buildup for the historical period of injection at the facility.



7.3.27 Nearby Oil and Gas Production

Hydrocarbons are actively produced within the area of interest surrounding the ExxonMobil facility refinery. However, all of the active production is from much deeper horizons. There is no nearby oil and gas production from the Frio Formation Injection Interval. Therefore, nearby oil and gas production will have no effect on the SWIFT model predicted lateral plume movement or predicted reservoir pressure buildup.

Injection Interval pressurization models were run to estimate reservoir pressure at the end-of-operation in the Frio D Sand, the Frio E/F Sand and the Frio AB Sand. The Injection Interval pressurization models use the minimum flow capacity (hydraulic conductivity) and maximum injectate density and viscosities. Injection Interval pressure buildup is determined by subtracting the initial Injection Interval pressures (10,000 days) from the Injection Interval pressures at the time of interest during the operational period. The simulated pressure buildup is indicative of the formation buildup outside the wellbore. A Table of Contents is included at the beginning of Appendix E which lists the pressure buildup cases by injection sand as well as showing the input and output file names for each of the model runs.

7.4.1 Cone of Endangering Influence

The cone of endangering influence (COI) is defined to be "the potentiometric surface area around the injection well within which increased Injection Zone pressures caused by injection of wastes would be sufficient to drive fluids into a USDW or a fresh water aquifer." The SWIFT model was used to determine the ExxonMobil pressure buildup and COI for this application. SWIFT models the pressure increase that will be created in the Injection Interval sands during, and at the end of the operational life of the ExxonMobil injection wells.

The methodology used in this petition for calculating the Cone of Endangering Influence (COI) was developed by E. I. du Pont de Nemours and Company (DuPont) for its injection well sites, and it is also generally consistent with previous methods (Price, 1971; Johnston and Greene, 1979; Barker, 1981; Collins, 1986; Davis, 1986; Johnston and Knape, 1986; Warner and Syed, 1986; Clark and others, 1987; Warner, 1988). The basic underlying assumption in the approach is that in the absence of naturally-occurring, vertically transmissive conduits (faults and fractures), the only potential pathway between the Injection Zone and USDW is through an artificial penetration (active or inactive oil and gas well(s). In order to pose a potential threat to a USDW (i.e., pressure build-up from injection operations must be sufficient to drive fluids into a USDW), the pressure increase in the Injection Zone would have to be greater than the pressure necessary to displace the material residing within the borehole. This pressure is defined as the allowable pressure build-up. At the

ExxonMobil facility location, a minimum 9.0 1b/gal mud is considered to be a conservative wellbore fluid (see Section 8.0).

The initial step in calculating the allowable pressure build-up (Cone of Influence) for the injection sands at the ExxonMobil site involved determining the maximum pressure build-up gradient. The formation pressure gradient of the injection sand (Frio D Sand for this calculation) is calculated by dividing the static BHP pressure by the depth where the pressure was estimated. As discussed in Section 7.3.3, the static BHP in the Frio E&F Sand at at reference depth of 6,628 feet GL is 2,884 psia. The formation gradient for the Frio D Sand is therefore equal to 0.433 psi/ft [((2,884 psia - 14,7 psi)/6,628 ft GL) = 0.433 psi/ft].

The maximum pressure build-up gradient is calculated by subtracting the original formation pressure gradient from a conservative 9.0 1b/gal mud column gradient, and is demonstrated by the following equation.

$$P_{max} = G_m - G_{fm}$$

where:

 P_{max} = Maximum Pressure Build-up Gradient

G_m = Mud Column Gradient (from Barker, 1981)

 $= (0.052 \text{ gal/ft-in}^2) (9.0 \text{ lb/gal}) = 0.468 \text{ psi/ft}$

G_{fm} = Formation Pressure Gradient

= 0.433 psi/ft (See discussion above)

Therefore:

$$P_{\text{max}} = (0.468 \text{ psi/ft}) - (0.433 \text{ psi/ft}) = 0.035 \text{ psi/ft}$$

Therefore, 0.035 psi/ft is considered to be a maximum pressure build-up gradient allowed in the injection sands prior to possible fluid movement initiation. At a reference depth of 6,628 feet GL (Frio D Sand), and allowing for 50 feet of fall back for the mud column, the reservoir pressure increase at an abandoned well with 9.0 lb/gal mud in the borehole would have to exceed 230 psi (6,578 ft x 0.035 psi/ft = 230.0 psi) before any upward movement of fluid would be possible. At a reference depth of 6,765 feet GL (Frio E&F Sand), and allowing for 50 feet of fall back for the mud column, the reservoir pressure increase at an abandoned well with 9.0 lb/gal mud in the borehole would have to exceed 235 psi (6,715 ft x 0.035 psi/ft = 235.0 psi) before any upward movement of fluid would



be possible. At a reference depth of 7,000 feet GL (Frio A/B Sand), and allowing for 50 feet of fall back for the mud column, the reservoir pressure increase at an abandoned well with 9.0 lb/gal mud in the borehole would have to exceed 243 psi (6,950 ft x 0.035 psi/ft = 243.3 psi) before any upward movement of fluid would be possible.

Another mechanism which contains waste fluid in the Injection Zone at an abandoned well is borehole collapse. It is well documented that the geologically young and unconsolidated sediments of the Gulf Coast Basin tend to slough and swell, and that uncased wells in this region of Texas commonly squeeze shut within a matter of hours or days (Johnson, 1986; Clark and others, 1991). In order to be conservative, however, no borehole collapse is assumed for abandoned boreholes.

In addition to the mud hydrostatic head and borehole collapse, a hydrologic barrier related to the strength of the drilling mud must be overcome before formation fluid can move upward through the borehole. When mud is allowed to remain quiescent for a period of time, a gel develops (Johnston and others, 1986). Until the structure of the mud gel is disrupted, the mud will resist displacement. As reported by Johnston and others (1986), drilling mud gel strengths can range from 25 to 120 pounds per 100 square feet. A copy of the relevant portion of the Johnston and others (1986) reference is included in Appendix D. Assuming a low gel strength, a mud plug with a gel strength of 25 pounds per 100 square feet, with a 6,578-foot mud column (reference depth in Frio D Sand less 50 feet of fall back of the mud column) in a borehole with an average diameter of 10.75 inches (conservative borehole size) should be capable of resisting a pressure of at least an additional 51 psi [(0.00333)(25)(6,578)/10.75]. A 6,715-foot mud column (reference depth in Frio E&F Sand less 50 feet of fall back of the mud column) in a borehole with an average diameter of 10.75 inches (conservative borehole size) should be capable of resisting a pressure of at least an additional 52 psi [(0.00333)(25)(6,715)/10.75]. A 6,950-foot mud column (reference depth in Frio A/B Sand less 50 feet of fall back of the mud column) in a borehole with an average diameter of 10.75 inches (conservative borehole size) should be capable of resisting a pressure of at least an additional 54 psi [(0.00333)(25)(6,950)/10.75].

Therefore, for the Frio D Sand, the hydrostatic weight of the mud to be overcome (230 psi), probable borehole closure (not included in this calculation), and the strength of the mud gel (51 psi) total to a pressure needed to initiate fluid movement of **281 psi** (230 psi + 51 psi) in a worst care borehole in the ExxonMobil AOR. Similarly, the pressure



needed to initiate fluid movement in a worst case borehole which penetrates the Frio E&F Sand would be **287** psi (235 psi to 52 psi). The pressure needed to initiate fluid movement in a worst case borehole which penetrates the Frio A/B Sand would be **297** psi (243 psi to 54 psi).

Therefore, for purposes of this demonstration, the COI for the ExxonMobil AOR is defined as that area around the ExxonMobil injection well(s) within which the modeled reservoir pressure increase due to injection operations exceeds **281 psi**.

7.4.2 SWIFT ExMob_Dprs Pressure Model

Reservoir pressure buildup in the Frio D Sand was considered for three (3) different scenarios. Although WDW-398 is not, and will not be completed to inject into the Frio D Sand, WDW-398 was incorporated into the Frio D Sand pressure modeling scenarios to The first scenario (ExMob Dprs A) assumed all future injection be conservative. (January 1, 2009 to December 31, 2020) into the Frio D Sand will occur only in WDW-397 at 360 gpm. The second scenario (ExMob_Dprs_B) assumes all future injection (January 1, 2009 to December 31, 2020) into the Frio D Sand will occur only in WDW-398 at 360 gpm. The third scenario (ExMob_Dprs_C) assumes all future injection (January 1, 2009 to December 31, 2020) into the Frio D Sand will occur into both WDW-397 and WDW-398 at 180 gpm (each). The SWIFT reservoir pressure model input parameters are summarized on Table 7-4. For each scenario, an injection rate of 140 gpm for WDW-397 from July 1, 2008 until December 31, 2008 was incorporated into the demonstration to account for historically injected volumes (see Section 7.3.1). Injection activities at the Merisol facility (WDW-147 and WDW-319), at the Lyondell facility (WDW-148 and WDW-162), and at the Equistar facility (WDW-36) were not considered in the demonstration, since none of these wells are completed to inject into the Frio D Sand. Historical and modeled flow rates into the wells are depicted on Table 7-9. The Frio D Sand pressure model(s) (ExMob_Dprs_A, ExMob_Dprs_B, and ExMob_Dprs_C) input and output data are included in Appendix E.

A summary discussion of the SWIFT model input parameters and Frio D Sand pressure model results for each of the three (3) scenarios is presented on Plate 7-7. The SWIFT model grid and end-of-operations pressure contours are also depicted on Plate 7-7. The stratigraphic pinchout of the Frio D Sand which occurs to the east and northeast of the well locations was modeled as noted on Plate 7-7. In the approximate area of the pinchout (defined as the area within the 10-foot contour interval), the grid block cells

were made inactive via use of the R1-26 Card (FPV = 0). Pressure buildup was determined by subtracting the initial Injection Interval pressures from the Injection Interval pressures at the end of the operational period. The initial pressures were determined from a pre-operation period (no injection) in which the model was run for 10,000 days. The initial Injection Interval pressures are included in the output files in Appendix E.

For the first scenario (ExMob_Dprs_A), the maximum predicted flowing bottom-hole grid block pressure on December 31, 2020 is 3,478 psia. The maximum predicted flowing bottom-hole well bore pressure on December 31, 2020 is 3,600 psia. The preinjection native static reservoir pressure is 2,884 psia. Therefore, the pressure buildup in the grid block cell is no more than 594 psi and the pressure buildup predicted at the well is no more than 716 psi.

For the second scenario (ExMob_Dprs_B), the maximum predicted flowing bottom-hole grid block pressure on December 31, 2020 is 3,469 psia. The maximum predicted flowing bottom-hole well bore pressure on December 31, 2020 is 3,590 psia. The pre-injection native static reservoir pressure at WDW-398 is 2,902 psia. Therefore, the pressure buildup in the grid block cell is no more than 567 psi and the pressure buildup predicted at the well is no more than 688 psi.

For the third scenario (ExMob_Dprs_C), the maximum predicted flowing bottom-hole grid block pressure in WDW-397 on December 31, 2020 is 3,334 psia. The maximum predicted flowing bottom-hole well bore pressure in WDW-397 on December 31, 2020 is 3,390 psia. The pre-injection native static reservoir pressure is 2,884 psia. Therefore, the pressure buildup in the grid block cell for WDW-397 is no more than 450 psi and the pressure buildup predicted at the well is no more than 506 psi. The maximum predicted flowing bottom-hole grid block pressure in WDW-398 on December 31, 2020 is 3,339 psia. The maximum predicted flowing bottom-hole well bore pressure in WDW-398 on December 31, 2020 is 3,400 psia. The pre-injection native static reservoir pressure is 2,902 psia. Therefore, the pressure buildup in the grid block cell for WDW-398 is no more than 437 psi and the pressure buildup predicted at the well is no more than 498 psi.

Of the three (3) scenarios, the first scenario (ExMob_Dprs_A) results in the greatest reservoir pressure buildup at the well (WDW-397) and has the largest areal extent of the area enclosed within the cone of endangering influence. The cone of endangering



influence includes the area within the pressure isopleth representing a 281-psi increase in reservoir pressure.

The simulated Injection Interval pressure buildup for the first scenario (ExMob_Dprs_A) at the end-of-operation (December 31, 2020) is shown in Figure 7-9. The figure shows pressure isobars, representing the pressure buildup (the difference between the injection pressure at the end-of-operation and initial reservoir pressure) within the Injection Interval, radiating outward from the injection wells. From WDW-397, the cone of endangering influence extends to the Frio D Sand pinchout to the northeast, to the trace of Fault B to the southeast, approximately 4,800 feet to the southwest, and approximately 4,200 feet to the northwest. The model predicted flowing BHPs for each scenario for WDW-397 and WDW-398 are included on Table 7-10. The reservoir pressure buildup for each scenario is graphically illustrated in Figure 7-10.

7.4.3 SWIFT ExMob_EF Pressure Model

Reservoir pressure buildup in the Frio E&F Sand was considered for three (3) different scenarios. The first scenario (ExMob_EF Pressure_A) assumed all future injection (January 1, 2009 to December 31, 2020) into the Frio E&F Sand will occur only in WDW-397 at 1,200 gpm. The second scenario (ExMob_EF Pressure_B) assumes all future injection (January 1, 2009 to December 31, 2020) into the Frio E&F Sand will occur only in WDW-398 at 1,200 gpm. The third scenario (ExMob_EF Pressure C) assumes all future injection (January 1, 2009 to December 31, 2020) into the Frio E&F Sand will occur into both WDW-397 and WDW-398 at 600 gpm (each). The SWIFT reservoir pressure model input parameters are summarized on Table 7-4. For each scenario, an injection rate of 700 gpm for WDW-397 from July 1, 2008 until December 31, 2008 was incorporated into the demonstration to account for historically injected volumes (see Section 7.3.1). Injection activities at the Merisol facility (WDW-147 and WDW-319), at the Lyondell facility (WDW-148 and WDW-162), and at the Equistar facility (WDW-36) were also included in the demonstration. Historical and modeled flow rates into the wells are depicted on Table 7-9. The Frio E&F Sand pressure model(s) (ExMob_EF Pressure A, ExMob_EF Pressure B, and ExMob_EF Pressure C) input and output data are included in Appendix E.

A summary discussion of the SWIFT model input parameters and Frio E&F Sand pressure model results for each of the three (3) scenarios is presented on Plate 7-8. The SWIFT model grid and end-of-operations pressure contours are also depicted on Plate 7-



8. Pressure buildup was determined by subtracting the initial Injection Interval pressures from the Injection Interval pressures at the end of the operational period. The initial pressures were determined from a pre-operation period (no injection) in which the model was run for 10,000 days. The initial Injection Interval pressures are included in the output files in Appendix E.

For the first scenario (ExMob_EF Pressure_A), the maximum predicted flowing bottom-hole grid block pressure on December 31, 2020 is 3,354 psia. The maximum predicted flowing bottom-hole well bore pressure on December 31, 2020 is 3,430 psia. The pre-injection native static reservoir pressure is 2,944 psia. Therefore, the pressure buildup in the grid block cell is no more than 410 psi and the pressure buildup predicted at the well is no more than 486 psi. For SWIFT pressure model run ExMob_EF Pressure_A.dat, the 281-psi pressure contour extends no farther than 425 feet from the WDW-397 wellbore.

For the second scenario (ExMob_EF Pressure_B), the maximum predicted flowing bottom-hole grid block pressure on December 31, 2020 is 3,358 psia. The maximum predicted flowing bottom-hole well bore pressure on December 31, 2020 is 3,440 psia. The pre-injection native static reservoir pressure at WDW-398 is 2,960 psia. Therefore, the pressure buildup in the grid block cell is no more than 398 psi and the pressure buildup predicted at the well is no more than 480 psi. For SWIFT pressure model run ExMob_EF Pressure_B.dat, the 281-psi pressure contour extends no farther than 300 feet from the WDW-398 wellbore.

For the third scenario (ExMob_EF Pressure_C), the maximum predicted flowing bottom-hole grid block pressure in WDW-397 on December 31, 2020 is 3,262 psia. The maximum predicted flowing bottom-hole well bore pressure in WDW-397 on December 31, 2020 is 3,300 psia. The pre-injection native static reservoir pressure is 2,944 psia. Therefore, the pressure buildup in the grid block cell for WDW-397 is no more than 318 psi and the pressure buildup predicted at the well is no more than 356 psi. The maximum predicted flowing bottom-hole grid block pressure in WDW-398 on December 31, 2020 is 3,269 psia. The maximum predicted flowing bottom-hole well bore pressure in WDW-398 on December 31, 2020 is 3,310 psia. The pre-injection native static reservoir pressure is 2,960 psia. Therefore, the pressure buildup in the grid block cell for WDW-398 is no more than 309 psi and the pressure buildup predicted at the well is no more than 350 psi. For SWIFT pressure model run ExMob_EF Pressure_C.dat, the 281-psi pressure



contour extends no farther than 100 feet from the WDW-397 wellbore and no more than 50 feet from the WDW-398 wellbore.

Of the three (3) scenarios, the first scenario (ExMob_EF Pressure_A) results in the greatest reservoir pressure buildup at the well (WDW-397) and has the largest areal extent of the area enclosed within the cone of endangering influence. The cone of endangering influence includes the area within the pressure isopleth representing a 281-psi increase in reservoir pressure. The simulated Injection Interval pressure buildup at the end-of-operation (December 31, 2020) for the ExMob_EF Pressure_A model run is shown in Figure 7-11. The figure shows pressure isobars, representing the pressure buildup (the difference between the injection pressure at the end-of-operation and initial reservoir pressure) within the Injection Interval, radiating outward from the injection wells. The 281-psi contour extends no farther than 425 feet from the WDW-397 injection well. The model predicted flowing BHPs for each of the three scenarios (ExMob_EF Pressure_A, ExMob_EF Pressure_B and ExMob_EF Pressure_C) are included on Table 7-11. The flowing BHPs are graphically illustrated in Figure 7-12.

7.4.4 SWIFT ExMob_AB Pressure Model

Reservoir pressure buildup in the Frio A/B Sand was also considered for three (3) different scenarios. The first scenario (ExMob_AB Pressure_A) assumed all future injection (January 1, 2009 to December 31, 2020) into the Frio A/B Sand will occur only in WDW-397 at 1,200 gpm. The second scenario (ExMob_AB Pressure_B) assumes all future injection (January 1, 2009 to December 31, 2020) into the Frio A/B Sand will occur only in WDW-398 at 1,200 gpm. The third scenario (ExMob AB Pressure C) assumes all future injection (January 1, 2009 to December 31, 2020) into the Frio A/B Sand will occur into both WDW-397 and WDW-398 at 600 gpm (each). The SWIFT reservoir pressure model (ExMob AB Pressure) model input parameters are summarized on Table 7-4. For each scenario, an injection rate of 700 gpm for WDW-397 from July 1, 2008 until December 31, 2008 was incorporated into the demonstration to account for historically injected volumes (see Section 7.3.1). Injection activities at the Merisol facility (WDW-147 and WDW-319), at the Lyondell facility (WDW-148 and WDW-162), and at the Equistar facility (WDW-36) and the Cobra saltwater disposal well were also included in the demonstration. Historical and modeled flow rates into the wells are depicted on Table 7-9. The Frio A/B Sand pressure model(s) (ExMob_AB Pressure_A, ExMob AB Pressure B and ExMob_AB Pressure_C) input and output data are included in Appendix E.



A summary discussion of the SWIFT model input parameters and Frio A/B Sand pressure model results for each of the three (3) scenarios is presented on Plate 7-9. The ExMob_AB Pressure SWIFT model grid and end-of-operations pressure contours are also depicted on Plate 7-9. Pressure buildup was determined by subtracting the initial Injection Interval pressures from the Injection Interval pressures at the end of the operational period. The initial pressures were determined from a pre-operation period (no injection) in which the model was run for some period of time (10,000 days). The initial Injection Interval pressures are included in the output file in Appendix E.

For the first scenario (ExMob_AB Pressure_A), the maximum predicted flowing bottom-hole grid block pressure in WDW-397 on December 31, 2020 is 3,500 psia. The maximum predicted flowing bottom-hole well bore pressure on December 31, 2020 is 3,590 psia. The pre-injection native static reservoir pressure is 3,047 psia. Therefore, the pressure buildup in the grid block cell is no more than 453 psi and the pressure buildup predicted at the well is no more than 543 psi. For SWIFT pressure model run ExMob_AB Pressure_A.dat, the 281-psi pressure contour extends no farther than 850 feet from the WDW-397 wellbore.

For the second scenario (ExMob_AB Pressure_B), the maximum predicted flowing bottom-hole grid block pressure in WDW-398 on December 31, 2020 is 3,505 psia. The maximum predicted flowing bottom-hole well bore pressure on December 31, 2020 is 3,600 psia. The pre-injection native static reservoir pressure at WDW-398 is 3,063 psia. Therefore, the pressure buildup in the grid block cell is no more than 442 psi and the pressure buildup predicted at the well is no more than 537 psi. For SWIFT pressure model run ExMob_AB Pressure_B.dat, the 281-psi pressure contour extends no farther than 625 feet from the WDW-398 wellbore.

For the third scenario (ExMob_AB Pressure_C), the maximum predicted flowing bottom-hole grid block pressure in WDW-397 on December 31, 2020 is 3,364 psia. The maximum predicted flowing bottom-hole well bore pressure in WDW-397 on December 31, 2020 is 3,440 psia. The pre-injection native static reservoir pressure is 3,047 psia. Therefore, the pressure buildup in the grid block cell for WDW-397 is no more than 347 psi and the pressure buildup predicted at the well is no more than 393 psi. The maximum predicted flowing bottom-hole grid block pressure in WDW-398 on December 31, 2020 is 3,402 psia. The maximum predicted flowing bottom-hole well bore pressure in WDW-

398 on December 31, 2020 is 3,450 psia. The pre-injection native static reservoir pressure is 3,063 psia. Therefore, the pressure buildup in the grid block cell for WDW-398 is no more than 339 psi and the pressure buildup predicted at the well is no more than 387 psi. For SWIFT pressure model run ExMob_AB Pressure_C.dat, the 281-psi pressure contour extends no farther than 100 feet from the WDW-397 wellbore and no more than 50 feet from the WDW-398 wellbore.

Of the three (3) scenarios, the first scenario (ExMob_AB Pressure_A) results in the greatest reservoir pressure buildup at the well (WDW-397) and has the largest areal extent of the area enclosed within the cone of endangering influence. The cone of endangering influence includes the area within the pressure isopleth representing a 281-psi increase in reservoir pressure. The simulated Injection Interval pressure buildup at the end-of-operation (December 31, 2020) for the ExMob_AB Pressure_A model run is shown in Figure 7-13. The figure shows pressure isobars, representing the pressure buildup (the difference between the injection pressure at the end-of-operation and initial reservoir pressure) within the Injection Interval, radiating outward from the injection wells. The 281-psi contour extends no farther than 850 feet from the WDW-397 injection well. The model predicted flowing BHPs for each of the three scenarios (ExMob_EF Pressure_A, ExMob_EF Pressure_B and ExMob_EF Pressure_C) are included on Table 7-12. The flowing BHPs are graphically illustrated in Figure 7-14.

7.5 SWIFT Model Results – Lateral Migration Modeling

The lateral SWIFT model was used to simulate lateral waste plume migration during the 10,000-year post operational period. Lateral migration modeling was performed independently for the Frio D Sand, the Frio E&F Sand and the Frio A/B Sand. A Table of Contents is included at the beginning of Appendix E which lists the plume migration cases by injection sand as well as showing the input and output file names for each model run.

The lateral transport model consists of three components: 1) fluid displacement due to injection; 2) buoyant fluid movement and 3) dispersive and diffusive contaminant transport for a conservative species (no adsorption, hydrolysis or other fate mechanism). In this fashion, the outline of the isopleth for the 5-order of magnitude reduction in initial concentration for a 10,000-year post-operational period is obtained. This is the appropriate concentration reduction factor in that it will render the initial waste constituent concentrations non-hazardous.

7.5.1 Low Density Injectate SWIFT Model (ExMob_D_C)

The up-dip lateral waste transport model (ExMob D C) incorporates variable structure, constant thickness and assumes a waste specific gravity of a light density fluid. The injected waste density was modeled as 61.64 lb/ft³ at 164 °F, and waste viscosity was 0.378 cP at 164 °F. The rate of ground water movement in the Injection Interval was assumed to be 0.0 ft/year. Historical injection from July 1, 2008 until December 31, 2008 was modeled at 140 gpm into WDW-397. Future injection from January 1, 2009 until December 31, 2020 was modeled at an injection rate of 360 gpm into WDW-397 (0 gpm into WDW-398). The lower model boundary is closed to represent the faultbounded area to the southeast and the remaining lateral model boundaries are left open (Carter-Tracy boundary conditions). The model results for ExMob D C are presented in the output file in Appendix E and are summarized on Plate 7-10. The ExMob D C SWIFT model grid, end-of-operations and 10,000-year waste plumes are also depicted on Plate 7-10. The waste plume orientations and dimensions at the end of the operational period and after 10,000 years are depicted on Plate 7-11. The base map for Plate 7-11 is the structure map on top of the Frio D Sand of the Injection Interval. The up-dip portion of the plume flows to, and surrounds, the Clinton Dome salt dome structure as illustrated on Plate 7-11. Plate 7-12 shows the buoyant plume outlines on the Frio D Sand isopach map and highlights the net thickness pinchout.



The end-of-operation waste plume is oval in shape. The end-of-operations waste plume (12/31/2020) is approximately 14,100 feet long and approximately 13,650 feet wide. The injected waste plume extends 38,500 feet up-gradient towards Clinton Dome, approximately 14,500 feet up-gradient towards the northeast and 6,600 feet downgradient from the WDW-397 injection well and is approximately 24,200 feet wide at its widest point after 10,000 years.

The up-dip lateral waste transport model (ExMob_EF_398) is identical to the ExMob_EF up-dip lateral waste transport model with the exception being that all future injection from January 1, 2009 until December 31, 2020 was modeled at an injection rate of 1,200 gpm into WDW-398 (0 gpm into WDW-397). The model results for ExMob_EF_398 are presented in the output file in Appendix K and are summarized on Plate 7-13. The ExMob_EF_398 SWIFT model grid, end-of-operations and 10,000-year waste plumes are also depicted on Plate 7-13. The waste plume orientations and dimensions at the end of the operational period and after 10,000 years are depicted on Plate 7-14A. The base map for Plate 7-14A is the structure map on top of the Frio E&F Sand of the Injection Interval. The up-dip portion of the plume flows to, and surrounds, the Clinton Dome salt dome structure as illustrated on Plate 7-14A. Plate 7-15A shows the buoyant plume outlines on the Frio E&F Sand isopach map.

The end-of-operation waste plume is oval in shape. The end-of-operations waste plume (12/31/2020) is approximately 15,400 feet long and approximately 13,500 feet wide. The injected waste plume extends 40,400 feet up-gradient towards Clinton Dome and 5,300 feet down-gradient from the WDW-398 injection well and is approximately 24,000 feet wide at its widest point after 10,000 years.

A discussion of the wells (non-freshwater artificial penetrations) that are intersected by the plumes during the modeled operational (end time of 12/31/2020) and post-operational (10,000-year) time periods is included in Section 8.0 (Area of Review). These wells meet non-endangerment standards (due to pressure increases) and/or no-migration standards (due to waste movement), as discussed in Section 8.0.

Sensitivity Analysis (Reservoir Thickness) (ExMob_EF_S and ExMob_EF_S_398): In order to assess the potential additional plume migration in the Frio E&F Sand due to thinning of the sand near the Clinton Dome, sensitivity runs were prepared which employed a constant reservoir thickness of 132 feet. This is the average net thickness of



The shape of both the end-of-operations waste plume and the 10,000-year waste plume are affected by the fault-bounded edge to the southeast and the stratigraphic thinning to the east and northeast. The end-of-operation waste plume is oval in shape. The end-of-operations waste plume is approximately 15,200 feet long along the north-south axis and approximately 13,800 feet wide along the east-west axis. The end-of-operations waste plume center of mass is shifted about 1,700 feet west northwest of the WDW-397 well location. The 10,000-year waste plume extends 48,200 feet up-gradient towards Clinton Dome and 14,000 feet to the northeast towards the area where the Frio D Sand pinches out (measured from the WDW-397 well location). The 10,000 year waste plume extends about 21,000 feet to the southwest and 7,625 feet southeast of WDW-397 and has a width of about 27,000 feet across the Clinton Dome.

A discussion of the wells (non-freshwater artificial penetrations) that are intersected by the plumes during the modeled operational (end time of 12/31/2020) and post-operational (10,000-year) time periods is included in Section 8.0 (Area of Review). These wells meet non-endangerment standards (due to pressure increases) and/or no-migration standards (due to waste movement), as discussed in Section 8.0.

7.5.2 Low Density Injectate SWIFT Model (ExMob EF and ExMob EF 398)

The up-dip lateral waste transport model (ExMob_EF) incorporates variable structure, constant thickness and assumes a waste specific gravity of a light density fluid. The injected waste density was modeled as 61.45 lb/ft³ at 169 °F, and waste viscosity was 0.364 cP at 169 °F. Historical injection from July 1, 2008 until December 31, 2008 was modeled at 700 gpm into WDW-397. Future injection from January 1, 2009 until December 31, 2020 was modeled at an injection rate of 1,200 gpm into WDW-397 (0 gpm into WDW-398). All lateral model boundaries are left open (Carter-Tracy boundary conditions). The model results for ExMob_EF are presented in the output file in Appendix E and are summarized on Plate 7-13. The ExMob_EF SWIFT model grid, end-of-operations and 10,000-year waste plumes are also depicted on Plate 7-13. The waste plume orientations and dimensions at the end of the operational period and after 10,000 years are depicted on Plate 7-14. The base map for Plate 7-14 is the structure map on top of the Frio E&F Sand of the Injection Interval. The up-dip portion of the plume flows to, and surrounds, the Clinton Dome salt dome structure as illustrated on Plate 7-14. Plate 7-15 shows the buoyant plume outlines on the Frio E&F Sand isopach map.



the Frio E&F Sand within the projected path of the 10,000-year buoyant plume. Carter-Tracy boundary conditions were adjusted to account for the revision in reservoir thickness. All other parameters were identical to those employed in the ExMob_EF and ExMob_EF_398 SWIFT model runs. The input parameters, text discussion, plates, SWIFT model input and output for ExMob_EF_S and ExMob_EF_S_398 are included in Appendix H.

The waste plume orientations and dimensions for the 5-order magnitude reduction for ExMob_EF_S and ExMob_EF_S_398 after 10,000 years are depicted on Plate H-1. To provide for comparison, the 5-order magnitude reduction for ExMob_EF and ExMob EF 398 after 10,000 years is also depicted on Plate H-1. Note that the waste plume outlines presented on Plate H-1 are composite boundaries of the waste plumes which collectively cover the largest area regardless of flow rate allocation. The base map for Plate H-1 is the structure map on top of the Frio E&F Sand of the Injection Interval. The ExMob_EF_S and ExMob_EF_S_398 composite modeled waste plume extends approximately 41,300 feet up-gradient towards Clinton Dome, approximately 14,800 feet up-gradient towards the northeast and 6,700 feet down-gradient from the WDW-397 injection well and is approximately 25,200 feet wide at its widest point after 10,000 years. By comparison, the ExMob_EF and ExMob-EF 398 composite injected waste plume extends 40,400 feet up-gradient towards Clinton Dome, approximately 14,500 feet up-gradient towards the northeast, and 6,700 feet down-gradient from the WDW-397 injection well and is approximately 24,200 feet wide at its widest point after 10,000 years.

The ExMob_EF_S and ExMob_EF_S_398 composite 10,000-year waste plume is slightly larger than the ExMob_EF and ExMob_EF_398 composite 10,000-year waste plume. The ExMob_EF_S and ExMob_EF_S_398 composite plume extends approximately 900 feet farther to the north and about 600 feet farther east of the Clinton Dome than the ExMob_EF plume and ExMob_EF_398 composite plume. The additional artificial penetrations enclosed with the expanded plume area have already been addressed in the discussion included in Section 8.0 (Area of Review) regarding wells (non-freshwater artificial penetrations) that are intersected by the plumes during the modeled operational (end time of 12/31/2020) and post-operational (10,000-year) time periods.



7.5.3 Low Density Injectate SWIFT Model (ExMob_AB and ExMob_AB 398)

The up-dip lateral waste transport model (ExMob_AB) incorporates variable structure, constant thickness and assumes a waste specific gravity of a light density fluid. The injected waste density was modeled as 61.38 lb/ft³ at 173 °F, and waste viscosity was 0.353 cP at 173 °F. Historical injection from July 1, 2008 until December 31, 2008 was modeled at 700 gpm into WDW-397. Future injection from January 1, 2009 until December 31, 2020 was modeled at an injection rate of 1,200 gpm into WDW-397 (0 gpm into WDW-398). All lateral model boundaries are left open (Carter-Tracy boundary conditions). The model results for ExMob_AB are presented in the output file in Appendix E and are summarized on Plate 7-16. The ExMob_AB SWIFT model grid, end-of-operations and 10,000-year waste plumes are also depicted on Plate 7-16. The waste plume orientations and dimensions at the end of the operational period and after 10,000 years are depicted on Plate 7-17. The base map for Plate 7-17 is the structure map on top of the Frio E&F Sand of the Injection Interval. The up-dip portion of the plume flows to, and surrounds, the Clinton Dome salt dome structure as illustrated on Plate 7-17. Plate 7-18 shows the buoyant plume outlines on the Frio A/B Sand isopach map.

The end-of-operation waste plume is oval in shape. The end-of-operations waste plume (12/31/2020) is approximately 16,700 feet long and approximately 14,600 feet wide. The injected waste plume extends 41,300 feet up-gradient towards Clinton Dome, approximately 15,500 feet up-gradient towards the northeast, and 7,100 feet downgradient from the WDW-397 injection well and is approximately 26,700 feet wide at its widest point after 10,000 years.

The up-dip lateral waste transport model (ExMob_AB_398) is identical to the ExMob_AB up-dip lateral waste transport model with the exception being that all future injection from January 1, 2009 until December 31, 2020 was modeled at an injection rate of 1,200 gpm into WDW-398 (0 gpm into WDW-397). The model results for ExMob_AB_398 are presented in the output file in Appendix K and are summarized on Plate 7-16. The ExMob_AB_398 SWIFT model grid, end-of-operations and 10,000-year waste plumes are also depicted on Plate 7-16. The waste plume orientations and dimensions at the end of the operational period and after 10,000 years are depicted on Plate 7-17A. The base map for Plate 7-17A is the structure map on top of the Frio E&F Sand of the Injection Interval. The up-dip portion of the plume flows to, and surrounds, the Clinton Dome salt dome structure as illustrated on Plate 7-17A. Plate 7-18A shows the buoyant plume outlines on the Frio A/B Sand isopach map.



The end-of-operation waste plume is oval in shape. The end-of-operations waste plume (12/31/2020) is approximately 16,500 feet long and approximately 14,500 feet wide. The injected waste plume extends 42,500 feet up-gradient towards Clinton Dome and 5,400 feet down-gradient from the WDW-398 injection well and is approximately 26,000 feet wide at its widest point after 10,000 years.

A discussion of the wells (non-freshwater artificial penetrations) that are intersected by the plumes during the modeled operational (end time of 12/31/2020) and post-operational (10,000-year) time periods is included in Section 8.0 (Area of Review). These wells meet non-endangerment standards (due to pressure increases) and/or no-migration standards (due to waste movement), as discussed in Section 8.0.

Sensitivity Analysis (Reservoir Thickness) (ExMob_AB_S and ExMob_AB_S_398): In order to assess the potential additional plume migration in the Frio A/B Sand due to thinning of the sand near the Clinton Dome, a sensitivity run was prepared which employed a constant reservoir thickness of 91 feet. This is the average net thickness of the Frio A/B Sand within the projected path of the 10,000-year buoyant plume. Carter-Tracy boundary conditions were adjusted to account for the revision in reservoir thickness. All other parameters were identical to those employed in the ExMob_AB and ExMob_AB_398 SWIFT model runs. The input parameters, text discussion, plates, SWIFT model input and output for ExMob_AB_S and ExMob_AB_S_398 are included in Appendix H.

The waste plume orientations and dimensions for the 5-order magnitude reduction for ExMob_AB_S and ExMob_AB_S_398 after 10,000 years are depicted on Plate H-2. To provide for comparison, the 5-order magnitude reduction for ExMob_AB and ExMob_AB_398 after 10,000 years is also depicted on Plate H-2. Note that the waste plume outlines presented on Plate H-2 are **composite** boundaries of the waste plumes which collectively cover the largest area regardless of flow rate allocation. The base map for Plate H-2 is the structure map on top of the Frio E&F Sand of the Injection Interval. The ExMob_AB_S and ExMob_AB_S_398 modeled composite waste plume extends 44,700 feet up-gradient towards Clinton Dome, approximately 17,000 feet up-gradient towards the northeast and 8,100 feet down-gradient from the WDW-397 injection well and is approximately 28,600 feet wide at its widest point after 10,000 years.



The ExMob_AB_S and ExMob_AB_S_398 10,000-year composite waste plume is larger than the ExMob_AB and ExMob_AB_398 10,000-year composite waste plume. The ExMob_AB_S and ExMob_AB_S_398 composite plume extends approximately 2,200 feet farther to the north and as much as 1,500 feet farther east of the Clinton Dome than the ExMob_AB and ExMob_AB_398 composite plume. The additional artificial penetrations enclosed with the expanded plume area have already been addressed in the discussion included in Section 8.0 (Area of Review) regarding wells (non-freshwater artificial penetrations) that are intersected by the plumes during the modeled operational (end time of 12/31/2020) and post-operational (10,000-year) time periods.

7.5.4 High Density Injectate SWIFT Model (ExMob_D HiDens)

The up-dip lateral waste transport model (ExMob_D HiDens) incorporates variable structure, constant thickness and assumes a waste specific gravity of a light density fluid. The injected waste density was modeled as 64.34 lb/ft³ at 164 °F, and waste viscosity was 0.452 cP at 164 °F. Historical injection from July 1, 2008 until December 31, 2008 was modeled at 140 gpm into WDW-397. Future injection from January 1, 2009 until December 31, 2020 was modeled at an injection rate of 360 gpm into WDW-397 (0 gpm into WDW-398). The lower model boundary is closed to represent the fault-bounded area to the southeast and the remaining lateral model boundaries are left open (Carter-Tracy boundary conditions). Downdip groundwater flow was set at 0 feet/year, since the Frio D Sand is faulted against shale and is effectively sealed to the southeast of the facility location. The model results for ExMob_D HiDens are presented in the output file in Appendix E and are summarized on Plate 7-19. The ExMob D HiDens SWIFT model grid, end-of-operations and 10,000-year waste plumes are also depicted on Plate 7-19. The waste plume orientations and dimensions at the end of the operational period and after 10,000 years are depicted on Plate 7-20. The base map for Plate 7-20 is the structure map on top of the Frio D Sand of the Injection Interval. The up-dip portion of the plume flows to, and surrounds, the Clinton Dome salt dome structure as illustrated on Plate 7-20.

The shape of both the end-of-operations waste plume and the 10,000-year waste plume are affected by the fault-bounded edge to the southeast and the stratigraphic thinning to the east and northeast. The end-of-operations waste plume is oval in shape. The end-of-operations waste plume is approximately 15,800 feet long along the north-south axis and approximately 13,900 feet wide along the east-west axis. The end-of-operations waste plume center of mass is shifted about 1,800 feet west of the WDW-397 well location.



The 10,000-year waste plume extends 39,200 feet up-gradient towards Clinton Dome and 14,000 feet to the northeast towards the area where the Frio D Sand pinches out (measured from the WDW-397 well location). The 10,000 year waste plume extends about 13,700 feet to the southwest and 7,625 feet southeast of WDW-397. The 10,000-year waste plume has a width of about 22,400 feet across the Clinton Dome.

A discussion of the wells (non-freshwater artificial penetrations) that are intersected by the plumes during the modeled operational (end time of 12/31/2020) and post-operational (10,000-year) time periods is included in Section 8.0 (Area of Review). These wells meet non-endangerment standards (due to pressure increases) and/or no-migration standards (due to waste movement), as discussed in Section 8.0.

7.5.5 High Density Injectate SWIFT Model (ExMob_EF HiDens and ExMob_EF_398 HiDens)

The heavy density lateral waste transport model (ExMob_EF HiDens) employs constant structure, constant thickness and assumes a waste specific gravity of a high density fluid. The injected waste density was modeled as 64.25 lb/ft³ at 169 °F, and waste viscosity was 0.439 cP at 169 °F. The reservoir brine density was modeled as 66.02 lb/ft³ at 169 °F, and brine viscosity was 0.487 cP at 169 °F. Historical injection from July 1, 2008 until December 31, 2008 was modeled at 700 gpm into WDW-397. Future injection from January 1, 2009 until December 31, 2020 was modeled at an injection rate of 1,200 gpm into WDW-397 (0 gpm into WDW-398). All lateral model boundaries are left open (Carter-Tracy boundary conditions). The model results for ExMob EF HiDens are presented in the output file in Appendix E and are summarized on Plate 7-21. The injected waste plume extends 7,400 feet up-gradient, 7,100 feet down-gradient, 6,950 feet to the northeast and 8,600 feet to the southwest from the WDW-397 injection well at the end of operation (12/31/2020). The end-of-operations waste plume is oval in shape and has a width of 15,550 feet on the long axis and 14,500 feet on the short axis. The injected waste plume extends 32,100 feet up-gradient and 6,950 feet down-gradient from the WDW-397 injection well and is approximately 15,550 feet wide at its widest point after 10,000 years. The ExMob_EF SWIFT model grid, end-of-operations and 10,000-year waste plumes are depicted on Plate 7-21.

In order to simulate plume movement in response to a background flow gradient of 1.2 ft/year, the 10,000-year waste plume center of mass was shifted down-dip by 12,000 feet (10,000 years x 1.2 ft/year). Plate 7-22 illustrates the position of the end-of-operations



waste plume and of the 10,000-year heavy density waste plume after repositioning of the waste plume. The base map for Plate 7-22 is the structure map on top of the Frio E&F Sand of the Injection Interval.

The heavy density lateral waste transport model (ExMob_EF_398 HiDens) is identical to the ExMob_EF HiDens up-dip lateral waste transport model with the exception being that all future injection from January 1, 2009 until December 31, 2020 was modeled at an injection rate of 1,200 gpm into WDW-398 (0 gpm into WDW-397). The model results for ExMob_EF_398 HiDens are presented in the output file in Appendix K and are summarized on Plate 7-21. The injected waste plume extends 7,500 feet up-gradient, 6,950 feet down-gradient, 7,950 feet to the northeast and 7,450 feet to the southwest from the WDW-398 injection well at the end of operation (12/31/2020). The end-of-operations waste plume is oval in shape and has a width of 15,400 feet on the long axis and 14,500 feet on the short axis. The injected waste plume extends 31,800 feet up-gradient and 6,800 feet down-gradient from the WDW-398 injection well and is approximately 15,200 feet wide at its widest point after 10,000 years. The ExMob_EF_398 SWIFT model grid, end-of-operations and 10,000-year waste plumes are depicted on Plate 7-21.

In order to simulate plume movement in response to a background flow gradient of 1.2 ft/year, the 10,000-year waste plume center of mass was shifted down-dip by 12,000 feet (10,000 years x 1.2 ft/year). Plate 7-22A illustrates the position of the end-of-operations waste plume and of the 10,000-year heavy density waste plume after repositioning of the waste plume. The base map for Plate 7-22A is the structure map on top of the Frio E&F Sand of the Injection Interval.

A discussion of the wells (non-freshwater artificial penetrations) that are intersected by the plumes during the modeled operational (end time of 12/31/2020) and post-operational (10,000-year) time periods is included in Section 8.0 (Area of Review). These wells meet non-endangerment standards (due to pressure increases) and/or no-migration standards (due to waste movement), as discussed in Section 8.0.



7.5.6 High Density Injectate SWIFT Model (ExMob AB HiDens and ExMob AB 398 HiDens)

The down-dip lateral waste transport model (ExMob_AB HiDens) employs constant structure, constant thickness and assumes a waste specific gravity of a high density fluid. The injected waste density was modeled as 64.18 lb/ft³ at 173 °F, and waste viscosity was 0.428 cP at 173 °F. The reservoir brine density was modeled as 66.55 lb/ft³ at 173 °F, and brine viscosity was 0.495 cP at 173 °F. Historical injection from July 1, 2008 until December 31, 2008 was modeled at 700 gpm into WDW-397. Future injection from January 1, 2009 until December 31, 2020 was modeled at an injection rate of 1,200 gpm into WDW-397 (0 gpm into WDW-398). All lateral model boundaries are left open (Carter-Tracy boundary conditions). The model results for ExMob_AB HiDens are presented in the output file in Appendix E and are summarized on Plate 7-23. The injected waste plume extends 8,050 feet up-gradient, 7,550 feet down-gradient, 7,600 feet to the northeast and 6,900 feet to the southwest from the WDW-397 injection well at the end of operation (12/31/2020). The end-of-operations waste plume is oval in shape and has a width of 15,600 feet on the long axis and 14,500 feet on the short axis. The injected waste plume extends 38,200 feet up-gradient and 7,300 feet down-gradient from the WDW-397 injection well and is approximately 16,500 feet wide at its widest point after 10,000 years. The ExMob AB SWIFT model grid, end-of-operations and 10,000-year waste plumes are depicted on Plate 7-23.

In order to simulate plume movement in response to a background flow gradient of 1.2 ft/year, the 10,000-year waste plume center of mass was shifted down-dip by 12,000 feet (10,000 years x 1.2 ft/year). Plate 7-24 illustrates the position of the end-of-operations waste plume and of the 10,000-year heavy density waste plume after repositioning of the waste plume. The base map for Plate 7-24 is the structure map on top of the Frio E&F Sand of the Injection Interval.

The down-dip lateral waste transport model (ExMob_AB_398 HiDens) is identical to the ExMob_AB HiDens up-dip lateral waste transport model with the exception being that all future injection from January 1, 2009 until December 31, 2020 was modeled at an injection rate of 1,200 gpm into WDW-398 (0 gpm into WDW-397). The model results for ExMob_AB_398 HiDens are presented in the output file in Appendix K and are summarized on Plate 7-23. The injected waste plume extends 8,050 feet up-gradient, 7,450 feet down-gradient, 8,350 feet to the northeast and 7,700 feet to the southwest from the WDW-398 injection well at the end of operation (12/31/2020). The end-of-



operations waste plume is oval in shape and has a width of 16,050 feet on the long axis and 15,500 feet on the short axis. The injected waste plume extends 38,150 feet upgradient and 7,200 feet down-gradient from the WDW-398 injection well and is approximately 16,400 feet wide at its widest point after 10,000 years. The ExMob_AB SWIFT model grid, end-of-operations and 10,000-year waste plumes are depicted on Plate 7-23.

In order to simulate plume movement in response to a background flow gradient of 1.2 ft/year, the 10,000-year waste plume center of mass was shifted down-dip by 12,000 feet (10,000 years x 1.2 ft/year). Plate 7-24A illustrates the position of the end-of-operations waste plume and of the 10,000-year heavy density waste plume after repositioning of the waste plume. The base map for Plate 7-24A is the structure map on top of the Frio E&F Sand of the Injection Interval.

A discussion of the wells (non-freshwater artificial penetrations) that are intersected by the plumes during the modeled operational (end time of 12/31/2020) and post-operational (10,000-year) time periods is included in Section 8.0 (Area of Review). These wells meet, non-endangerment standards (due to pressure increases) and/or no-migration standards (due to waste movement), as discussed in Section 8.0.

7.6 Vertical Advective and Diffusive Waste Transport Model

The determination of vertical transport of injected waste constituents included two components. The first component is advection, which arises from pressurization of the Injection Interval during the operational period. The second component is diffusion, which arises from the concentration gradient of injectate from the Injection Interval vertically upward into the overlying Injection Zone strata. The two components of transport are added together to obtain the total predicted vertical plume migration.

The vertical transport model, which includes both advection and diffusion, was designed to focus on the worst-case vertical movement of injection constituents over the total time frame (operational period and 10,000-year post-operational period). This was done by employing a one-dimensional model, whereby no dilution through lateral dispersion is allowed and invoking conservative constraints and input parameters. Also, the injectate constituent which was modeled, chromium, was modeled as a fully conservative species with no transport retardation through sorption, and no decay through hydrolysis or reaction.

In the advective component of vertical transport, the primary transport mechanism (pressure buildup within the Injection Interval during the operational period) is set at the maximum value from the beginning of operations (assumed to be July 1, 2008), through the end of the future operational period (December 31, 2020), and for an additional five years after the operational period (17.5 years total). The additional five years of advective movement was included in the calculation to account for the time required for the reservoir pressure to return to a static level. Although it is anticipated that reservoir pressure will decline rapidly at the end-of-operations, and that near static reservoir pressures will be reached in a matter of a few months, five years is included in the calculation to be conservative. The Injection Interval pressure buildup is determined from the SWIFT pressure buildup model (ExMob_Dprs_A), and is calculated to occur at the end of the future operational period (December 31, 2020), just before the well is shut in. In reality, the pressure during the majority of the operational period is significantly less, since the historical injection rates are less than the future injection rates. The result An additional is a conservatively higher value for the vertical pressure gradient. advective component arises from the buoyancy of the injectate (light density case) due to the density contrast between the injectate and native formation brine. The advective component due to the density contrast is calculated for both the operational and 10,000year post-operational periods. In this model, it is conservatively assumed that the density



contrast remains at its maximum, without allowing any decrease in the density contrast through dispersion or diffusion.

In calculating the diffusive component of vertical transport, it is assumed that the source strength within the Injection Interval remains constant at its maximum value during the entire 10,000-year post operational period. In reality, the source strength within the Injection Interval decreases after injection ceases, since no additional injectate mass is added to the Injection Interval. The result is a conservatively greater transport distance, since the concentration gradient remains at the initial maximum value during the entire 10,000-year period.

7.6.1 Advective Transport Model and Results

The vertical advective transport of the injectate is made up of two components: 1) transport due to pressure buildup within the Injection Interval during operational period; and, 2) transport due to buoyancy of injectate arising from density contrast between injectate and native formation fluid (for light density case) over entire operational and 10,000-year post-operational periods.

To ensure the most conservative case, it is assumed that the Injection Interval pressure buildup reaches the maximum value at the beginning of the operational period on July 1, 2008, and remains at this maximum value for a period of 5 years after injection has ceased (injection ceased on December 31, 2020), for a total pressure buildup period of 17.5 years at the maximum pressure. Additionally, it is assumed that the density contrast between the injectate and formation fluid remains at its maximum during the entire operational and 10,000-year post-operational periods. In this way, the advective component of transport is over-estimated.

7.6.1.1 Vertical Advection During Operational Period

The advective component of transport in general can be found through Darcy's Law written in terms of the total head gradient and hydraulic conductivity:

$$q = -K \frac{\Delta h}{\Delta l}$$
 where,
$$q = \text{Darcy velocity}$$

$$\frac{\Delta h}{\Delta l} = \text{total head gradient}$$

$$K = \text{hydraulic conductivity}$$



Vertical Head Gradient During Operational Period

The total head gradient was defined in terms of pressure buildup within the Injection Interval, elevation and buoyancy (due to a density contrast between injectate and native formation fluid):

$$\frac{\Delta h}{\Delta l} = \frac{\frac{\Delta p}{\rho g} + \Delta z + H_{\text{buoy}}}{L}$$

where.

L = distance

 Δp = pressure change across distance L

 ρg = fluid specific weight (density)

 Δz = elevation change across L

H_{buoy} = buoyant head

The quantities in the equation were specified using the conditions at the ExxonMobil facility to define the total vertical head gradient across the first containing shale sequence overlying the Injection Interval.

The distance, L, and elevation change, Δ z, were both defined as the thickness of the first, 60 feet of shale above the upper completion depth limit of 6,178 feet GL (in WDW-397) or 6,251 feet GL (in WDW-398). The total net shale thickness between the upper completion depth limit of 6,178 feet GL and the top of the Injection Interval at 5,900 feet GL is approximately 105 feet. The total net shale thickness between the upper completion depth limit of 6,251 feet GL and the top of the Injection Interval at 5,940 feet GL (log correlated) is approximately 110 feet. There are additional shale sequences within the containment interval overlying the Injection Interval (260 feet net shale thickness). Therefore, the gradient determined here is greater than would be determined for the net containing interval. This results in a conservative overestimate of the advective transport. In addition, since the elevation head gradient (Δ z/L) acts opposite to the pressure head gradient and buoyant gradient, it was omitted from the calculation. This also results in a conservative overestimate of the advective transport.

The pressure change was defined as the difference between the maximum pressure in the Injection Interval (which occurs at the end-of-operation), and the initial pressure within the Injection Interval. The SWIFT lateral pressurization model (ExMob_Dprs_A) output was used to determine the maximum Injection Interval pressure at the end-of-operation. The initial pressure within the Injection Interval was determined based on the initial



(before operation) pressure measured in the Injection Interval at WDW-397. The maximum Injection Interval pressure buildup, 716 psi (wellbore pressure), occurs at the end of the operation period at WDW-397, as shown in the SWIFT output file (ExMob_Dprs_A).

The buoyant head (H_{buoy}) is defined as a function of the maximum possible density contrast between the injectate and formation fluid (assuming light density injectate), and of the diameter of the total waste-swept pore volume (as determined through a piston-type displacement). The Frio D Sand is considered in this demonstration, since it is the shallowest interval which is utilized for injection. The waste swept pore radius, r, of the Frio D Sand was determined as follows at WDW-397:

$$V = \pi \phi r^2 h$$

Where: V

V = volume injected = (140 gpm from July 1, 2008 to December 31, 2008) + (360 gpm from January 1, 2009 to December 31, 2020)

 $V = 2,309,040,000 \text{ gal} = 308,718,648 \text{ ft}^3$ h = unit thickness = 25 feet (Frio D Sand)

 $\phi = \text{porosity} = 0.28$

 $r = \text{waste swept radius} = (V/\pi\phi h)^{1/2}$

r = 3,747 feet

With these definitions of terms, the equation now becomes:

$$\frac{\Delta h}{\Delta l} = \frac{\frac{\Delta p_{inj}}{\rho g} + \frac{\Delta \rho g D}{(\rho g)_{inj}}}{L}$$

Where:

 Δp_{inj} = injection pressure differential = 716 psi

 ρg = formation fluid density at reservoir temperature = 66.11 lb/ft³ (at reservoir temperature, 164 °F)

 $(\rho g)_{ini}$ = injectate density at reservoir temperature = 61.64 lb/ft³ (least dense waste density at 164 °F)

 $\Delta \rho g$ = maximum possible density contrast between injectate and formation fluid = 4.47 lb/ft³

D = diameter of total waste-swept pore volume by piston-type displacement = 7,494 feet

L = shale thickness = 60 feet (first 60 feet of shale above the upper completion depth limit)

The vertical head gradient across the thickness of the first shale sequence overlying the Injection Interval for the operational period was then determined using the parameters defined above:



$$\frac{\Delta h}{\Delta l} = \frac{\frac{(716 \text{ lb/in}^2)(144 \text{ in}^2/\text{ft}^2)}{66.11 \text{ lb/ft}^3} + \frac{(4.47 \text{ lb/ft}^3)(7,494 \text{ ft})}{61.64 \text{ lb/ft}^3}}{60 \text{ ft}} = 35.0 \text{ ft/ft}$$

Vertical Hydraulic Conductivity

The total head gradient calculated above, along with the vertical hydraulic conductivity for the containing shale sequence overlying the Injection Interval were used to determine the vertical Darcy velocity through the first shale sequence overlying the Injection Interval (using a shale permeability of 5×10^{-4} mD). A discussion of shale permeability is included in Section 7.3.2. The hydraulic conductivity was determined to be 3.10×10^{-6} ft/day using an injectate viscosity of 0.438 cP, and an injectate specific weight of 61.80 lb/ft³ (at reservoir conditions):

With the vertical head gradient defined from the top of the Injection Interval through the first overlying shale, and the vertical hydraulic conductivity of the shale overlying the Injection Interval, the Darcy flow velocity can be calculated from the Darcy equation as written above:

$$q = 3.10 \times 10^{-6} \text{ ft/day } (35.0 \text{ ft/ft}) = 1.09 \times 10^{-4} \text{ ft/day}$$

Using the vertical Darcy velocity determined above, and the shale porosity of 0.21, the vertical average linear velocity was determined by dividing the Darcy velocity by the porosity:

$$v = (1.09 \times 10^{-4} \text{ ft/day})/0.21 = 5.19 \times 10^{-4} \text{ ft/day}$$

The vertical advective transport was then calculated by applying the average linear velocity for the entire 12.5-year operational and 5 post-operational period (17.5 years total) in which Injection Interval pressure was elevated due to injection operations. This is an over-estimation because the maximum pressure buildup (and therefore velocity) is used for the entire combined period. In reality, the pressure gradient builds up to the maximum value over time, and then falls off sharply when injection is ceased.

Using the approach outlined above, the advective transport distance of waste into the first containing shale sequence overlying the Injection Interval is found by:



$z_{advection1} = v \cdot t$

where, $v = vertical average linear velocity = 5.19 x <math>10^{-4}$ ft/day t = advective transport period = 17.5 yr x 365.25 day/yr

 $z_{advection1} = 5.19 \times 10^{-4} \text{ ft/day} \times 17.5 \text{ yr} \times 365.25 \text{ day/yr} = 3.3 \text{ feet of advective transport during modeled period}$

7.6.1.2 Vertical Advection During 10,000-Year Post-Operational Period

As discussed above, an additional component of advective transport may also arise due to the continued density contrast between the injectate and native brine, which remains even after the operational period has ended.

Vertical Head Gradient During 10,000 Post-Operational Period

If it is assumed that the injectate is not diluted due to dispersion or other mixing, the advective transport due to this density contrast arising from the buoyant component of the head gradient as defined above can be calculated over the 10,000-year post-operational period.

$$\frac{\Delta h}{\Delta l} = \frac{\frac{(4.47 \text{ lb/ft}^3) 7,494 \text{ ft}}{61.64 \text{ lb/ft}^3}}{60 \text{ ft}} = 9.06 \text{ ft/ft}$$

The resulting Darcy flow velocity from the buoyant head component can be calculated using the vertical hydraulic conductivity as calculated above in the Darcy equation:

$$q = 3.10 \times 10^{-6} \text{ ft/day } (9.06 \text{ ft/ft}) = 2.81 \times 10^{-5} \text{ ft/day}$$

Using the vertical Darcy velocity determined above, and the shale porosity of 0.21, the vertical average linear velocity was determined by dividing the Darcy velocity by the porosity:

$$v = (2.81 \times 10^{-5} \text{ ft/day})/0.21 = 1.34 \times 10^{-4} \text{ ft/day}$$

The vertical advective transport due to the buoyant head gradient during the 10,000-year post-operational period is then calculated by applying the average linear velocity for the entire 10,000-year period.



$z_{advection2} = v \cdot t$

where, $v = vertical average linear velocity = 1.34 x <math>10^{-4}$ ft/day t = advective transport period = 10,000 yr x 365.25 day/yr

 $z_{advection2}$ = 1.34 x 10⁻⁴ ft/day x 10,000 yr x 365.25 day/yr = 504 feet advective transport during 10,000-year post-operational period due to buoyancy of injectate

The total advective transport of injectate during the operational and 10,000-year postoperational periods is the sum of the two advective transport distances:

 $Z_{\text{(advection)Total}} = z_{\text{advection1}} + z_{\text{advection2}} = 3.3 \text{ feet} + 504 \text{ feet} = 507.3 \text{ feet}$

The total advective distance, 507.3 feet, is less than the containment interval thickness of 575 feet (top of Injection Zone at 5,325 feet GL and top of Injection Interval at 5,900 feet GL), of which 260 feet is composed of shale. This is very conservative, since as stipulated in the petition parameter request in Section 2.0), injection of restricted waste shall be limited to completion intervals which are within the permitted Injection Interval and below a depth of 6,178 feet GL in WDW-397 and below a depth of 6,251 feet GL in WDW-39.

The advective transport calculated here is over-estimated due to several reasons. First, the Injection Interval pressure buildup was assumed to reach its maximum value at the beginning of injection operations on July 1, 2008, and continue at this maximum value through the post-operational fall-off period, for a total Injection Interval pressure buildup period of 17.5 years at the maximum value (in reality, the pressure builds up to its maximum value, and then falls of rapidly during the post-operational fall-off period). Secondly, the first shale sequence overlying the Injection Interval was used to define the hydraulic gradient over which vertical advection occurred. The thickness of this shale sequence, 60 feet, is only 23 percent of the 260 feet of the cumulative net shale thickness in the Injection Zone overlying the Injection Interval. Finally, it is assumed that the density contrast between the injectate and native formation fluid remains at its maximum during the entire operational and 10,000-year post-operational periods. By invoking these model considerations, the model results were conservatively overestimated.

7.6.2 Diffusive Transport Model and Results

The second component of vertical transport is diffusion which arises from the concentration gradient of injectate from the Injection Interval vertically upward into the



overlying Injection Zone strata. The governing equation for diffusive transport through a porous medium in one-dimension is given by Fick's second law (Freeze and Cherry, 1979; Daniel and Shackelford, 1988; Carslaw and Jaeger, 1959):

$$\frac{\partial \mathbf{c}}{\partial \mathbf{t}} = \mathbf{D} * \frac{\partial^2 \mathbf{c}}{\partial \mathbf{z}^2}$$

The vertical extent of molecular diffusion through a porous media in one dimension at any time, t, is calculated from the following solution (Freeze and Cherry, 1979) to Fick's second law:

$$\frac{C(z,t)}{C_0} = \text{erfc}\left[\frac{z}{\sqrt{4D^*t}}\right]$$

where:

z,t) = concentration at location z and time t;

 C_0 = initial concentration at t = 0, z = 0;

 $C(z,t)/C_0$ = inverse of concentration reduction factor = 1 x 10⁻⁵ for the ExxonMobil facility's waste;

z = diffusive plume extent = quantity to be calculated;

t = time = 10,000 years;

 D^* = effective molecular diffusivity = $D_0 \times G = 0.163 \text{ ft}^2/\text{yr}$ using:

 D_0 = molecular diffusivity of arsenic in water = 1.09 x 10⁻⁸ m²/sec = 3.70 ft²/yr;

 $G = geometric correction factor = \phi^n$ where n is approximately 2 for shales

 $\phi = porosity = 0.21$

erfc = complimentary error function = 1- erf (error function)

It should be noted that an inherent boundary condition required for the above solution is that the source strength remains constant $(C(z,t)=C_0)$ at the top of the Injection Interval for all times, namely, during the entire 10,000-year post-operational period. This is conservative since the source strength of injectate will begin to decay after the end of the operational period, and no additional mass will be introduced to the Injection Interval to keep the source strength constant at its maximum value.

$$1x10^{-5} = 1 - \text{erf} \left[\frac{z}{\sqrt{(4)(0.163)(10,000)}} \right]$$
$$0.99999 = \text{erf} \left[\frac{z}{80.7} \right]$$

from error function tables;

$$3.12 = \frac{z}{80.7}$$

$$z_{\text{diffusion}} = 252 \text{ feet}$$



The total vertical transport for the injected waste at the ExxonMobil facility, as determined using the one-dimensional analytical models for both advection, due to injection pressure buildup and density contrast, and diffusion, due to concentration gradient between the Injection Interval and overlying Injection Zone is the sum of the two:

$$Z_{total} = Z_{(advection)Total} + Z_{diffusion}$$

$$Z_{total} = 507.3 \text{ feet} + 252 \text{ feet}$$

$$Z_{total} = 759.3 \text{ feet}$$

Thus, the calculated total vertical transport distance is 759.3 feet. The top of the Frio D Sand is separated from the top of the Injection Zone by 1,288 feet of alternating sand and shale sequences, with more than 650 feet of total net shale present within the sequence. As discussed earlier in this document, ExxonMobil will stipulate that neither WDW-397 nor WDW-398 will be completed to inject into Injection Interval sands which are higher in the subsurface than 6,178 feet GL (6,200 feet KB) in WDW-397 or 6,251 feet GL (6,276 feet KB) in WDW-398. Subtracting 759.3 feet from 6,200 feet KB, places the top of vertical migration in 10,000 years at approximately 5,441 feet KB in WDW-397, which is well below the top of the permitted Injection Zone which is present at 5,347 feet KB. Subtracting 759.3 feet from 6,276 feet KB, places the top of vertical migration in 10,000 years at approximately 5,517 feet KB in WDW-398, which is well below the top of the permitted Injection Zone which is present at 5,370 feet KB. Therefore, the standard for no-migration is met for the vertical model simulation.

7.7 Molecular Diffusion Through Mud Filled Boreholes

The modeling results discussed in Section 7.6 above address the issue of vertical waste movement by advection-diffusion through a porous medium. This section assesses the extent of vertical diffusion over 10,000 years through a mud filled borehole that could penetrate the Injection Zone (Frio D Sand) and intersect the location of the 10,000 year plume.

The calculation is conservative because it assumes that full strength waste would be at the location of a mud filled borehole for 10,000 years. Also, the calculation employs a tortuosity of 0.5 and porosity of 0.9 for the drilling mud. This provides the maximum calculated vertical diffusion distance for the given molecular diffusivity.

The vertical extent of molecular diffusion through a mud filled borehole is calculated from the following solution (Freeze and Cherry, 1979) to Fick's second law:

$$\frac{C(z,t)}{C_o} = erfc \left[\frac{z}{\sqrt{4D^*t}} \right]$$

where:

C(z,t) = concentration at location z and time t; C_0 = initial concentration at t = 0, z = 0;

 $C_0 = 1 \times 10^{-5}$ for ExxonMobil's waste; 1×10^{-5} for arsenic at 5,000 mg/L

z = diffusive extent = quantity to be calculated;

t = time = 10,000 years;

 $D_o = \text{molecular diffusivity of arsenic in water} = 3.70 \text{ ft}^2/\text{yr}$;

G = geometric correction factor = 0.5 for tortuosity x 0.9 porosity (drilling mud)

 $D^* = D_0 \times G = 1.665 \text{ ft}^2/\text{yr}$

As demonstrated in the above equation, the vertical diffusive distance is a function of the concentration reduction factor and the molecular diffusivity of the compound in water. As reported previously, arsenic had the highest molecular diffusivity in water for the chemical species of interest to this demonstration. The concentration reduction factor necessary to reach the health based limit given the petitioned concentration of 5,000 mg/L is 1.00 x 10⁻⁵. Therefore, the diffusive contaminant transport was calculated as follows:



$$1.00x10^{-5} = 1 - erf \left[\frac{z}{\sqrt{(4)(1.665)(10,000)}} \right]$$
$$0.99999 = erf \left[\frac{z}{258.07} \right]$$

from error function tables;

$$3.12 = \frac{z}{258.07}$$

$$z_{diffusion} = 805 \text{ feet}$$

Following is a list of selected compounds or chemical species having large calculated vertical migration distances (calculated for the Frio D Sand). The list also shows the vertical migration distance for those selected compounds having the highest concentration reduction factor.

Chemical Name	Petitioned Concentration (mg/L)	Concentration Reduction Factor	Vertical Migration Distance (feet)
Arsenic	5,000	1.0E-05	805
Chromium	10,000	1.0E-05	757
Vanadium	400	1.0E-05	711
Nickel	100	1.0E-05	657
Lead	100	1.0E-05	596
Cadmium	500	1.0E-05	554
Mercury	200	1.0E-05	520
Barium	200,000	1.0E-05	472
o-cresol	5,000	1.0E-05	195
p-cresol	1,000	1.0E-05	195
m-cresol	5,000	1.0E-05	194
2,4-Dinitrotoluene	200	1.0E-05	179

Table 7-8 lists concentration reduction factors for constituents with assigned waste codes and includes the calculated vertical migration through a mud-filled borehole for those compounds for which molecular diffusivity information is available. The maximum calculated total vertical transport distance is approximately 805 feet (Frio D Sand). As discussed earlier in this document, neither WDW-397 nor WDW-398 will be completed to inject into Injection Interval sands which are higher in the subsurface than 6,178 feet GL (6,200 feet KB) in WDW-397 or 6,251 feet GL (6,276 feet KB) in WDW-398.



Subtracting 805 feet from 6,200 feet KB, places the top of vertical migration in 10,000 years at approximately 5,395 feet KB in WDW-397, which is below the top of the permitted Injection Zone which is present at 5,347 feet KB. Subtracting 805 feet from 6,276 feet KB, places the top of vertical migration in 10,000 years at approximately 5,471 feet KB in WDW-398, which is below the top of the permitted Injection Zone which is present at 5,370 feet KB. Therefore, the standard for no-migration is met for the vertical model simulation with respect to a mud-filled borehole.

7.8 Model Conclusions

This modeling effort provides a demonstration of "no-migration" in accordance with applicable regulations. This has been accomplished by demonstrating that the ExxonMobil facility's injected waste will not migrate out of the Injection Zone and will be contained both vertically and laterally within the Injection Zone for a period of at least 10,000 years.

The modeling accounts for: (1) Injection Interval pressurization during the operational period; (2) end-of-operations light density injectate lateral waste transport; (3) post-operation light density injectate 10,000-year lateral waste transport; (4) end-of-operations heavy density injectate lateral waste transport; (5) post-operation heavy density injectate 10,000-year lateral waste transport; and (6) vertical waste transport. Conservative numerical and analytical models have been constructed and used to determine the maximum pressure buildup, and lateral and vertical waste transport distances. The modeling results demonstrate that no harm or impairment to the environment will occur from continued injection operations at the ExxonMobil facility, through either endangerment (Injection Interval pressurization), lateral waste transport (up-dip or downdip) or vertical waste transport.

For the Frio Formation Injection Interval, lateral (low density) plume migration is depicted on Plates 7-11, 7-14, 7-14A, 7-17, 7-17A, H-1 and H-2. The **composite** low density injectate model results (ExMob_D_C, ExMob_EF, ExMob_EF_398, ExMob_AB, ExMob_AB_398, ExMob_EF_S, ExMob_EF_S_398, ExMob_AB_S, and ExMob_AB_S_398) indicate that, for a 1 x 10⁵ order of magnitude reduction in the initial concentration, the end-of-operations (12/31/2020) is approximately 20,800 feet long (east west) and approximately 18,750 feet wide(north-south). In 10,000 years, the **composite** light density waste plume will migrate up-dip and collect within, and around, the structural high created by the presence of the Clinton Dome Salt Dome. The light density plume extends approximately 48,200 feet up gradient, from WDW-397, and extends laterally approximately 28,600 feet at the waste plumes widest point.

For the Frio Formation Injection Interval, lateral (high density) plume migration is depicted on Plates 7-20, 7-22, 7-22A, 7-24 and 7-24A. The **composite** high density injectate model results (ExMob_D HiDens, ExMob_EF HiDens, ExMob_EF_398 HiDens, ExMob_AB HiDens and ExMob_AB_398 HiDens) indicate that the end-of-operations waste plume (for a 1 x 10⁵ order of magnitude reduction in the initial



concentration) is approximately 18,200 feet long and approximately 17,200 feet wide. In 10,000 years, the **composite** injected waste plume extends 39,200 feet up-gradient and 19,300 feet down-gradient from the injection wells (after repositioning the plume to account for background flow in the injection interval) and is approximately 22,400 feet wide at its widest point after 10,000 years.

Injection interval pressure buildup isopleths are depicted on Figures 7-9, 7-11 and 7-13. The calculated cone of endangering influence is defined as that area around the ExxonMobil injection well(s) within which the modeled reservoir pressure increase due to injection operations exceeds 281 psi. For the SWIFT pressure model run ExMob Dprs A Pressure, the maximum pressure buildup in the grid block cell in which WDW-397 is located occurs at the end-of-operations (December 31, 2020) and is 594 psi. For the SWIFT pressure model run ExMob EF Pressure A, the maximum pressure buildup in the grid block cell in which WDW-397 is located occurs at the end-ofoperations (December 31, 2020) and is 398 psi. For the SWIFT pressure model run ExMob AB Pressure, the maximum pressure buildup in the grid block cell in which WDW-397 is located occurs at the end-of-operations (December 31, 2020) and is 453 psi. The cone of endangering influence is greatest for the Frio D Sand pressure model The cone of endangering influence extends northeast to the Frio D Sand pinchout, to the trace of Fault B to the southeast, approximately 4,800 feet to the southwest, and approximately 4,200 feet to the northwest.

A conservative analytical model was used to determine the vertical advective transport resulting from the pressure buildup during the historical and projected operational periods. The results indicate that the vertical advective transport during the operational period would be 507.3 feet above the top of the Frio D Sand within the Injection Interval. In addition, 252 feet of vertical migration was calculated by the 10,000-year molecular diffusion analytical model for arsenic, for a total modeled predicted vertical migration in 10,000 years of 759.3 feet above the top of Frio D Sand within the Injection Interval. The vertical distance between the top of the stipulated completion interval [6,178 feet GL (6,200 feet KB) in WDW-397 and 6,251 feet GL (6,276 feet KB) in WDW-398] and the top of the Injection Zone is a minimum 853 feet.

A conservative analytical model was also used to determine the vertical transport resulting from the vertical migration through a mud-filled borehole. The results indicate that the vertical transport during the 10,000-year modeled timeframe would be 805 feet



above the top of the Injection Interval. The vertical migration was calculated by the 10,000-year molecular diffusion analytical model for arsenic (worst case constituent). The vertical distance between the top of the stipulated completion interval [6,178 feet GL (6,200 feet KB) in WDW-397 and 6,251 feet GL (6,276 feet KB) in WDW-398] and the top of the Injection Zone is a minimum 853 feet.

In conclusion, the modeling results demonstrate no harm to the environment will occur from continued operations at the facility resulting from endangerment or migration of waste. All of the artificial penetrations located within the boundaries of the waste plumes are plugged or constructed to prevent the migration of waste from the Injection Zone to satisfy the no-migration standard.

REFERENCES

Adams, E.E., and L.W. Gelhar, 1992, "Field Study of Dispersion in a Heterogeneous Aquifer: 2. Spatial Moments Analysis", <u>Water Resources Research</u>, v. 28, n. 12, p. 3293-3307.

Anderson, M.P., 1984, Movement of Contaminants in Groundwater: Groundwater Transport-Advection and Dispersion: Groundwater Contamination, National Academy Press, Washington, D.C., p. 37-45.

Barker, S. E., 1981, Determining the Area of Review for Hazardous Waste Disposal Wells: M.S. Thesis, University of Texas at Austin.

Baroid, 1931, Composition and method for dual function soil grouting excavating or boring fluid, Baroid Corporation, 1931.

Bethke, C. M., 1986, Inverse hydrologic analysis of the distribution and origin or Gulf Coast-type geopressured zones: Journal of Geophysical Research, 91, 6535-6545 (also 93, 9211).

Borst, R. L., 1983, Methods of Calculating Shale Permeability: Society of Petroleum Engineers, Paper No. 11768.

Bryant, W. D., W. R. Hoffman, and P. Trabant, 1975, Permeability of Unconsolidated and Consolidated Marine Sediments, Gulf of Mexico: Marine Geotechnology, v. 1, p. 1-14.

Carslaw, H. S., and J. C. Jaeger, 1959, Conduction of heat in Solids, Oxford University Press, Oxford England, 2nd Edition, 510 p.

Clark, J. E., M. R. Howard, and D. K. Sparks, 1987, Factors that can Cause Abandoned Wells to Leak as Verified by Case Histories from Class II injection, Texas Railroad Commission files: International Symposium on Subsurface Injection of Oilfield Brines, Underground Injection Practices Council, New Orleans, La., p. 166-223.

Clark, J. E., 1989, Groundwater Flow in Deep Saline Aquifers: Proceedings of the International Symposium on Class I and II Injection Well Technology, p. 151-176.

Clark, J. E., P. W. Papadeas, D. K. Sparks, and R. R. McGowen, 1991, Gulf Coast Borehole Closure Test Well, Orangefield, Texas, *in* Proceedings of the UIPC Underground Injection Practices Council, 1991 Winter and Summer Meetings: Underground Injection Practices Council, Oklahoma City, OK, p. 219-238.

Collins, R. E. 1986, Technical basis for area of review, an engineering study prepared for Chemical Manufacturers Association: CMA Reference Number 80 160 000 4. (0110859).



Constant, W. D. and D. A. Clark, 1989, Evaluation of Shale Permeability Associated With Deep-Well Hazardous Waste Injection Zone Confining Layers: Proceedings of the International Symposium on Class I and II Injection Well Technology, pp. 257-280.

CRC Handbook of Chemistry and Physics, 1979, Lide, D. R., editor, CRC Press, Boston, 58th Edition.

CRC Handbook of Chemistry and Physics, 1991, Lide, D. R., editor, CRC Press, Boston, 83th Edition.

Daniel, D. E., and C. D. Shackelford, 1988, Disposal Barriers that Release Contaminants Only by Molecular Diffusion, Nuclear and Chemical Waste Management, v. 8, p. 299-305.

Davis, S.N., D.J. Campbell, H.W. Bentley, and T.J. Flynn, 1985, Ground-Water Tracers, National Water Well Assn. and U.S. EPA Robert S. Kerr Environmental Research Laboratory, U.S. EPA and University of Arizona cooperative agreement CR-81003601-0, 200 p.

Davis, K. E., 1986, Factors Effecting the Area of Review for Hazardous Waste Disposal Wells: Proceedings of the International Symposium on Subsurface Injection of Liquid Wastes, New Orleans, National Water Well Association, Dublin, OH, p. 148-194.

Domenico, P. A., and F. W. Schwartz, 1990, Physical and Chemical Hydrogeology, J. Wiley and Sons, New York, 824 p.

Earlougher, R.C., 1977, Advances in Well Test Analysis: H.L. Doherty Series, Monograph Vol. 5, Society of Petroleum Engineers of AIME, 264 p.

Finley, N.C., and M. Reeves, 1982, SWIFT Self-Teaching Curriculum: NUREG/CR-1968, SAND81-0410, Sandia National Laboratories, Albuquerque, NM, 169 p.

Freeze, A.R., and J.A. Cherry, 1979, Groundwater: Prentice-Hall, Inc., Englewood Cliffs, N.J., 604 p.

Gelhar, L.W., 1986, Stochastic Subsurface Hydrology From Theory to Applications: Water Resources Research, v. 22, n. 9, p. 135s-145s.

Gelhar, L.W., A.L. Gutjahr, and R.L. Naff, 1979, Stochastic Analysis of Macrodispersion in a Stratified Aquifer: Water Resources Research, v. 15, p. 1387-1397.

Gelhar, L. W., C. Welty, and K. R. Rehfeldt, 1992, A Critical Review of Data on Field-Scale Dispersion in Aquifers, Water Resources Research, v. 28, p. 1955-1974.

Hewlett Packard, 1982, HP41C Petroleum Fluids Pac Manual, Hewlett Packard Corporation, Fort Collins, Colorado, 199 p.



HSI Geotrans, 2000, Swift for Windows Sandia Waste Isolation Flow and Transport Model, 45060 Manekin Pl, Suite 100 C, Sterling, VA 20166.

Intercomp Resources Development and Engineering, Inc., 1976, Development of Model for Calculating Disposal in Deep Saline Aquifers, Parts I and II: USGS/WRI 76-61, National Technical Information Service, Washington, D.C., 236 p.

Johnson, R. L., J. A. Cherry, and J. F. Pankow, 1989, Diffusive Contaminant Transport in Natural Clay: A field Example and Implications for Clay-Lined Waste Disposal Sites: Environmental Science and Technology, v. 23, p. 340-349.

Johnston, O. C., and Green, C. J., 1979, Investigation of Artificial Penetrations in the Vicinity of Subsurface Disposal Wells: Texas Department of Water Resources.

Johnston, O. C. and B. K. Knape, 1986, Pressure Effects of the Static Mud Column in Abandoned Wells: Texas Water Commission, Limited Publication 86-06, Austin, Texas.

Lerman, A., 1979, Geochemical Processes Water and Sediment Environments: John Wiley and Sons, New York, N.Y., 481 p.

MacKay, D.M., P.V. Roberts, and J.A. Cherry, 1985, Transport of Organic Contaminants in Groundwater: Environmental Science and Technology, v. 19, n. 5, p. 384-392.

Magara, K., 1969, "Porosity-Permeability Relationship of Shale," Society of Petroleum Engineers Paper No. 2430.

Neuman, S. P., 1993, Comment on A Critical Review of Data on Field-Scale Dispersion in Aquifers by L. W. Gelhar, C. Welty, and K. R. Rehfeldt, Water Resources Research, v. 29, p. 1863-1865.

Neuman, S. P., 1990, Universal Scaling of Hydraulic Conductivities and Dispersivities in Geologic Media, Water Resources Research, v. 26, p. 1749-1758.

Numbere, D., W. E. Brigham, and M. B. Standing, 1977, Correlations for Physical Properties of Petroleum Reservoir Brines, Petroleum Research Institute, Stanford University, November, 1977, p. 16.

Perry, R.H., 1984, Perry's Chemical Engineers' Handbook: Sixth Edition, McGraw-Hill Book Company, New York, N.Y.

Perry, R.H., 1979, Perry's Chemical Engineers' Handbook: McGraw-Hill Book Company, New York, N.Y.

Perry, R.H., 1997, Perry's Chemical Engineers' Handbook: Seventh Edition, McGraw-Hill Book Company, New York, N.Y.



Reeves, M.D., and D.S. Ward, 1986, SWIFT II Self-Teaching Curriculum: NUREG/CR-3925, Sandia National Laboratories, Albuquerque, NM, 105 p.

Reeves, M.D., D.S. Ward, N.D. Johns, and R.M. Cranwell, 1986, Theory and Implementation for SWIFT II, the Sandia Waste-Isolation Flow and Transport Model for Fractured Media, Release 4.84: NUREG/CR-3328 or SAND83-1159, Sandia National Laboratories, Albuquerque, NM, 189 p.

Reeves, M.D., D.S. Ward, P.A. Davis, and E.J. Bonano, 1987, SWIFT II Self-Teaching Curriculum: Illustrative Problems for the Sandia Waste-Isolation Flow and Transport Model for Fractured Media: NUREG/CR-3925 or SAND84-1586, Sandia National Laboratories, Albuquerque, NM, 94 p.

Sandia Technologies, LLC., 2000, Merisol 2000 HWDIR Exemption Petition Reissuance Request.

URM 1986, Technical Report.

Ward, D.S., M. Reeves, and L.E. Duda, 1984, "Verification and Field Comparison of the Sandia Waste-Isolation Flow and Transport Model (SWIFT)", <u>NUREG/CR-3316 or SAND83-1154</u>, Sandia National Laboratories, Albuquerque, NM.

Ward, D.S., M. Reeves, and L.E. Duda, 1984, Verification and Field Comparison of the Sandia Waste-Isolation Flow and Transport Model (SWIFT): NUREG/CR-3316 or SAND83-1154, Sandia National Laboratories, Albuquerque, NM.

Ward, D.S., D.R. Buss, J.W. Mercer, and S.S. Hughes, 1987, Evaluation of a Groundwater Corrective Action at the Chem-Dyne Hazardous Waste Site Using a Telescopic Mesh Refinement Modeling Approach: Water Resources Research, v. 23, n. 4, p. 603-617.

Warner, D. L., and T. Syed, 1986, Confining layer study-supplemental report: prepared for U.S. EPA Region V, Chicago, Illinois

Warner, D. L., 1988, Abandoned oil and gas industry wells and their environmental implications: prepared for the American Petroleum Institute.

Schlumberger, 1989, Cased Hole Log Interpretation Principles/Applications: Schlumberger Educational Services.

Xu, M. and Y Eckstein, 1995, Use of Weighted Least-Squares Method in Evaluation of the Relationship Between Dispersivity and Field Scale, Ground Water, v. 33, pp 905-90.



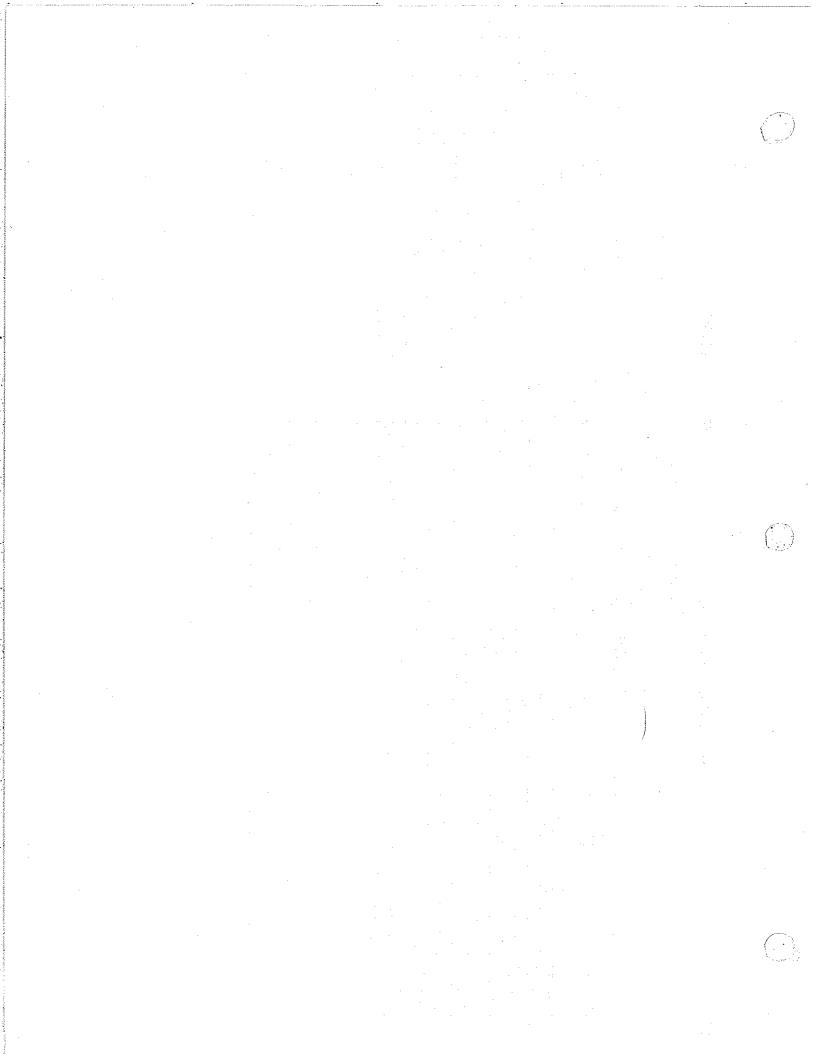


TABLE 7-4

SWIFT MODEL PARAMETER VALUES

Exxon Mobil Corporation Pasadena, Texas

			FRIO	FRIO	FRIO	
PARAMETER	SYMBOL, UNITS	SWIFT MNEMONIC	D SAND	E&F SAND	A&B SAND	
NATIVE FORMATION FLUID						
Specific Gravity	γ (60/60, 1 atm; surface)		1,0803	1.0803	1.0906	
Density	p (T, P), lb/ft3 (at reference temperature)	BWRN	66.11	66,02	66.55	
Viscosity	μ (T, P), cP (at reference temperature)	VISRR .	0.507	0.487	0.495	
Compressibility	C (T, P), psi-1	CW	2.43E-06	2.43E-06	2.39E-06	
WASTE, Least Dense						
Specific Gravity	γ (T/60, p) [γ (60/60, atm; surface):		1.00	1.00	1,00	
Density	ρ(T, P), lb/ft3 (at reference temperature)	BWRI	61.54	61.45	61.38	
Viscosity	μ (T, P), cP (at reference temperature)	VISIR	0,378	0.364	0.353	
WASTE, Most Dense						
Specific Gravity	γ (T/60, P) [γ 60/60, 1 atm; surface):	·	1,05	1.05	1.05	
Density	ρ (T, P), lb/ft3 (at reference temperature)	BWRI ·	64.34	64.25	64,18	
Viscosity	μ (T, P), cP (at reference temperature)	VISIR	0.452	0.439	0.428	
INJECTION INTERVAL	y :					
Reference Depth	D, ft (subsea)	HINIT	6,618	6,755	6,990	
Initial Pressure (at reference depth)	P, psia	PBWR, PINIT	2,884	2,944	3,047	
Temperature (at reference depth)	T, ° F	TBWR, TRR, TIR, TD, TO	164	169	173	
Hydraulic Conductivity						
Plume movement:	K (kρ/μ), feet/day	KX, KY	11.46	11.915	11,816	
Pressurization:	K (kρ/μ), feet/day	KX, KY	3.725	3.872	3.840	
Rock Density	p, lb/ft ³	BROCK	165	165	165	
Porosity	φ.	PHI	0.28	0.28	0.28	
Rock Compressibility	C, psi ⁻¹	CR	3.20E-06	3.20E-06	3.20E-06	
Dispersivity						
Longitudinal	α_L , feet	ALPHL	100	100	100	
Transverse	α_T , feet	ALPHT	10	10	10	
Molecular Diffusivity (effective)	$D^* \cdot \hat{\pi}^2 / d (D^* = D^\circ \tau \phi)$	DMEFF	7.93E-04	8.33E-04	8.24E-04	
Molecular Diffusivity (free water)	D°, ft ² /d (free water)		1.01E-02	1,06E-02	1.05E-02	
Tortuosity					l	
Sand	τ		0.28	0.28	0.28	
Shale	τ	And the second	0.21	0.21	0.21	
Thickness	ft	DELZ(K), UTH	25	150	125	
Well Index	ft²/day	WI .				
High Conductivity	ft²/day	WI	589.9	3,680.1	3,041.2	
Low Conductivity	ft²/day	WI	191.8	1,195.9	988.4	
Carter-Tracy Boundary					1	
Permeability-Thickness (high conductivity)	Kh	KH	286.5	1,787.3	1,477.0	
Permeability-Thickness (low conductivity)	Kh	KH	93.1	580.0	480.0	
Porosity-Thickness	φh	РНІН	7	42	35	
Coefficient of thermal expansion	ok-1	CTW	0,00	0.00	0.00	
Fluid heat capacity	BTU/lb-°F	CPW	. 1	.1	1	
Rock heat capacity	BTU/lb-°F	CPR	. 1	1	1	
Thermal conductivity	BTU/ft-d-°F	UKTX, UKTY, UKTZ	116	116	116	



TABLE 7-5

HISTORICAL RESERVOIR TEST RESULTS OF MERISOL USA LLC INJECTION WELLS

Exxon Mobil Corporation Pasadena, Texas

Merisol USA LLC WDW-147 (Frio E&F Sand)

Date	Test Type	Analysis	Transmissibility	k*
		Technique	kh/μ, mD-ft/cP	mD
Mar-90 /	Fall-off	Semilog	593,041	1,469
Dec-91	Fall-off	Semilog	858,516	2,127
Sep-93	Fall-off	Semilog	691,141	1,712
Sep-94	Fall-off	Semilog	524,815	1,300
Sep-95	Fall-off	Semilog	682,259	1,690
Dec-96	Fall-off	Semilog	806,196	1,997
Sep-97	Fall-off	Semilog	641,666	1,589
Oct-98 /	Fall-off	Semilog	573,649	1,421
May-01	Fall-off	Semilog	984,633	2,439
Jul-02 /	Fall-off	Semilog	779,498	1,931
Jul-03 /	Fall-off	Semilog	645,522	1,599
Aug-04 //	Fall-off	Semilog	831,523	2,060
Jul-05 //	Fall-off	Semilog	945,119	2,341
Sep-06 '	Fall-off	Semilog	775,447	1,921
* assumes a reservoir thickness	of 218 feet, and a fluid viscosit	y of 0.54 cp	Average	
i .			Transmissibility	738,073
			Minimum k	1,300
		•	Average k	1,828
<u></u>			Maximum k	2,439

Merisol USA LLC WDW-319 (Frio A&C and Frio C Sands)

Date	Test Type	Analysis	Transmissibility	k*
		Technique	kh/μ, mD-ft/cP	mD
Sep-00	Fall-off	Semilog	459,910	1,035
Sep-01	Fall-off	Semilog	131,027	860
Mar-02	Fall-off	Semilog	372,018 /	1,245
Mar-03	Fall-off	Semilog	343,834	1,151
Apr-04	Fall-off	Semilog	349,549	1,170
Jul-05	Fall-off	Semilog	384,198	1,286
Sep-06	Fall-off	Semilog	288,875	967
Aug-07	Fall-off	Semilog	258,137	864
assumes a reservoir thickness o	f 245 feet, and a fluid viscosi	ty of 0.82 cP	Average	
(Sept 2000 reservoir thickness of	-		Transmissibility	323,444
(Sept 2001 reservoir thickness of	f 125 feet and fluid viscosity	of 0.82 cP)	Minimum k	860
			Average k	1,072
			Maximum k	1,286

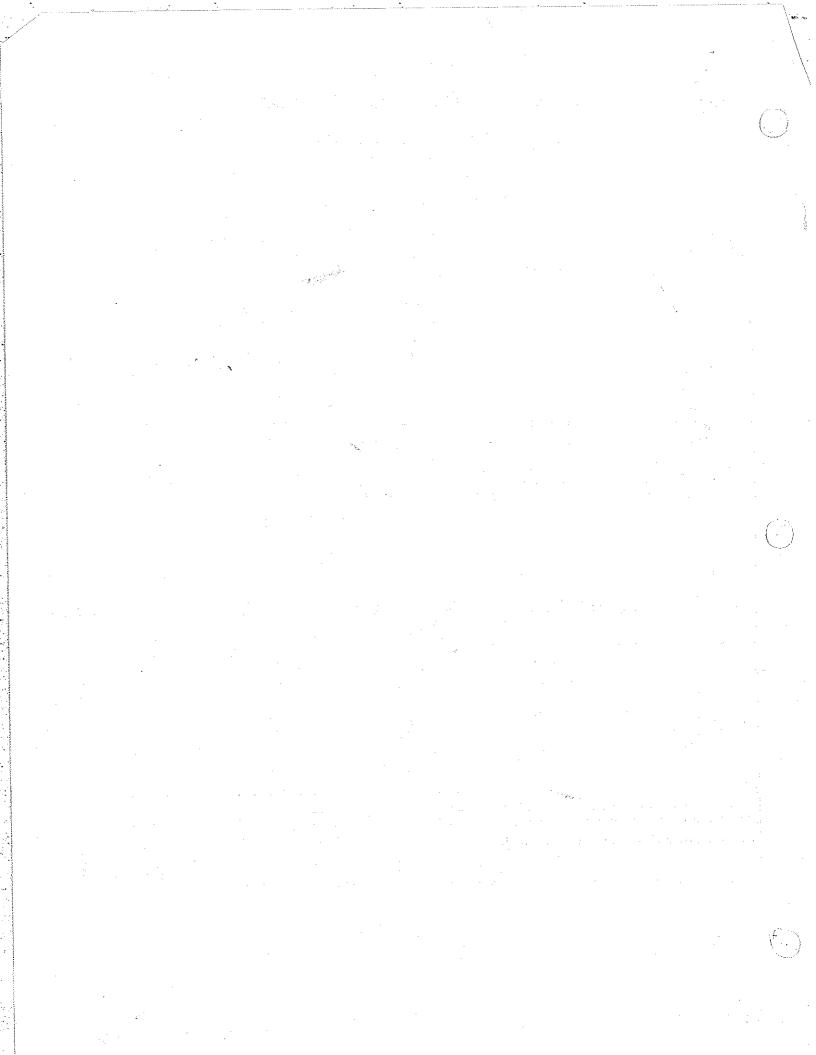


TABLE 7-6

DEPTH, PRESSURE, VOID RATIO, POROSITY AND DENSITY RELATIONSHIPS FOR A TYPICAL SILTY CLAY FROM THE GULF OF MEXICO

Exxon Mobil Corporation Pasadena, Texas

Depth of	Cumulative	Void		Density of Saturated
Sediments, m	Pressure, kPa	Ratio	Porosity	Sediments, mg/m ³
0	· 0	4.05	0.80	1.36
10	30	3.04	0.75	1.44
20	70	2.54	0.71	1.50
30	120	2.20	0.68	1.55
40	160	1.98	0.66	1.59
50	220	1.84	0.64	1.61
70	340	1.67	0.62	1.65
100	530	1.52	0.60	1.69
150	880	1.30	0.56	1.75
200	1,250	1.19	0.54	1.79
300	2,040	1.02	0.50	1.85
400	2,890	0.90	0.47	1.90
500	3,790	0.83	0.45	1.94
600	4,710	0.76	0.43	1.97
700	5,670	0.71	0.41	2.00
800	6,650	0.67	0.40	2.02
900	7,660	0.64	0.39	2.04
1,000	8,690	0.60	0.37	2.07
1,200	10,810	0.53	0.34	2.11
1,400	13,030	0.47	0.32	2.15
1,600	15,330	0.43	0.30	2.19
1,800	17,690	0.39	0.28	2.22
2,000	20,100	0.36	0.26	2.25
2,500	26,370	0.29	0.23	2.31
3,000	32,920	0.24	0.19	2.36
4,000	46,700	0.18	0.15	2.44
5,000	61,130	0.13	0.11	2.50

(from Bryant and others, 1975)



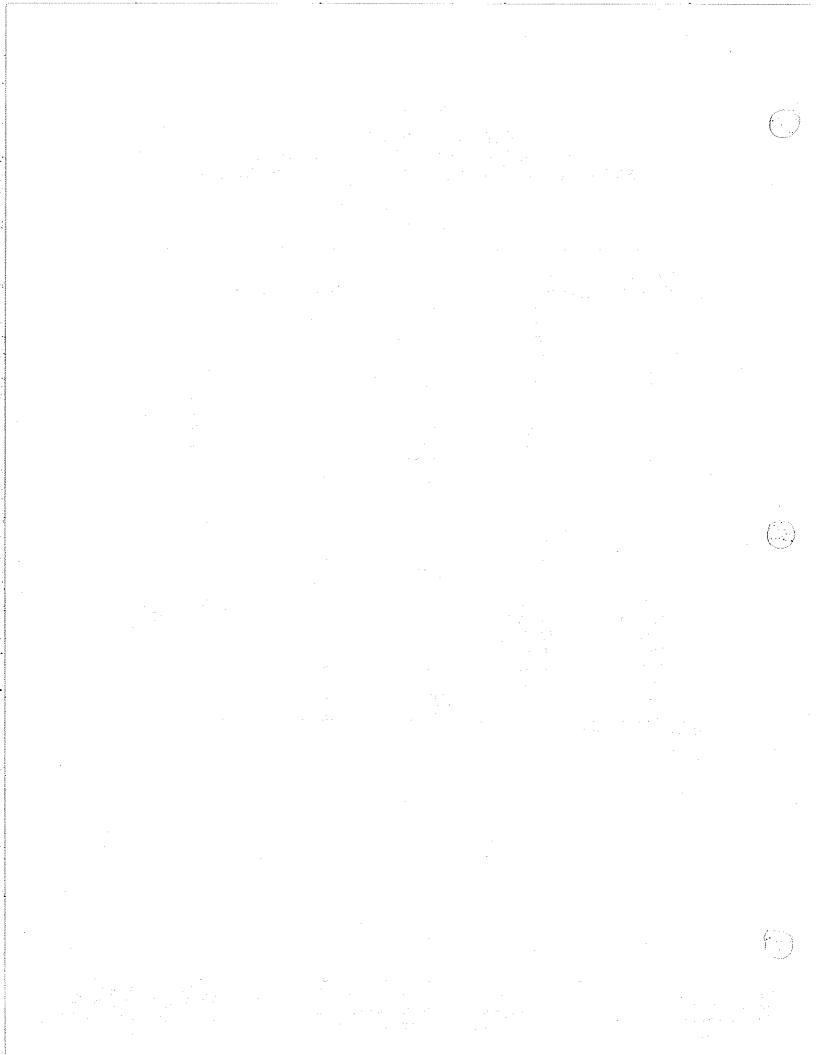


TABLE 7-7

EQUATIONS FOR PERMEABILITY-POROSITY RELATIONSHIPS

Exxon Mobil Corporation Pasadena, Texas

Sediment Group	Sediment Type	Equation
1	80% clay	$k=(e)^{n(15.05)-27.37}$
2	60%-80% clay	$k=(e)^{n(14.18)-26.50}$
3	silty clays and clayey silts	$k=(e)^{n(15.59)-26.65}$
4	sandy clays and silts	$k=(e)^n(17.51)-26.93$
all data		$k=(e)^{n(14.30)-26.30}$
		Note: n = porosity (fraction)

k = coefficient of permeability in cm/s (from Bryant and others, 1975)

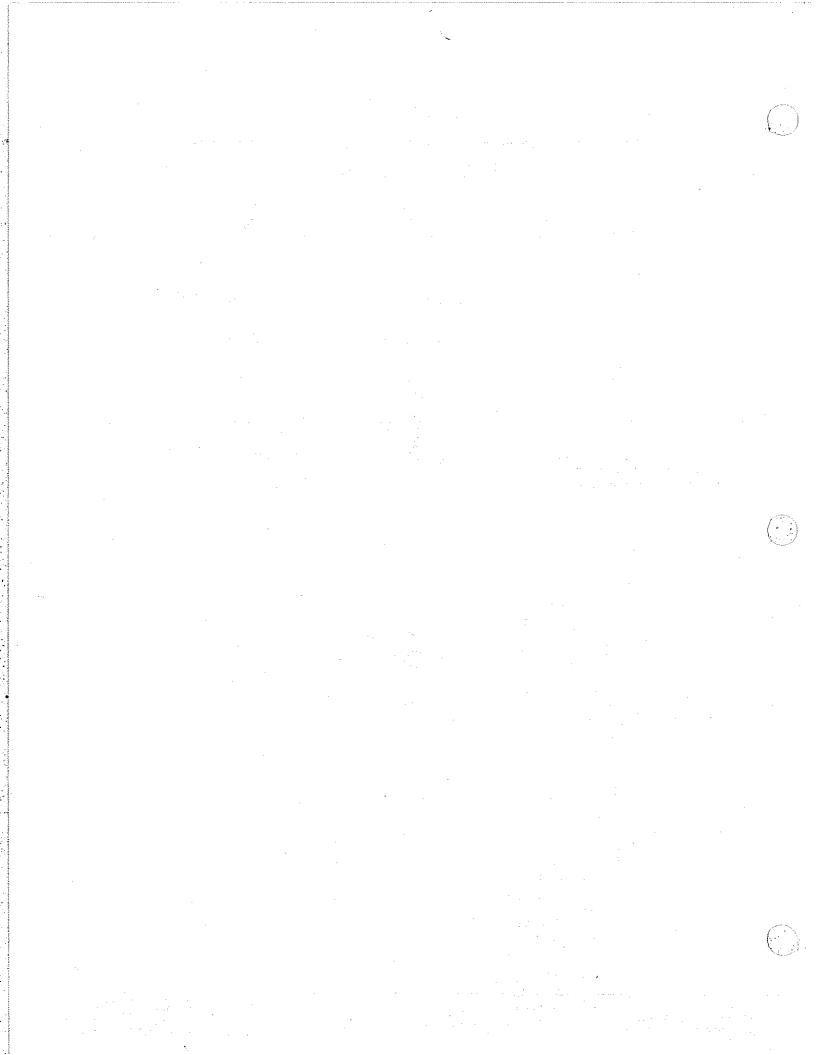


TABLE 7-8

VERTICAL DIFFUSION DISTANCES FOR PETITIONED CONSTITUENTS THROUGH ROCK AND MUD-FILLED BOREHOLES

Exxon Mobil Corporation Pasadena, Texas

		-				ECULAR DIFFUS				A STATE OF THE STA	
Chemical Name	Waste Codes	Land Ban Health Based Limit (mg/L)	Detection Limit (1) (mg/L)	Injected Fluid Maximum Concentration (2) (mg/L)	Concentration Reduction Factor (C/Co)	Molecular Diffusivity In Water (3) (cm2/sec)	Molecular Diffusivity In Water (ft2/day)	Effective Diffusion Coefficient in Injection Interval (ft2/day)	Effective Diffusion Coefficient in Containment Interval (ft2/day)	Vertical Diffusion Distance Through Containment Interval (ft)	Vertical Diffusion Distance Through Mud-Filled Borehole (ft)
Arsenic	D004, F039	5.0E-02		5,000	1.0E-05	1.09E-04	1.01E-02	7.93E-04	4,46E-04	252	805
Chromium	D007, F039	1.0E-01		10,000	1.0E-05	9.63E-05	8.95E-03	7.02E-04	3.95E-04	237	757
Vanadium	F039	2.1E+01		210,000	1.0E-04	8.48E-05	7.89E-03	6.19E-04	3.48E-04	196	626
Nickel	F039		1.0E-03	100	1.0E-05	7.25E-05	6.75E-03	5.29E-04	2.98E-04	206	657
Lead	D008, F039		1.0E-03	100	1.0E-05	5.96E-05	5.54E-03	4.34E-04	2.44E-04	186	596
Cadmium	D006, F039	5.0E-03		500	1.0E-05	5.16E-05	4.80E-03	3.76E-04	2.12E-04	173	554
Mercury	D009, F039	2.0E-03		200	1.0E-05	4.55E-05	4.23E-03	3.32E-04	1.87E-04	163	520
Barium	D005, F039	2.0E+00		200,000	1.0E-05	3.74E-05	3.47E-03	2.72E-04	1.53E-04	148	472
o-cresol	D024, F039	5.0E-02	Ī	5,000	1.0E-05	6.40E-06	5.95E-04	4.66E-05	2,62E-05	61	195
o-cresol	D025, F039		1.0E-02	1,000	1.0E-05	6.37E-06	5.92E-04	4.64E-05	2.61E-05	61	195
n-cresol	D023, F039	5.0E-02		5,000	1.0E-05	6.35E-06	5.90E-04	4.63E-05	2.60E-05	61	194
2,4-Dinitrotoluene	D030, F039	2.0E-03		200	1.0E-05	5.38E-06	5.00E-04	3,92E-05	2.21E-05	56	179

FRIO E&F SAND MOLECULAR DIFFUSION DISTANCES											
Chemical Name	Waste Codes	Land Ban Health Based Limit (mg/L)	Detection Limit (1) (mg/L)	Injected Fluid Maximum Concentration (2) (mg/L)	Concentration Reduction Factor (C/Co)	Molecular Diffusivity In Water (3) (cm2/sec)	Molecular Diffusivity In Water (ft2/day)	Effective Diffusion Coefficient in Injection Interval (ft2/day)	Effective Diffusion Coefficient in Containment Interval (ft2/day)	Vertical Diffusion Distance Through Centainment Interval (ft)	Vertical Diffusion Distance Through Mud-Filled Borehole (ft)
Arsenic	D004, F039	5.0E-02		5,000	1.0E-05	1.14E-04	1.06E-02	8.33E-04	4.68E-04	258	824
Chromium	D007, F039	1.0E-01	1	10,000	1.0E-05	1.01E-04	9.39E-03	7.37E-04	4.14E-04	243	775
Vanadium	F039	2.1E+01		210,000	1.0E-04	8.90E-05	8.28E-03	6.49E-04	3.65E-04	201	642
Nickel	F039		1.0E-03	100	1.0E-05	7.61E-05	7.08E-03	5.55E-04	3.12E-04	211	673
Lead	D008, F039		1.0E-03	100	1.0E-05	6.25E-05	5.82E-03	4.56E-04	2.56E-04	191	610
Cadmium	D006, F039	5.0E-03		500	1.0E-05	5.42E-05	5.04E-03	3.95E-04	2.22E-04	178	568
Mercury	D009, F039	2.0E-03		200	1.0E-05	4.78E-05	4.44E-03	3.48E-04	1.96E-04	167	533
Barium	D005, F039	2.0E+00		200,000	1.0E-05	3.92E-05	3.65E-03	2.86E-04	1.61E-04	151	483
o-cresol	D024, F039	5.0E-02		5,000	1.0E-05	6.40E-06	5.95E-04	4.66E-05	2.62E-05	61	195
p-cresol	D025, F039		1.0E-02	1,000	1.0E-05	6.37E-06	5.92E-04	4.64E-05	2.61E-05	61	195
m-cresol	D023, F039	5.0E-02		5,000	1.0E-05	6.35E-06	5.90E-04	4.63E-05	2.60E-05	61	194
2,4-Dinitrotoluene	D030, F039	2.0E-03		200	1.0E-05	5.38E-06	5.00E-04	3.92E-05	2.21E-05	56	179

FRIO A&B SAND MOLECULAR DIFFUSION DISTANCES											
Chemical Name	Waste Codes	Land Ban Health Based Limit (mg/L)	Detection Limit (1) (mg/L)	Injected Fluid Maximum Concentration (2) (mg/L)	Concentration Reduction Factor (C/Co)	Molecular Diffusivity In Water (3) (cm2/sec)	Molecular Diffusivity In Water (ft2/day)	Effective Diffusion Coefficient in Injection Interval (ft2/day)	Effective Diffusion Coefficient in Containment Interval (ft2/day)	Vertical Diffusion Distance Through Containment Interval (ft)	Vertical Diffusion Distance Through Mud-Filled Borehole (ft)
Arsenic	D004, F039	5.0E-02		5,000	1.0E-05	1.13E-04	1.05E-02	8.24E-04	4.64E-04	257	820
Chromium	D007, F039	1.0E-01		10,000	1.0E-05	1.00E-04	9.30E-03	7.29E-04	4.10E-04	242	772
Vanadium	F039	2.1E+01	The second second second second	210,000	1.0E-04	8.81E-05	8.20E-03	6.43E-04	3.62E-04	200	638
Nickel	F039		1.0E-03	100	1.0E-05	7.54E-05	7.01E-03	5.50E-04	3.09E-04	210	670
ead	D008, F039		1.0E-03	100	1.0E-05	6.19E-05	5.76E-03	4.51E-04	2.54E-04	190	607
Cadmium	D006, F039	5.0E-03		500	1.0E-05	5.36E-05	4.99E-03	3.91E-04	2.20E-04	177	565
Mercury	D009, F039	2.0E-03		200	1.0E-05	4.73E-05	4.40E-03	3.45E-04	1.94E-04	166	530
Barium	D005, F039	2.0E+00		200,000	1.0E-05	3.88E-05	3.61E-03	2.83E-04	1.59E-04	150	481
-cresol	D024, F039	5.0E-02		5,000	1.0E-05	6.40E-06	5.95E-04	4.66E-05	2.62E-05	61	195
-cresol	D025, F039		1.0E-02	1,000	1.0E-05	6.37E-06	5.92E-04	4.64E-05	2.61E-05	61	195
n-cresol	D023, F039	5.0E-02	Name and Advantage of the State	5,000	1.0E-05	6.35E-06	5.90E-04	4.63E-05	2.60E-05	61	194
,4-Dinitrotoluene	D030, F039	2.0E-03	Aller	200	1.0E-05	5.38E-06	5.00E-04	3.92E-05	2.21E-05	56	179

RfD - Reference Dose

RSD- Risk Specific Dose

MCL taken from Drinking Water Regulations and Health Advisories, 10/96.

RFD and RSD taken from IRIS, 3/97.

 $RfD (mg/L) = RfD (mg/kg/day) \times 70 kg / 2L/day$

- (1) The Practical Quantitation Limit (PQL) was employed when available, using a ground water matrix.
- (2) Maximum yearly averages. See Appendix K for measured concentrations in waste stream.
- (3) Calculated using methodology given by Johnson and others (1989), p. 347.
 - Molecular diffusivity of inorganic constituents with multiple valences calculated using highest valence ion (Daniel & Shackleford, 1988)